

Electronic Thesis and Dissertation Repository

6-26-2017 12:00 AM

Pore-Lining Residues and Intracellular Magnesium Concentration Influence Connexin50 Gap Junction Unitary Channel Conductance

Mary Grace M. Tejada, *The University of Western Ontario*

Supervisor: Dr. Donglin Bai, *The University of Western Ontario*

A thesis submitted in partial fulfillment of the requirements for the Master of Science degree in Neuroscience

© Mary Grace M. Tejada 2017

Follow this and additional works at: <https://ir.lib.uwo.ca/etd>



Part of the [Molecular and Cellular Neuroscience Commons](#), and the [Molecular Biology Commons](#)

Recommended Citation

Tejada, Mary Grace M., "Pore-Lining Residues and Intracellular Magnesium Concentration Influence Connexin50 Gap Junction Unitary Channel Conductance" (2017). *Electronic Thesis and Dissertation Repository*. 4616.

<https://ir.lib.uwo.ca/etd/4616>

This Dissertation/Thesis is brought to you for free and open access by Scholarship@Western. It has been accepted for inclusion in Electronic Thesis and Dissertation Repository by an authorized administrator of Scholarship@Western. For more information, please contact wlsadmin@uwo.ca.

Abstract

Gap junction (GJ) channels mediate direct intercellular communication. Each GJ channel consists of two hemichannels and each hemichannel is a hexamer of connexins. GJs formed by different connexins display different unitary channel conductance (γ_j) and intracellular magnesium modulation. The underlying mechanisms are not fully clear. The present study investigates the effect of mutating putative pore-lining residues (G8, G46, and V53 individually or together) into glutamate in Cx50 on homotypic GJ channel properties. Expression of the triple and individual mutants in GJ-deficient N2A cells resulted in the formation of functional GJ channels similar to that of Cx50 GJs. However, the γ_j s of G8EG46EV53E, G8E, G46E, but not V53E, GJs significantly increased Cx50 GJ γ_j . Increasing intracellular magnesium concentration from 0 to 3 mM significantly reduced the γ_j s of Cx50 and all mutant GJs. These results and our homology structural model indicate that these residues are likely pore-lining.

Keywords

Gap junction channel, connexin, unitary channel conductance, Cx50, patch clamp, magnesium sensitivity

Co-Authorship Statement

Chapter 2 will be submitted as a manuscript for publication. Electrophysiological data was collected by Mary Grace Tejada. Nicholas Kim assisted in minor electrophysiological data on Cx50 V53E single channel recordings. Honghong Chen generated vectors for all Cx50 mutant cDNA. Homology structural models of Cx50 and mutations were generated by Hiroshi Aoyama from Osaka University.

Acknowledgments

Firstly, I would like to thank my supervisor, Dr. Donglin Bai, for the opportunity to work in his lab. I greatly appreciate your guidance throughout my masters and you have instilled the importance of critical thinking. I would also like to thank my advisory committee members, Dr. Wataru Inoue and Dr. Susanne Schmid, for their insight and assistance in shaping my project. I wish to extend my gratitude to all my fellow lab members, both past and present, for their camaraderie and their assistance in editing so many drafts of this thesis. Thank you especially to John Cameron and Benny Yue for training me on the dual whole-cell patch clamp set-up. Thank you Honghong Chen for always being so reliable and being a great mentor in the cell culture room. Thank you Nicholas Kim, Swathy Sudhakar, and fellow office mates for keeping me sane throughout the whole process. Finally, I would like to thank my family and my friends for their continual support and encouragement.

Table of Contents

Abstract.....	i
Co-Authorship Statement.....	ii
Acknowledgments.....	iii
List of Figures and Tables.....	vii
Abbreviations.....	ix
Chapter 1 – Introduction.....	1
1.1 Gap Junction Channels.....	1
1.2 Connexins.....	4
1.3 GJ Channel Regulation and Modulation.....	5
1.3.1 Voltage Regulation.....	5
1.3.2 Chemical Regulation.....	8
1.4 Structural Determinants of Channel Conductance.....	10
1.5 Connexin 50.....	14
1.5.1 Localization and Physiological Functions.....	14
1.5.2 Cx50 GJ Properties and Structural Determinants.....	18
1.5.3 Cataracts and Magnesium Deficiency.....	19
1.6 Rationale and Hypothesis.....	20
1.7 Objectives.....	24
1.8 References.....	25
Chapter 2 – Manuscript.....	35
2.1 Abstract.....	35
2.2 Introduction.....	36
2.3 Materials and Methods.....	40
2.3.1 Construction of Cx50 mutants.....	40

2.3.2 Cell culture and transient transfection	40
2.3.3 Homology structure modeling	41
2.3.4 Electrophysiological recordings	41
2.3.5 Data analysis.....	44
2.4 Results.....	45
2.4.1 Single channel conductance (γ_j) of Cx50 G8EG46EV53E GJ	45
2.4.2 γ_j s of G8E, G46E, and V53E GJs	48
2.4.3 V_j -gating properties of GJs formed by G8G46V53 and individual mutants	51
2.4.4 $[Mg^{2+}]_i$ modulated the γ_j s of G8G46V53 and Cx50	55
2.4.5 $[Mg^{2+}]_i$ modulate γ_j s of G8E, G46E, and V53E GJs.....	58
2.4.6 V_j -gating properties of Cx50 and each mutant GJs under different $[Mg^{2+}]_i$	61
2.4.7 Homology model and pore surface electrostatic potentials of Cx50, G8E, G46E, V53E, and G8G46V53	68
2.5 Discussions	70
2.5.1 Structural determinants of γ_j and V_j -gating in Cx50.....	71
2.5.2 Intracellular magnesium modulation	75
2.5.3 Pathologies associated with mutations in NT, M1, E1 domains.....	78
2.5.4 Resolving the structure-function relationship in NT, M1, E1 domains in Cx50.....	79
2.5.5 Conclusion	80
2.6 References.....	81
Chapter 3 – Discussions.....	95
3.1 Overall Study	95
3.2 The role of pore-lining residues in γ_j and V_j -gating.....	96
3.3 Intracellular magnesium modulation in Cx50 mutant GJ channels	99
3.4 Physiological and pathological role of intracellular magnesium in the lens	101
3.5 Limitations and future directions	102

3.6 Summary	104
3.7 References	106
Curriculum Vitae	120

List of Figures and Tables

Figure 1-1. Gap junction (GJ) channel composition and structural topology of a single connexin.....	3
Figure 1-2. Structural model of Cx26 GJ pore-lining domains NT, M1, and E1.	13
Figure 1-3. Distribution of Cx43, Cx46, and Cx50 in the lens.....	17
Figure 1-4. Homology models of Cx50 GJ and triple mutation (G8EG46EV53E).	23
Figure 2-1. Sequence alignment of the amino terminal, first transmembrane, and early portion of the first extracellular domain of Cx50 and Cx37.....	39
Figure 2-2. The γ_j of Cx50 G8EG46EV53E GJ is drastically higher than that of Cx50.....	47
Figure 2-3. γ_j of G8E and G46E, but not V53E, GJ channels were higher than that of Cx50 GJ.....	50
Figure 2-4. The GJs of Cx50 mutants showed little change in V_j -gating.....	53
Table 2-1. Boltzmann fitting parameters for Cx50 and mutants showed minor differences in V_j -gating parameters.....	54
Figure 2-5. G8G46V53 GJ channels shows greater decrease in γ_j with increasing $[Mg^{2+}]_i$ than Cx50 GJ.....	57
Figure 2-6. The γ_j s of individual mutation GJs reduced in 3 mM $[Mg^{2+}]_i$	60
Figure 2-7. $[Mg^{2+}]_i$ showed little influence on the V_j -gating properties of Cx50 GJ.....	62
Table 2-2. Boltzmann fitting parameters for the V_j -gating of Cx50 GJ at different $[Mg^{2+}]_i$..	63
Figure 2-8. $[Mg^{2+}]_i$ showed little influence on the V_j -gating properties of Cx50 mutant GJs.....	65
Table 2-3. Boltzmann fitting parameters for the V_j -gating of Cx50 mutant GJ at different $[Mg^{2+}]_i$	66

Figure 2-9. Homology models and pore-electrostatic potentials in G8E, G46E, V53E, and G8G46V53 in comparison to Cx50. 69

Abbreviations

[Mg²⁺]_i	Intracellular magnesium concentration
AChR	Acetylcholine receptor
ATP	Adenosine triphosphate
BK	Large-conductance Ca ²⁺ -dependent K ⁺ channels
CaM	Calmodulin
CL	Cytoplasmic loop of a connexin
CT	Carboxyl-terminus of a connexin
Cx	Connexin
DIC	Differential interference contrast
DMEM	Dulbecco's modified Eagle's medium
EGTA	Ethylene glycol-bis(β-aminoethyl ether)-N,N,N',N'-tetraacetic acid
eGFP	Enhanced green fluorescent protein
E1	The first extracellular loop of a connexin
E2	The second extracellular loop of a connexin
ECS	Extracellular solution
GJA8	Human gap junction alpha 8 gene
GJ	Gap junction
G_j	Junctional conductance
G_{j,ss}	Normalized steady state transjunctional conductance

HEPES	4-(2-hydroxyethyl)-1-piperazineethanesulfonic acid
ICS	Intracellular solution
I_j	Junctional current
i_j	Unitary junctional current
kDa	Kilo Dalton
M1 – M4	Transmembrane domain 1 – 4 of a connexin
ms	Millisecond
mV	Millivolts
N2A	Mouse neuroblastoma cells
nS	Nanosiemens
NT	Amino terminus
PEG	Polyethylene glycol probe
pIRES	Plasmid containing internal ribosome entry site
pS	Picosiemens
SEM	Standard error of the mean
SCAM	Substituted cysteine accessibility method
V_j	Transjunctional voltage
V_m	Transmembrane voltage
γ_j	Gap junction unitary channel conductance

Chapter 1 – Introduction

1.1 Gap Junction Channels

Gap junction (GJ) channels are fundamental to synchronizing physiological activities in multicellular organisms. These intercellular channels form a communication network by directly linking cytoplasm between neighboring cells. This enables GJ-connected cells to exchange ions (e.g. K^+), small metabolites (e.g. ATP and glutamate), and other biological molecules (e.g. cyclic AMP) under 1 kDa (Dunlap, Takeda, & Brehm, 1987; Goldberg, Lampe, & Nicholson, 1999; Lawrence, Beers, & Gilula, 1978; Simpson, Rose, & Loewenstein, 1977). A GJ channel forms when two hemichannels on adjacent cells are in close proximity of each other (Bruzzone, White, & Paul, 1996). Two identical hemichannels docking head-to-head form a homotypic GJ channel, whereas two different (yet docking compatible) hemichannels can form a functional heterotypic GJ channel (Figure 1-1). Typically multiple GJ channels aggregate together to form clusters along the cell-to-cell interface known as GJ plaques; yet, a single functioning GJ channel can also exist (Johnson, Hammer, Sheridan, & Revel, 1974).

The communication networks formed by GJ channels are ubiquitously expressed in all tissues of the body. Depending on tissue localization, GJs can mediate a wide range of physiological activities. During tissue differentiation, different types of GJ channels in the embryonic and postnatal brain are up-regulated and down-regulated depending on the developmental stage (Dermietzel et al., 1989). Excitable cells, such as neurons and cardiac myocytes, use GJs to mediate propagation and synchronize electrical signals (Bennett, 1997; Kanter, Saffitz, & Beyer, 1992). Moreover, GJs regulate metabolic

homeostasis in avascular organs, such as the lens, by importing nutrients and exporting waste products between individual cells (Gong et al., 1997). Finally, GJs are involved in regulating cell growth through apoptosis. Cancer cells, in particular, use GJs to propagate apoptotic signals to healthy surrounding cells (Krutovskikh, Piccoli, & Yamasaki, 2002). Therefore, it is evident that GJs are highly involved in mediating many physiological and pathological activities.

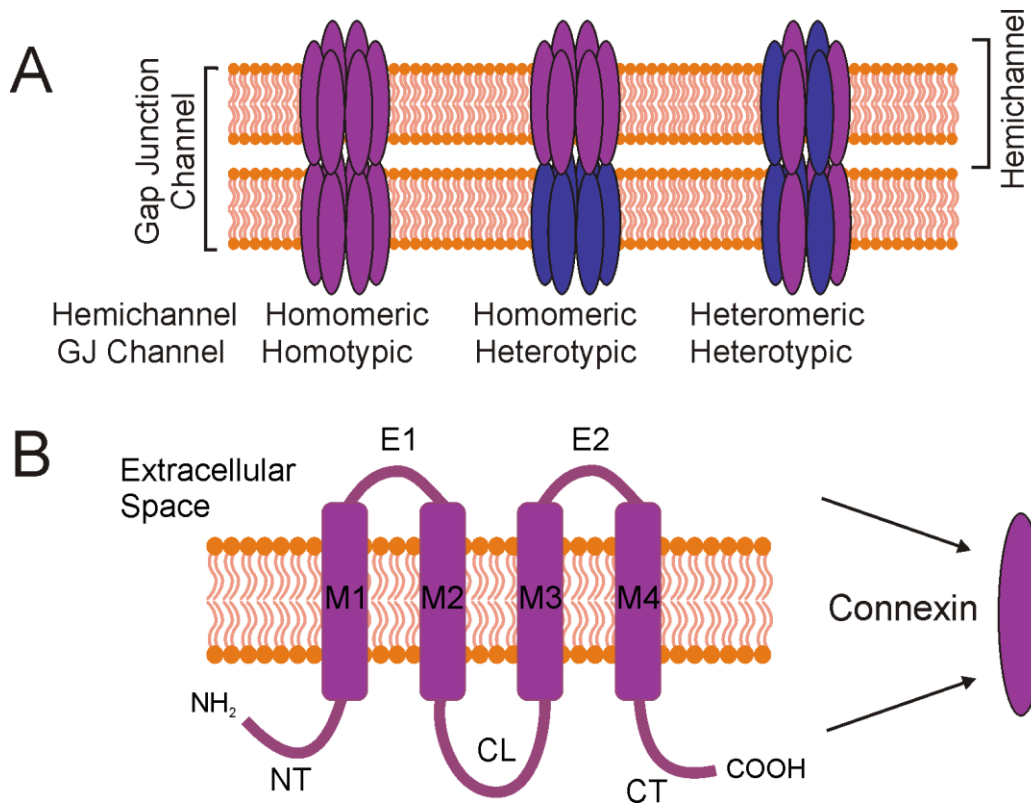


Figure 1-1. Gap junction (GJ) channel composition and structural topology of a single connexin.

A. GJ channels consist of two docked hemichannels localized at the plasma membrane of neighbouring cells. GJ classification varies based on hemichannel composition, which is dependent upon connexin isoform oligomerization. **B.** General structural topology of a connexin monomer.

1.2 Connexins

The diversity in GJ channel properties is partially due to its composition of connexin (Cx) monomers. Connexins are a family of homologous proteins that oligomerize into a hexamer to form a hemichannel. There are 21 identified connexin gene isoforms in the human genome and 20 in the mouse (Sohl & Willecke, 2004). Connexins are classified into phylogenetic groups based on their sequence homology (α , β , γ , δ , and ϵ) (Sohl & Willecke, 2004). Furthermore, connexin nomenclature is based on species and molecular mass; for instance, mCx50 is a mouse connexin with a calculated molecular mass of approximately 50 kDa (Beyer, Paul, & Goodenough, 1990; Kumar & Gilula, 1992). Each connexin has a distinct function and pattern of distribution yet connexins can be co-expressed in tissues with other connexins (Kumar & Gilula, 1992). Consequently, there is a wide array of connexin combinations, thereby creating a variety of functional hemichannels and fully formed GJ channels.

Connexin structural topology is very well characterized. All are assumed to have four hydrophobic transmembrane domains (M1-M4), two extracellular loops (E1 and E2), a cytoplasmic loop (CL), and an amino and carboxyl termini (NT and CT, respectively) found within the intracellular space (Kumar & Gilula, 1992) (Figure 1-1). When six identical connexin isoforms oligomerize it creates homomeric hemichannels, whereas more than one connexin may oligomerize to create heteromeric hemichannels (Figure 1). The oligomerization process may begin in the rough endoplasmic reticulum and continue along the secretory pathway to the Golgi network (George, Kendall, & Evans, 1999; Laird, 1996; Yeager, Unger, & Falk, 1998). Nevertheless, variability in trafficking

pathways are connexin specific; for instance, Cx32 and Cx43 can oligomerize in different intracellular compartments (Maza, Mateescu, Das Sarma, & Koval, 2003; Sarma, Wang, & Koval, 2002). After hemichannels are fully formed they are shuttled and inserted into the plasma membrane where they can then act as individual, functional hemichannels. Alternatively, they can move laterally and potentially dock with a hemichannel from a neighbouring cell membrane to form a complete GJ channel (Laird, 1996; Segretain & Falk, 2004).

Connexin isoform identity originates from differences in amino acid sequence and consequently, GJ structure. Sequence analysis reveals that the extracellular domains are highly conserved across connexins and the most variability is found in the cytoplasmic domains (Bruzzone et al., 1996; Kumar & Gilula, 1992). High sequence identity may be necessary for the extracellular domains as they are responsible for docking between two hemichannels to form a complete GJ channel (Kumar & Gilula, 1992). However, E2 sequence variability dictates heterotypic docking compatibility thereby limiting the possible heterotypic combinations (Bai & Wang, 2014).

1.3 GJ Channel Regulation and Modulation

The activity of a GJ channel, also known as the permeability and conductance, can be modulated by several factors, including two large categories: voltage and chemical.

1.3.1 Voltage Regulation

To a certain extent, all GJs display voltage-dependent deactivation or “gating” (Bukauskas & Weingart, 1994; Moreno, Rook, Fishman, & Spray, 1994; Bukauskas & Verselis, 2004; González, Gómez-Hernández, & Barrio, 2007). Two types of electrical

fields influence GJ channel properties: membrane potential (V_m), which refers to the voltage difference between the interior and exterior of the cell, and transjunctional voltage (V_j), the voltage difference between the interior of the two GJ-linked cells (González et al., 2007). V_j -dependent gating, the deactivation of GJs in response to changes in V_j , is a common characteristic for all GJ channels. The amount of channels undergoing V_j -dependent deactivation (voltage sensitivity), V_j -gating polarity, and kinetic properties, such as the time-course of conductance transitions when V_j is reversed, varies on connexin type (Bennett & Verselis, 1992). Electrophysiological recordings made using dual whole-cell patch clamp in *in vitro* expression systems such as *Xenopus* oocytes and mouse neuroblastoma (N2A) cells are commonly used to observe V_j -dependent gating properties of different connexin GJ channels. This involves taking a GJ-deficient cell line, such as N2A cells, transfecting with a connexin of interest, artificially inducing changes in V_j and recording subsequent changes in current responses (Tong, Aoyama, Tsukihara, & Bai, 2014; Xin, Gong, & Bai, 2010). Macroscopic current recordings, showing the activity of multiple GJ channels, are used to create normalized steady state-to-peak conductance ratios ($G_{j,ss}$) and are then analyzed using a two-state Boltzmann fitting (Harris, Spray, & Bennett, 1981). The V_j -gating parameters obtained from the fitting include: G_{min} , normalized voltage-insensitive residual conductance; V_o , voltage at which conductance is reduced by half; and A , slope of the curve reflecting V_j -gating sensitivity (Harris et al., 1981). These parameters are commonly used to characterize GJs of varying connexin compositions.

It was proposed that one GJ channel contains two V_j -sensitive sensors (one per hemichannel) connected in series that act as “gates” by controlling the closure of the GJ

channel (Harris et al., 1981; Paulauskas, Pranevicius, Pranevicius, & Bukauskas, 2009). Contingent gating theory proposes that these gates act in a contingent manner, such that the state of one hemichannel gate is contingent upon the other hemichannel gate's state (Harris et al., 1981). When one hemichannel gate closes, the V_j experienced by the other gate is altered rendering a closure of the second hemichannel (Harris et al., 1981). On a single channel level, multiple conductance states are exhibited: a fully open state, a residual or subconducting state, and a closed state (Bukauskas & Weingart, 1994). Single channel analysis recorded from insect cells proposed that GJs exhibit two distinct V_j -gating mechanisms per hemichannel defined by their time course of gating transitions between different conducting states (Bukauskas & Weingart, 1994). Fast V_j -gating is the transition between the main open state and a residual state (<1 – 2 ms), whereas slow V_j -gating is the transition between an open or residual state to a completely closed state (tens of ms) (Bukauskas & Weingart, 1994; Bukauskas & Verselis, 2004; Moreno, Rook, Fishman, & Spray, 1994).

Molecular domains responsible for determining V_j -gating mechanisms are still under investigation. Verselis, Ginter, & Bargiello (1994) proposed that the NT forms a charged complex with the M1/E1 domains forming a V_j -sensor responsible for gating polarity and the cytoplasmic movement of the NT initiated V_j -gating. Furthermore, it was found that single amino acid mutations in the NT is able to reverse gating polarity possibly attributing to the differences in gating sensitivity between connexins (Verselis et al., 1994). The importance of the NT in V_j -gating is also seen in domain exchange studies between Cx50 and Cx36 (Xin et al., 2010). When the NT of Cx50 was replaced with the NT of Cx36 V_j -gating properties resembled that of Cx36. Overall, even a small change

via a single point mutation in the NT is able to drastically alter V_j -gating properties further illustrating that molecular differences along the NT could attribute to differences in V_j -gating parameters between connexins (Xin et al., 2010).

1.3.2 Chemical Regulation

Chemical factors are involved in regulating levels of GJ expression and permeability. Depending on GJ connexin composition, hormones and phosphorylation (via protein kinases) alter cell coupling by regulating connexin protein synthesis and insertion/removal of hemichannels from the plasma membrane (Decker, 1976; Kwak et al., 1995; Burghardt et al., 1995). Cell coupling can also be regulated through intracellular acidification. An increase in protons or CO_2 decreases the open-channel probability of GJ channels (Hermans, Kortekaas, Jongsma, & Rook, 1995). A study examining the effects of CO_2 sensitivity indicated that CO_2 activates slow gating mechanisms which structurally changes the GJ channel from an open state to a closed state, thereby reducing junctional conductance (G_j) (Bukauskas & Peracchia, 1997). Again, the extent of GJ channel closure in response to changing levels of pH is connexin-dependent (Hermans et al., 1995). For instance, when comparing two cardiac connexins at a pH_i 6.7, GJ channels expressing Cx45 deactivated 80% of its channels, whereas GJs expressing Cx43 deactivated 30% of its channels relative to a control pH_i of 7.0 (Hermans et al., 1995).

Divalent cations are also known to regulate GJ communication. Increased intracellular calcium (Ca^{2+}) and magnesium (Mg^{2+}) concentrations have consistently shown a marked decrease in junctional permeability by stabilizing a closed channel conformation, thereby uncoupling GJ linked cells (Loewenstein & Rose, 1978; Noma & Tsuboi, 1987; Oliveira-

Castro & Loewenstein, 1971; Palacios-Prado et al., 2013). The effect of intracellular Ca^{2+} and Mg^{2+} is usually seen at higher than normal physiological concentrations; for instance, a lenticular intracellular concentration higher than 0.0005 mM and 1 mM, respectively (Peracchia & Peracchia, 1980). In pathological situations, abnormally high concentrations of divalent cations may induce uncoupling as a protective mechanism to isolate injured cells (Loewenstein, Nakas, & Socolar, 1967).

Nevertheless, sensitivity to divalent cation modulations is still connexin-dependent. An extensive amount of literature has looked into the role and mechanisms of intracellular Ca^{2+} modulation; however, the molecular mechanism underlying intracellular Mg^{2+} modulation is still under investigation. Peracchia & Peracchia (1980) proposed that divalent cations aggregate along the negative charges found within the channel possibly narrowing the channel and impeding conductance. Further examination of intracellular Mg^{2+} concentrations in Cx36, Cx26, Cx32, Cx43, Cx45, and Cx47 have proposed that Mg^{2+} binding within the electrostatic regions of the channel lumen stabilizes the closed conformation of the slow gates (Palacios-Prado et al., 2013). In particular, Palacios-Prado and colleagues (2014) identified the E1 domain in Cx36 as a region of interest for Mg^{2+} sensitivity. Site-directed mutagenesis identified D47, a negatively charged aspartate located in the E1 domain possible facing the pore, as a site of high Mg^{2+} sensitivity directly influencing Cx36 GJ gating characteristics (Palacios-Prado et al., 2014). Intracellular Mg^{2+} modulation on an individual channel level has yet to be investigated in several connexins, including Cx50. All things considered, molecular determinants for connexin specific Mg^{2+} -sensitivity may be due to charged residues found in the E1 domain.

1.4 Structural Determinants of Channel Conductance

GJs formed by different connexins show different channel properties, including differences in single (or unitary) channel conductance. Unitary conductance (γ_j) refers to the rate of ion permeation through one single channel and ranges between 9 pS (mCx30.2) to 300 pS (Cx37) (Kreuzberg et al., 2005; Veenstra et al., 1994). The molecular differences between GJs of different connexins remain unclear. Pore properties such as the pore size (or diameter) and electrostatic charge have been proposed as potential determinants to γ_j differences (Gong & Nicholson, 2001; Tong et al., 2015; Veenstra et al., 1994; Weber, Chang, Spaeth, Nitsche, & Nicholson, 2004).

One classic assumption proposed that pore diameter limits the ion flow through the channel, thereby restricting γ_j suggesting that GJ channels with larger pore diameters have larger γ_j s. Dye studies involving Cx37, known to have one of the largest γ_j s, have consistently demonstrated that Cx37 was the least permeable to larger dyes, consequently negating this theory (Gong & Nicholson, 2001; Veenstra et al., 1994; Weber, Chang, Spaeth, Nitsche, & Nicholson, 2004). For instance, Gong & Nicholson (2001) used different sized polyethylene glycol probes (PEG) to assess physical limits of Cx26, Cx32, and Cx37. Here it was demonstrated that Cx32, which had a relatively small γ_j , had a larger PEG size cut-off than Cx37 suggesting channel size is a poor indicator of conductance (Gong & Nicholson, 2001). Using different sized Alexa dyes, Weber and colleagues (2004) demonstrated that Cx37 was the least permeable to the largest Alexa dyes. Also, predicted permeability of Cx43, Cx32, Cx26, Cx40, and Cx37 GJs based on hindered pore diffusion was much smaller than absolute experimental permeability, providing more evidence negating the pore diameter assumption (Weber et al., 2004).

Moreover, a site-directed mutagenesis study in Cx50 involving many putative pore-lining residue mutations altering estimated channel diameters demonstrated a weak correlation between pore diameter and γ_j (Tong et al., 2015).

Experimental efforts have focused on pore-lining domains as major influencers of γ_j . Currently, human Cx26, also known as β_2 protein, is the only connexin to have a high resolution crystal structure of the GJ channel (Maeda et al., 2009). Due to the high degree of sequence homology between connexins (Bai & Wang, 2014), Cx26's structure has been used as a model for many structure-function studies. This structural model indicated that the NT, M1, and E1 domains are pore-lining regions (Figure 1-2) that are crucial in the involvement in charge selectivity through the channel lumen. Therefore, mutations within these regions would change the GJs properties, including γ_j (Maeda et al., 2009). Substituted cysteine accessibility method (SCAM) used in Cx46 identified pore-lining residues along the M1-E1 border, particularly E43, G46, and D51, that greatly reduced γ_j when methanethiosulfonate reagents were added (Kronengold, Trexler, Bukauskas, Bargiello, & Verselis, 2003). Zhou and colleagues (1997) also conducted cysteine scanning mutagenesis in Cx46 and Cx32E₁43 revealing pore-lining residues again in the latter half of M1. Tryptophan scanning in Cx32 revealed pore-lining M1 residues, especially in the M1-E1 border region, were highly sensitive to tryptophan substitutions and significantly reduced coupling (Brennan et al., 2015). M1 domain exchange between Cx46 and Cx32E₁43 created chimeras exhibiting γ_j similar to their 'donor' GJs (Hu, Ma, & Dahl, 2006). Moreover, exchanging the latter half of M1 in Cx46 with Cx37 resulted in a chimera exhibiting a γ_j close to that of Cx37 (Hu et al., 2006). NT exchange between Cx50 and Cx36 resulted in altered γ_j and introducing positively charged amino acids at

position N9 reduced γ_j (Xin et al., 2010). Mutational changes altering electrostatic potentials along Cx50's E1 domain also showed a change in γ_j (Tong et al., 2015). Overall, these studies indicate that pore-lining properties of NT, M1, and E1 domains are important determinants in γ_j .

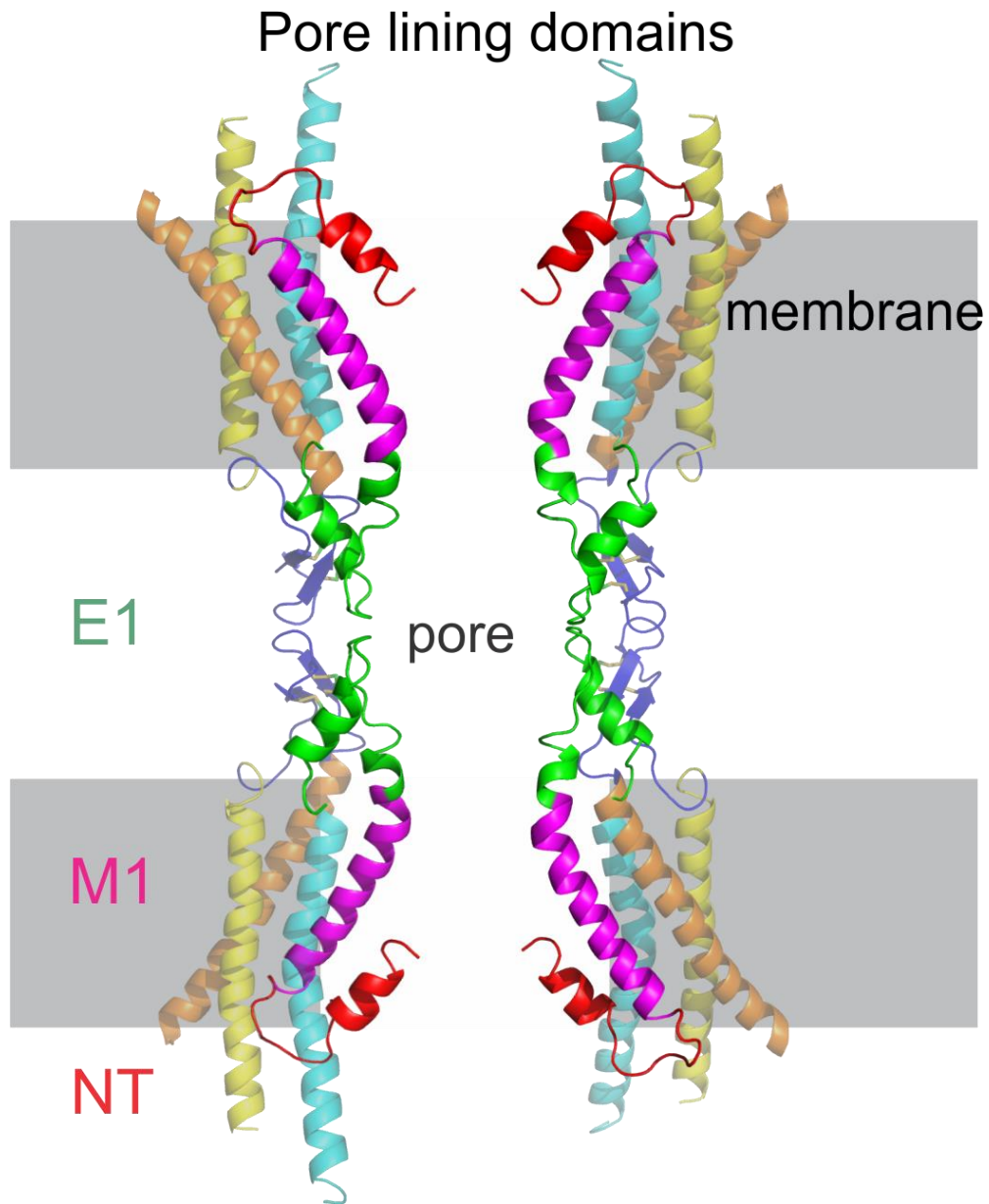


Figure 1-2. Structural model of Cx26 GJ pore-lining domains NT, M1, and E1.

Open view of four Cx26 monomers forming a GJ channel. Colour code illustrates different structural domains of the connexin. NT (red), M1 (magenta), and E1 (green) are highlighted to signify pore-lining domains.

1.5 Connexin 50

1.5.1 Localization and Physiological Functions

Cx50, also known as membrane protein 70 and α_8 protein, is encoded by gene *GJA8* (Kistler, Kirkland, & Bullivant, 1985; Shiels et al., 1998). *GJA8* is located on human chromosome 1, homologous to mouse chromosome 3 (Church, Wang, & Steele, 1995; Kerscher, Church, Boyd, & Lyon, 1995). Cx50 was shown to be expressed in the ciliary body epithelium, retinal astrocytes, retinal müller cells, and the atrioventricular valves; however, it is primarily found in the lens (Goodenough, 1992; Gourdie, Green, Severs, & Thompson, 1992; Schütte, Chen, Buku, & Wolosin, 1998; Wolosin, Schütte, & Chen, 1997).

The lens is an avascular organ that is highly dependent on proper GJ functioning to maintain metabolic and mineral homeostasis. The lens consists of two cell types: lens epithelium (mainly regulated by Cx43) and lens fibers (regulated by Cx46 and Cx50) (Fig. 1-3) (Goodenough, 1992; White, Bruzzone, Goodenough, & Paul, 1992). Epithelial cells cover the anterior surface of the lens and are metabolically active. During embryonic lens development, epithelial cells differentiate into lens fibers, which forms the bulk of the lens. Organelles in newly differentiated fibers degenerate forming an organelle-free zone and fiber cells gain high concentrations of soluble crystallins creating optical transparency and a high refractive index characterizing the lens (Bassnett & Beebe, 1992; Goodenough, 1992; White et al., 1992). GJs are necessary to form a syncytium between the epithelium and fiber cells to maintain intracellular ionic conditions to prevent precipitation of crystallins and cataract formation (Chang et al.,

2002; Gong et al., 1997; Goodenough, 1992; Rong et al., 2002; White, Goodenough, & Paul, 1998).

Although Cx50 and Cx46 are co-localized within the deep cortical regions of the lens fibers, they have unique physiological properties. These two connexins can form functional individual hemichannels or full GJ channels. Homotypic, heterotypic, and heteromeric Cx50 and Cx46 GJs can exist; however, Cx46 can form functional lens-to-epithelium heterotypic channels with Cx43 while Cx50 cannot (Hopperstad, Srinivas, & Spray, 2000; White, Bruzzone, Wolfram, Paul, & Goodenough, 1994). Experimental knockouts of either connexin in mouse models result in phenotypically different congenital cataracts, showing that one connexin cannot rescue the loss-of-function of the other (Gong et al., 1997; White, Goodenough, & Paul, 1998). Cx50 knockout mice exhibit microphthalmia (abnormally small eyes) with zonular pulverulent nuclear cataracts in addition to delayed lens growth and lens fiber maturation, demonstrating Cx50's importance in proper fiber cell maturation and ocular growth (Chang et al., 2002; Rong et al., 2002; White et al., 1998). Additionally, many missense mutations in Cx50 result in congenital cataracts (Li et al., 2013; Shiels et al., 1998; Tong et al., 2011; Vanita, Singh, Singh, Varon, & Sperling, 2008; Wang, Luo, Wen, Zhang, & Lu, 2011). Missense mutations such as D47H, W45S, and D47H impair trafficking of the hemichannel to the plasma membrane, resulting in nonfunctional GJ channels (Li et al., 2013; Vanita et al., 2008; Wang et al., 2011). In comparison, other missense mutations, such as G46V, have been shown to enhance hemichannel functioning causing increased metabolite and ion entry and exit of the cells reducing cell viability (Tong et al., 2011). Li and colleagues (2013) created an illustrated summary of identified human Cx50

congenital cataract mutations that highlights prevalence of mutations along the M1-E1 regions including G46V (Li et al., 2013). Understanding how these regions are involved in normal GJ functioning may provide insight into their role in pathological conditions.

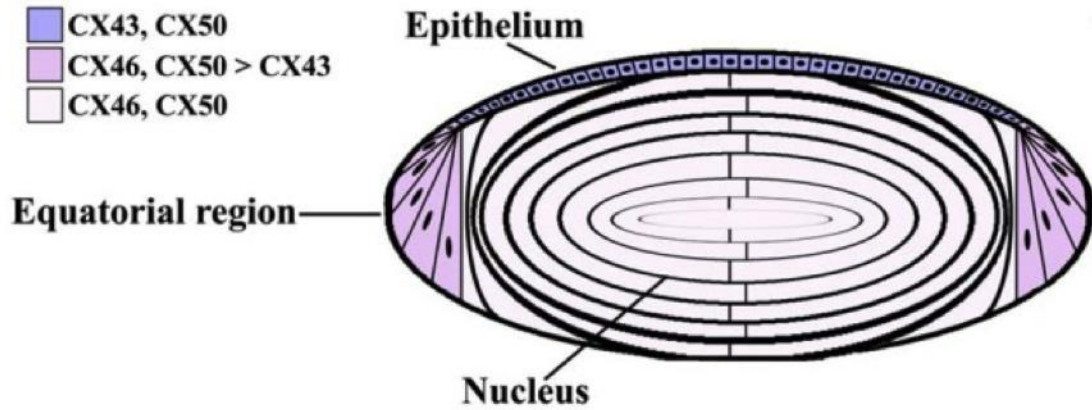


Figure 1-3. Distribution of Cx43, Cx46, and Cx50 in the lens.

Anterior epithelial cells express Cx43 and Cx50, differentiating fiber cells at the equatorial region express Cx43, Cx46, and Cx50, and fiber cells located in the nucleus express Cx46 and Cx50 (Beyer & Berthoud, 2014).

1.5.2 Cx50 GJ Properties and Structural Determinants

The properties of Cx50 GJ channels have been well characterized: they display one of the largest γ_j s (200–220 pS), preference of cation permeation through its channels, and high sensitivity to both transjunctional voltage and cytoplasmic acidification (Srinivas, Rozental, et al., 1999; Tong et al., 2014; White et al., 1992). Using Cx26 as a structural template, extensive research on Cx50 has been done to elucidate the Cx50 GJ structure and GJ channel function relationship (White et al., 1994; Tong et al., 2015; Tong et al., 2014; Xin et al., 2010; Xin, Nakagawa, Tsukihara, & Bai, 2012).

Many studies utilize a domain-exchange approach to examine how one connexin domain influences GJ properties. As previously mentioned, although Cx50 and Cx46 are co-localized in the lens fibers, only Cx46 is able to form functional heterotypic GJs with lens epithelium connexin Cx43 (Hopperstad et al., 2000; White et al., 1994). Using the domain-exchange approach, it has been shown that the E2 domain is responsible for discriminating heterotypic compatibility between connexins (White et al., 1994). Exchanging the E2 domain in Cx46 with the E2 domain of Cx50 rendered nonfunctional heterotypic channels with Cx43; however, the reciprocal chimera gained the ability to form functional heterotypic channels with Cx43 (White et al., 1994). Exchanging the NT domain of Cx50 and Cx36 resulted in dramatically modified V_j -gating sensitivity, kinetics, and single channel properties in Cx50 GJ highlighting the effects of the NT domain on Cx50 GJ V_j -gating properties and γ_j (Xin et al., 2010). Similarly, exchanging the E1 domain of Cx50 with Cx36 emphasized the importance of this domain in determining Cx50 GJ γ_j (Tong et al., 2015). Domain-exchange studies provide foundational information regarding how each domain is involved in GJ properties.

Nevertheless, to fully examine the exact structural determinants of GJ properties such as V_j -gating and γ_j , site-directed mutagenesis on individual residues is necessary. Pore surface electrostatic potentials have been of particular interest in determining Cx50 GJ channel properties. When charged residues are introduced at certain putative pore-lining positions in the primary sequence of the NT and M1-E1 border alterations in V_j -gating and γ_j are apparent (Tong et al., 2014; Xin et al., 2010; Xin, Nakagawa, Tsukihara, & Bai, 2012). The influence of pore surface electrostatic potential on Cx50 GJ channel properties is still unclear.

1.5.3 Cataracts and Magnesium Deficiency

GJs create a microcirculatory system in the lens to maintain homeostasis and transparency. A normal mammalian lens maintains precise intracellular ionic composition, characterized by low levels of Ca^{2+} and sodium (Na^+) as well as high levels of potassium (K^+) and Mg^{2+} (Dilsiz, Olcucu, & Atas, 2000). Alterations in lenticular GJ functionality reverses intracellular ionic composition consequently resulting in a cataract (Dilsiz, Olcucu, & Atas, 2000). Much of the literature focuses on altered lens GJ properties induced by high concentrations of Ca^{2+} . In comparison, there is a lack of information on how intracellular Mg^{2+} modifies lens GJ properties.

Intracellular Mg^{2+} is an important divalent cation necessary for maintaining structural and functional integrity of the lens (Agarwal, Iezhitsa, Agarwal, & Spasov, 2012). Mg^{2+} is a cofactor for several enzymes that regulates many metabolic activities, many of which occur when it is bound to ATP (Agarwal, Iezhitsa, & Agarwal, 2014; McGahan, Chin, & Bentley, 1983). Intracellular Mg^{2+} concentration is not uniform in the lens; instead

concentrations gradually decrease further into the inner tissue layers. There, internal “free” Mg^{2+} concentration is estimated to be 3 mM in the mammalian lens (McGahan et al., 1983). It is normal for intracellular Mg^{2+} concentrations to gradually decrease with age, yet concentrations less than 20 mg/lens gram reduce lens transparency enough to be classified as a cataract (Swanson & Truesdale, 1971). Lens phosphatase activity and membrane transport mechanisms such as Na^+K^+ -ATPase and Ca^{2+} -ATPase are highly dependent on Mg^{2+} (Agarwal, Iezhitsa, Agarwal, & Spasov, 2013; Umeda, Kashiwa, Nakata, & Nishigori, 2003). A deficiency in intracellular Mg^{2+} thereby causes an ionic imbalance initiating the formation of a cataract (Agarwal et al., 2012). Mg^{2+} is also involved in glutathione synthesis, a non-enzymatic factor required to protect the lens against oxidative stress (Minnich, Smith, Brauner, & Majerus, 1971). It is not fully understood how increased intracellular Mg^{2+} modulates lens GJ properties, in particular Cx50 GJ channels. Elucidating its influence on GJ properties would give insight into potential treatment for Mg^{2+} -deficient induced cataracts.

1.6 Rationale and Hypothesis

The relationship between molecular structure and GJ channel properties, such as V_j -gating and unitary channel conductance, are still under investigation. Current literature suggests the pore-lining domains, NT, latter half of M1, and E1, are responsible for the differences in channel properties (Kronengold et al., 2003; Tong et al., 2015). These domains have been of particular interest in determining Cx50's GJ channel properties. Domain exchange studies between Cx50 and Cx36 have unveiled the importance of NT and E1 in V_j -gating and single channel properties in Cx50 GJs (Tong et al., 2015; Xin et al., 2010). Moreover, mutagenesis of residue G46 in Cx50's M1-E1 region indicate the

importance of pore surface electrostatic potentials in dictating Cx50's unitary conductance (Tong et al., 2014). In particular, increasing negative charge at this pore-lining residue with a glutamic acid (E) increases Cx50 GJ channel γ_j to approximately 293 pS, almost reaching the highest γ_j of Cx37 of 300 pS (Tong et al., 2014; Veenstra, Wang, Beyer, Ramanan, & Brink, 1994).

Based on this observation, we aligned the sequences of alpha family connexins Cx50 and Cx37 to further investigate the molecular determinants underlying such large single channel γ_j s. Sequence alignment of Cx50 and Cx37 revealed differences at two key residues in the NT and E1 domains, In particular, G8 and V53 in Cx50 are E8 and E53 in Cx37. The added negative charges on the side chain at these positions in Cx37 may be contributors to its high γ_j . The present study investigates the influence of increased negative charge within the pore by creating triple mutation Cx50 G8EG46EV53E (G8G46V53) (Figure 1-4). To identify which residue is critical for any observed changes, single mutations G8E, G46E, and V53E was also examined.

Furthermore, intracellular Mg^{2+} (Mg^{2+}_i) has been shown to alter GJ properties (Noma & Tsuboi, 1987; Oliveira-Castro & Loewenstein, 1971; Palacios-Prado et al., 2013; Palacios-Prado et al., 2014). Since intracellular Mg^{2+} is critical for maintaining mineral homeostasis of the lens, its influence on Cx50 GJ properties was also investigated (Agarwal et al., 2012). Perhaps the increase in negative charges in the pore could modify intracellular Mg^{2+} modulation (Palacios-Prado et al., 2013). Overall, the current study examines potential determinants of Cx50 GJ channel properties. We hypothesize that

increasing negative charges along speculated pore-lining residues and increasing $[Mg^{2+}]_i$ will alter Cx50 GJ γ_j and V_j -gating properties.

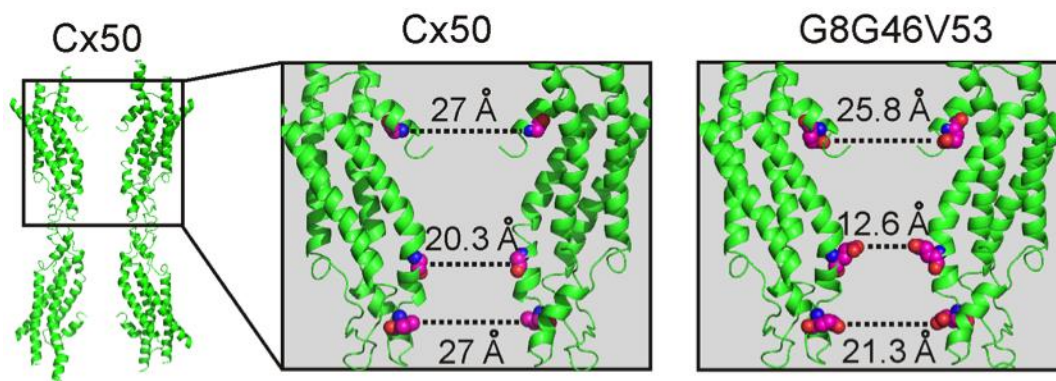


Figure 1-4. Homology models of Cx50 GJ and triple mutation (G8EG46EV53E).

Cx50 GJ homology structural model containing only four of the twelve subunits for simplification. Boxed region is enlarged area of wildtype Cx50 highlighting putative pore-lining residues with estimated pore diameters at mutagenesis sites prior to mutagenesis. G8EG46EV53E (or G8G46V53) mutant structural models based on wildtype Cx50. Highlighted mutant residues with estimated pore diameters after mutagenesis are shown.

1.7 Objectives

- i. Investigate the effect of introducing negatively charged residues in the pore-lining domains, NT, M1, and E1 on Cx50 GJ single channel unitary conductance (γ_j) and V_j -gating. Specifically, site-directed mutagenesis performed at residues G8, G46, and V53 to glutamic acid to create individual mutants and a triple mutation G8EG46EV53E (which will be referred to as G8G46V53). GJs formed by these mutants are characterized for changes in γ_j and V_j -gating properties.
- ii. Investigate the effect of $[Mg^{2+}]_i$ on the γ_j and V_j -gating properties of the GJs of these Cx50 mutants.

1.8 References

- Agarwal, R., Iezhitsa, I., Agarwal, P., & Spasov, A. (2012). Magnesium deficiency: Does it have a role to play in cataractogenesis? *Experimental Eye Research*, *101*, 82–89.
- Agarwal, R., Iezhitsa, I. N., Agarwal, P., & Spasov, A. a. (2013). Mechanisms of cataractogenesis in the presence of magnesium deficiency. *Magnesium Research*, *26*(1), 2–8.
- Agarwal, R., Iezhitsa, L., & Agarwal, P. (2014). Pathogenetic role of magnesium deficiency in ophthalmic diseases. *BioMetals*, *27*(1), 5–18.
- Bai, D., & Wang, A. H. (2014). Extracellular domains play different roles in gap junction formation and docking compatibility. *The Biochemical Journal*, *458*(1), 1–10.
- Bassnett, S., & Beebe, D. C. (1992). Coincident loss of mitochondria and nuclei during lens fiber cell differentiation. *Developmental Dynamics*, *194*(2), 85–93.
- Bennett, M. V. (1997). Gap junctions as electrical synapses. *Journal of Neurocytology*, *26*(6), 349–66.
- Bennett, M. V., & Verselis, V. K. (1992). Biophysics of gap junctions. *Seminars in Cell Biology*, *3*(1), 29–47.
- Beyer, E. C., & Berthoud, V. M. (2014). Connexin hemichannels in the lens. *Frontiers in Physiology*, *5*, 20.
- Brennan, M. J., Karcz, J., Vaughn, N. R., Woolwine-Cunningham, Y., DePriest, A. D., Escalona, Y., ... Skerrett, I. M. (2015). Tryptophan Scanning Reveals Dense Packing of Connexin Transmembrane Domains in Gap Junction Channels Composed of Connexin32. *Journal of Biological Chemistry*, *290*(28), 17074–17084.
- Bruzzone, R., White, T. W., & Paul, D. L. (1996). Connections with connexins: the molecular basis of direct intercellular signaling. *European Journal of Biochemistry / FEBS*, *238*(1), 1–27.

- Bukauskas, F. F., & Peracchia, C. (1997). Two distinct gating mechanisms in gap junction channels: CO₂-sensitive and voltage-sensitive. *Biophysical Journal*, 72(5), 2137–42.
- Bukauskas, F. F., & Verselis, V. K. (2004). Gap junction channel gating. *Biochimica et Biophysica Acta*, 1662(1-2), 42–60.
- Bukauskas, F. F., & Weingart, R. (1994). Voltage-dependent gating of single gap junction channels in an insect cell line. *Biophysical Journal*, 67(2), 613–625.
- Burghardt, R. C., Barhoumi, R., Sewall, T. C., & Bowen, J. A. (1995). Cyclic AMP induces Rapid increases in gap junction permeability and changes in the cellular distribution of connexin43. *New York*, 253, 243–253.
- Chang, B., Wang, X., Hawes, N. L., Ojakian, R., Davisson, M. T., Lo, W. K., & Gong, X. (2002). A Gja8 (Cx50) point mutation causes an alteration of alpha 3 connexin (Cx46) in semi-dominant cataracts of Lop10 mice. *Hum Mol Genet*, 11(5), 507–513.
- Church, R. L., Wang, J., & Steele, E. (1995). The human lens intrinsic membrane protein MP70 (Cx50) gene: clonal analysis and chromosome mapping. *Current Eye Research*, 14(3), 215–221.
- Decker, R. S. (1976). Hormonal regulation of gap junction differentiation. *The Journal of Cell Biology*, 69(3).
- Dermietzel, R., Traub, O., Hwang, T. K., Beyer, E., Bennett, M. V, Spray, D. C., & Willecke, K. (1989). Differential expression of three gap junction proteins in developing and mature brain tissues. *Proceedings of the National Academy of Sciences*, 86(December), 10148–10152.
- Dilsiz, N., Olcucu, A., & Atas, M. (2000). Determination of calcium, sodium, potassium and magnesium concentrations in human senile cataractous lenses. *Cell Biochemistry and Function*, 18(4), 259–262.

- Dunlap, K., Takeda, K., & Brehm, P. (1987). Activation of a calcium-dependent photoprotein by chemical signalling through gap junctions. *Nature*, 325(6099), 60–62.
- George, C. H., Kendall, J. M., & Evans, W. H. (1999). Intracellular trafficking pathways in the assembly of connexins into gap junctions. *Journal of Biological Chemistry*, 274(13), 8678–8685.
- Goldberg, G. S., Lampe, P. D., & Nicholson, B. J. (1999). Selective transfer of endogenous metabolites through gap junctions composed of different connexins. *Nature Cell Biology*, 1(7), 457–459.
- Gong, X., Li, E., Klier, G., Huang, Q., Wu, Y., Lei, H., ... Gilula, N. B. (1997). Disruption of $\alpha 3$ connexin gene leads to proteolysis and cataractogenesis in mice. *Cell*, 91(6), 833–843.
- Gong, X. Q., & Nicholson, B. J. (2001). Size selectivity between gap junction channels composed of different connexins. *Cell Communication & Adhesion*, 8, 187–192.
- González, D., Gómez-Hernández, J. M., & Barrio, L. C. (2007). Molecular basis of voltage dependence of connexin channels: An integrative appraisal. *Progress in Biophysics and Molecular Biology*, 94(1-2), 66–106.
- Goodenough, D. A. (1992). The crystalline lens. A system networked by gap junctional intercellular communication. *Semin Cell Biol*, 3(1), 49–58.
- Gourdie, R., Green, C., Severs, N., & Thompson, R. (1992). Immunolabelling patterns of gap junction connexins in the developing and mature rat heart. *Anatomy and Embryology*, 185(4), 363–378.
- Harris, A. L., Spray, D. C., & Bennett, M. V. (1981). Kinetic properties of a voltage-dependent junctional conductance. *The Journal of General Physiology*, 77(1).

- Hermans, M. M. P., Kortekaas, P., Jongsma, H. J., & Rook, M. B. (1995). pH sensitivity of the cardiac gap junction proteins, connexin 45 and 43. *Pflügers Archiv European Journal of Physiology*, *431*(1), 138–140.
- Hopperstad, M. G., Srinivas, M., & Spray, D. C. (2000). Properties of gap junction channels formed by Cx46 alone and in combination with Cx50. *Biophysical Journal*, *79*(4), 1954–66.
- Hu, X., Ma, M., & Dahl, G. (2006). Conductance of Connexin Hemichannels Segregates with the First Transmembrane Segment. *Biophysical Journal*, *90*(1), 140–150.
- Johnson, R., Hammer, M., Sheridan, J., & Revel, J. P. (1974). Gap junction formation between reaggregated Novikoff hepatoma cells. *Proc Natl Acad Sci U S A*, *71*(11), 4536–4540.
- Kanter, H. L., Saffitz, J. E., & Beyer, E. C. (1992). Cardiac myocytes express multiple gap junction proteins. *Circulation Research*, *70*(2), 438–444.
- Kerscher, S., Church, R. L., Boyd, Y., & Lyon, M. F. (1995). Mapping of four mouse genes encoding eye lens-specific structural, gap junction, and integral membrane proteins: Cryba1 (crystallin beta A3/A1), Crybb2 (crystallin beta B2), Gja8 (MP70), and Lim2 (MP19). *Genomics*, *29*(2), 445–450.
- Kistler, J., Kirkland, B., & Bullivant, S. (1985). Identification of a 70,000-D protein in lens membrane junctional domains. *Journal of Cell Biology*, *101*(1), 28–35.
- Kreuzberg, M. M., Söhl, G., Kim, J.-S., Verselis, V. K., Willecke, K., & Bukauskas, F. F. (2005). Functional properties of mouse connexin30.2 expressed in the conduction system of the heart. *Circulation Research*, *96*(11), 1169–77.
- Kronengold, J., Trexler, E. B., Bukauskas, F. F., Bargiello, T. A., & Verselis, V. K. (2003). Single-channel SCAM Identifies Pore-lining Residues in the First Extracellular Loop and First Transmembrane Domains of Cx46 Hemichannels. *The Journal of General Physiology*, *122*(4), 389–405.

- Krutovskikh, V. a, Piccoli, C., & Yamasaki, H. (2002). Gap junction intercellular communication propagates cell death in cancerous cells. *Oncogene*, *21*(13), 1989–1999.
- Kumar, N. M., & Gilula, N. B. (1992). Molecular biology and genetics of gap junction channels. *Seminars in Cell Biology*, *3*(1), 3–16.
- Kwak, B. R., Hermans, M. M., De Jonge, H. R., Lohmann, S. M., Jongma, H. J., & Chanson, M. (1995). Differential regulation of distinct types of gap junction channels by similar phosphorylating conditions. *Molecular Biology of the Cell*, *6*(12), 1707–1719.
- Laird, D. W. (1996). The life cycle of a connexin: gap junction formation, removal, and degradation. *Journal of Bioenergetics and Biomembranes*, *28*(4), 311–318.
- Lawrence, T. S., Beers, W. H., & Gilula, N. B. (1978). Transmission of hormonal stimulation by cell-to-cell communication. *Nature*, *272*, 501–506.
- Li, J., Wang, Q., Fu, Q., Zhu, Y., Zhai, Y., Yu, Y., ... Yao, K. (2013). A novel connexin 50 gene (gap junction protein, alpha 8) mutation associated with congenital nuclear and zonular pulverulent cataract. *Molecular Vision*, *19*(April), 767–774.
- Loewenstein, W. R., Nakas, M., & Socolar, S. J. (1967). Junctional Membrane Uncoupling: Permeability transformations at a cell membrane junction . *The Journal of General Physiology* , *50* (7) , 1865–1891.
- Loewenstein, W. R., & Rose, B. (1978). Calcium in (Junctional) Intercellular Communication and a Thought on Its Behavior in Intracellular Communication. *Annals of the New York Academy of Sciences*, *307*(1), 285–307.
- Maeda, S., Nakagawa, S., Suga, M., Yamashita, E., Oshima, A., Fujiyoshi, Y., & Tsukihara, T. (2009). Structure of the connexin 26 gap junction channel at 3.5 Å resolution. *Nature*, *458*(7238), 597–602.

- Maza, J., Mateescu, M., Das Sarma, J., & Koval, M. (2003). Differential oligomerization of endoplasmic reticulum-retained connexin43/connexin32 chimeras. *Cell Communication & Adhesion*, *10*, 319–322.
- McGahan, M. C., Chin, B., & Bentley, P. J. (1983). Some Observations on the Magnesium Metabolism of the Rabbit Lens. *Exp. Eye Res*, *36*, 67–73.
- Minnich, V., Smith, M. B., Brauner, M. J., & Majerus, P. W. (1971). Glutathione biosynthesis in human erythrocytes. I. Identification of the enzymes of glutathione synthesis in hemolysates. *Journal of Clinical Investigation*, *50*(3), 507–513.
- Moreno, a P., Rook, M. B., Fishman, G. I., & Spray, D. C. (1994). Gap junction channels: distinct voltage-sensitive and -insensitive conductance states. *Biophysical Journal*, *67*(1), 113–9.
- Noma, a, & Tsuboi, N. (1987). Dependence of junctional conductance on proton, calcium and magnesium ions in cardiac paired cells of guinea-pig. *J. Physiol.*, *382*(1), 193–211.
- Oliveira-Castro, G. M., & Loewenstein, W. R. (1971). Junctional membrane permeability - Effects of divalent cations. *The Journal of Membrane Biology*, *5*(1), 51–77.
- Palacios-Prado, N., Chapuis, S., Panjkovich, A., Fregeac, J., Nagy, J. I., & Bukauskas, F. F. (2014). Molecular determinants of magnesium-dependent synaptic plasticity at electrical synapses formed by connexin36. *Nature Communications*, *5*, 4667.
- Palacios-Prado, N., Hoge, G., Marandykina, A., Rimkute, L., Chapuis, S., Paulauskas, N., ... Bukauskas, F. F. (2013). Intracellular Magnesium-Dependent Modulation of Gap Junction Channels Formed by Neuronal Connexin36. *J Neurosci.*, *33*(11), 4741–4753.
- Paulauskas, N., Pranevicius, M., Pranevicius, H., & Bukauskas, F. F. (2009). A stochastic four-state model of contingent gating of gap junction channels containing two “fast” gates sensitive to transjunctional voltage. *Biophysical Journal*, *96*(10), 3936–3948.

- Peracchia, C., & Peracchia, L. L. (1980). Gap junction dynamics: reversible effects of divalent cations. *The Journal of Cell Biology*, 87(3).
- Rong, P., Wang, X., Niesman, I., Wu, Y., Benedetti, L. E., Dunia, I., ... Gong, X. (2002). Disruption of Gja8 (alpha8 connexin) in mice leads to microphthalmia associated with retardation of lens growth and lens fiber maturation. *Development (Cambridge, England)*, 129(1), 167–74.
- Rubinos, C., Villone, K., Mhaske, P. V, White, T. W., & Srinivas, M. (2014). Functional effects of Cx50 mutations associated with congenital cataracts. *American Journal of Physiology. Cell Physiology*, 306(3), C212–20.
- Sarma, J. Das, Wang, F., & Koval, M. (2002). Targeted gap junction protein constructs reveal connexin-specific differences in oligomerization. *Journal of Biological Chemistry*, 277(23), 20911–20918.
- Schütte, M., Chen, S., Buku, A., & Wolosin, J. M. (1998). Connexin50, a Gap Junction Protein of Macrogliia in the Mammalian Retina and Visual Pathway. *Experimental Eye Research*, 66(5), 605–613.
- Segretain, D., & Falk, M. M. (2004). Regulation of connexin biosynthesis, assembly, gap junction formation, and removal. *Biochimica et Biophysica Acta - Biomembranes*, 1662(1-2), 3–21.
- Shiels, a, Mackay, D., Ionides, a, Berry, V., Moore, a, & Bhattacharya, S. (1998). A missense mutation in the human connexin50 gene (GJA8) underlies autosomal dominant “zonular pulverulent” cataract, on chromosome 1q. *American Journal of Human Genetics*, 62(3), 526–32.
- Simpson, I., Rose, B., & Loewenstein, W. R. (1977). Size limit of molecules permeating the junctional membrane channels. *Science (New York, N.Y.)*, 195(4275), 294–6.
- Sohl, G. (2004). Gap junctions and the connexin protein family. *Cardiovascular Research*, 62(2), 228–232.

- Srinivas, M., Rozental, R., Kojima, T., Dermietzel, R., Mehler, M., Condorelli, D. F., ... Spray, D. C. (1999). Functional properties of channels formed by the neuronal gap junction protein connexin36. *The Journal of Neuroscience : The Official Journal of the Society for Neuroscience*, *19*(22), 9848–9855.
- Swanson, A. a., & Truesdale, A. W. (1971). Elemental analysis in normal and cataractous human lens tissue. *Biochemical and Biophysical Research Communications*, *45*(6), 1488–1496.
- Tong, J.-J., Minogue, P. J., Guo, W., Chen, T.-L., Beyer, E. C., Berthoud, V. M., & Ebihara, L. (2011). Different consequences of cataract-associated mutations at adjacent positions in the first extracellular boundary of connexin50. *American Journal of Physiology. Cell Physiology*, *300*(5), C1055–64.
- Tong, X., Aoyama, H., Sudhakar, S., Chen, H., Shilton, B. H., & Bai, D. (2015). The first extracellular domain plays an important role in unitary channel conductance of Cx50 gap junction channels. *PLoS ONE*, *10*(12), 1–20.
- Tong, X., Aoyama, H., Tsukihara, T., & Bai, D. (2014). Charge at the 46th residue of connexin 50 is crucial for the gap-junctional unitary conductance and transjunctional voltage-dependent gating. *The Journal of Physiology*, *592*(23), 5187–5202.
- Umeda, I. O., Kashiwa, Y., Nakata, H., & Nishigori, H. (2003). Predominant phosphatase in the ocular lens regulated by physiological concentrations of magnesium and calcium. *Life Sciences*, *73*(9), 1161–1173.
- Vanita, V., Singh, J. R., Singh, D., Varon, R., & Sperling, K. (2008). A novel mutation in GJA8 associated with jellyfish-like cataract in a family of Indian origin. *Molecular Vision*, *14*(August 2007), 323–326.
- Veenstra, R. D., Wang, H. Z., Beyer, E. C., Ramanan, S. V., & Brink, P. R. (1994). Connexin37 forms high conductance gap junction channels with subconductance state activity and selective dye and ionic permeabilities. *Biophysical Journal*, *66*(June), 1915–1928.

- Verselis, V. K., Ginter, C. S., & Bargiello, T. a. (1994). Opposite voltage gating polarities of two closely related connexins. *Nature*, *368*, 348–351.
- Wang, L., Luo, Y., Wen, W., Zhang, S., & Lu, Y. (2011). Another evidence for a D47N mutation in GJA8 associated with autosomal dominant congenital cataract. *Molecular Vision*, *17*(May), 2380–2385.
- Weber, P. a, Chang, H. C., Spaeth, K. E., Nitsche, J. M., & Nicholson, B. J. (2004). The permeability of gap junction channels to probes of different size is dependent on connexin composition and permeant-pore affinities. *Biophys J*, *87*(2), 958–973.
- White, T. W., Bruzzone, R., Goodenough, D. a, & Paul, D. L. (1992). Mouse Cx50, a functional member of the connexin family of gap junction proteins, is the lens fiber protein MP70. *Molecular Biology of the Cell*, *3*(7), 711–20.
- White, T. W., Bruzzone, R., Wolfram, S., Paul, D. L., & Goodenough, D. a. (1994). Selective interactions among the multiple connexin proteins expressed in the vertebrate lens: The second extracellular domain is a determinant of compatibility between connexins. *Journal of Cell Biology*, *125*(4), 879–892.
- White, T. W., Goodenough, D. A., & Paul, D. L. (1998). Targeted ablation of connexin50 in mice results in microphthalmia and zonular pulverulent cataracts. *Journal of Cell Biology*, *143*(3), 815–825.
- Wolosin, J. M., Schütte, M., & Chen, S. (1997). Connexin distribution in the rabbit and rat ciliary body: A case for heterotypic epithelial gap junctions. *Investigative Ophthalmology and Visual Science*, *38*(2), 341–348.
- Xin, L., Gong, X. Q., & Bai, D. (2010). The role of amino terminus of mouse Cx50 in determining transjunctional voltage-dependent gating and unitary conductance. *Biophysical Journal*, *99*(7), 2077–2086.
- Xin, L., Nakagawa, S., Tsukihara, T., & Bai, D. (2012). Aspartic Acid Residue D3 Critically Determines Cx50 Gap Junction Channel Transjunctional Voltage-Dependent Gating and Unitary Conductance. *Biophysj*, *102*(5), 1022–1031.

Yeager, M., Unger, V. M., & Falk, M. M. (1998). Synthesis, assembly and structure of gap junction intercellular channels. *Current Opinion in Structural Biology*, 8(4), 517–524.

Zhou, X. W., Pfahnl, a, Werner, R., Hudder, a, Llanes, a, Luebke, a, & Dahl, G. (1997). Identification of a pore lining segment in gap junction hemichannels. *Biophysical Journal*, 72(5), 1946–53.

Chapter 2 – Manuscript

2.1 Abstract

Gap junction (GJ) channels facilitate intracellular communication and consist of a dodecamer of connexins. GJs formed by different connexins display a wide range in unitary channel conductance (γ_j) and intracellular magnesium (Mg^{2+}) modulation; yet, underlying molecular determinants are not fully clear. The amino terminal (NT), first transmembrane and first extracellular domain (M1-E1) border of several connexins are proposed to line the pore and are implicated to play important roles in GJ properties. To test the roles of speculated pore-lining residues in Cx50 GJ channels, we generated a triple glutamate substitution at three putative pore-lining positions (G8, G46, and V53). The triple mutation and individual mutations G8E and G46E, but not V53E, drastically increased Cx50 GJ γ_j . Increasing intracellular Mg^{2+} from 0 mM to 3 mM reduced γ_j in Cx50 and mutant GJs. These results and our homology structural model indicate that these residues are likely pore-lining.

2.2 Introduction

Cellular communication is necessary to synchronize the many physiological activities occurring in multicellular organisms. Gap junction (GJ) intercellular channels enable direct cell-to-cell communication between neighboring cells by facilitating the exchange of ions, small metabolites, and other biological molecules under 1kDa in size (Dunlap et al., 1987; Goldberg et al., 1999; Lawrence et al., 1978; Simpson et al., 1977). GJs are ubiquitously expressed throughout the body and are essential for maintaining metabolic and electrical homeostasis (Bennett, 1997; Gong et al., 1997; Kanter, Saffitz, & Beyer, 1992). Each GJ channel consists of two hemichannels docked together at the extracellular space between plasma membranes of two adjacent cells (Bruzzone et al., 1996). GJs are classified as homotypic, if composed of two identical homomeric hemichannels, or heterotypic, if docked hemichannels are dissimilar. Hemichannels are oligomers of six connexins and can be further classified as homomeric or heteromeric depending on connexin composition. There are 21 identified connexin isoforms in the human genome and 20 in the mouse, each of which have distinct patterns of tissue distribution (Söhl & Willecke, 2004). All connexins are assumed to have the same structural topology consisting of four transmembrane domains (M1 – M4), two extracellular loops (E1 and E2), a cytoplasmic loop (CL), and an amino and carboxyl termini (NT and CT, respectively) found in the cytosol (Kumar & Gilula, 1992). Depending on component connexin isoform, GJs can display a wide variety of biophysical properties including unitary channel conductance (γ_j), transjunctional voltage-dependent deactivation (known as V_j -gating), and modulations by intracellular divalent cations, such as calcium (Ca^{2+})

and magnesium (Mg^{2+}). Molecular mechanisms behind these channel properties are still under investigation.

Homotypic GJ single channel conductance (γ_j), defined as the rate of ion permeation through one single channel, ranges between 9 pS (mCx30.2 GJ) to 300 pS (Cx37 GJ) (Kreuzberg et al., 2005; Veenstra et al., 1994). Structural determinants to this wide range in γ_j are not fully understood; however, it has been hypothesized that pore properties are probable contributors. One hypothesis suggests that pore diameter restricts ion flow, thereby limiting γ_j (Hille, 2001). Contradictorily, studies on GJ dye transfer using different sized dyes have consistently demonstrated that Cx37 GJ was the least permeable to large dyes despite having the largest γ_j (Gong & Nicholson, 2001; Veenstra et al., 1994; Weber, Chang, Spaeth, Nitsche, & Nicholson, 2004). Several experimental evidence suggests that electrostatic properties of pore-lining domains are an important determinant to unitary channel conductance (Kronengold, 2003; Maeda et al., 2009; Tong et al., 2015, 2014; Xin et al., 2012). Currently, Cx26 is the only connexin to have a high-resolution crystal structure. This crystal structure of Cx26 GJ indicates NT, M1, and E1 are pore-lining domains (Maeda et al., 2009). These domains of Cx50 and Cx37 showed high sequence identity with those of Cx26 (71% and 68%, respectively), suggesting that these domains are likely to have a similar structure in lining the pore as that of Cx26 GJ. Exchanging these specific domains between connexins of distinct GJ channel properties confirm that these regions influence γ_j and V_j -gating (Hu et al., 2006; Tong et al., 2015; Xin et al., 2010). Point mutations in the pore-lining residues of Cx50 NT and E1 highlight the importance of electrostatic charge at locations facing the channel lumen (Tong et al., 2014; Xin et al., 2012). For instance, introducing negatively charged

glutamic acid (E) at the 46th position in Cx50 (G46E) increases γ_j to 293 pS, almost reaching the highest γ_j of all known homotypic GJs of 300 pS attributed to Cx37 GJs (Tong et al., 2014; Veenstra et al., 1994).

This observation prompted us to look further into the molecular differences between Cx50 and Cx37 that could play a role in determining γ_j . Sequence alignment of Cx50 and Cx37 revealed two key residue differences at the 8th and 53rd positions in the NT and E1 domains, respectively. At these positions, negatively charged glutamic acid residues (E8 and E53) were found in Cx37, whereas much smaller non-polarized residues (G8 and V53) were in Cx50 (Figure 2-1). As both Cx50 and Cx37 GJs display cation-preference (Maeda et al., 2009; Srinivas, Costa, et al., 1999), we propose that these negatively charged residues in Cx37 GJ channels may facilitate the rate of cation permeation, consequently possessing a larger γ_j . To test the effects of negatively charged residues on homotypic GJ γ_j , we generated a triple mutation G8EG46EV53E in Cx50. Dual patch clamp on Cx50 G8EG46EV53E GJ channels revealed a significantly increased γ_j compared to wildtype Cx50 GJs. Furthermore, changes in intracellular Mg^{2+} concentrations ($[Mg^{2+}]_i$) have been shown to alter GJ properties (Noma & Tsuboi, 1987; Oliveira-Castro & Loewenstein, 1971a; Palacios-Prado et al., 2013, 2014). It is not clear how this $[Mg^{2+}]_i$ -dependent modulation affects individual homotypic GJ channels in Cx50 and the Cx50 triple mutant. Here we demonstrate that the γ_j s of Cx50 and G8EG46EV53E GJ channels were reduced with increasing $[Mg^{2+}]_i$. Our data are consistent with a model where the electrostatic properties of Cx50 pore lining residues are important determinants for Cx50 GJ γ_j and sensitivity to $[Mg^{2+}]_i$.

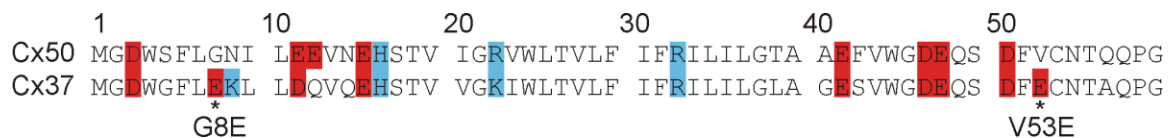


Figure 2-1. Sequence alignment of the amino terminal, first transmembrane, and early portion of the first extracellular domain of Cx50 and Cx37.

Cx50 residues 1 – 22, 22 – 46, and 47 – 59 represent the NT, M1, and early portion of E1, respectively. Two residues (asterisks) indicate a negative charge in Cx37 aligned with a neutral charge in Cx50. Mutations generated in Cx50 are named according to their residue number in Cx50. Positively charged residues (blue) and negatively charged residues (red) are highlighted.

2.3 Materials and Methods

2.3.1 Construction of Cx50 mutants

Untagged expression vector of mouse Cx50 cDNA was generated by polymerase chain reaction and inserted into pIRES2-EGFP vector (Tong et al., 2014). The untagged Cx50 construct was used as a template to generate single point mutations, G8E, G46E, and V53E using the QuikChange site-directed mutagenesis kit (Stratagene, La Jolla, CA). The primer for G8E and V53E are as follows:

Cx50G8E Forward: 5' TGG AGT TTC CTG GAA AAC ATC TTG GAA 3'

Reverse: 5' TTC CAA GAT GTT TTC CAG GAA ACT CCA 3'

Cx50V53E Forward: 5' G CAA TCT GAT TTT GAA TGC AAC ACC CAG 3'

Reverse: 5' CTG GGT GTT GCA TTC AAA ATC AGA TTG C 3'

Primers for G46E have been described previously (Tong et al., 2014). The Cx50 triple mutant, G8EG46EV53E (or G8G46V53), was generated using sequential mutagenesis.

2.3.2 Cell culture and transient transfection

GJ-deficient mouse neuroblastoma (N2A) cells were obtained from the American Type Culture Collection (ATCC, Manassas, VA) and cultured in Dulbecco's Modified Eagle Medium (DMEM) (Life Technologies Corporation, Grand Island, NY, USA) containing 10% fetal bovine serum (FBS), 1% penicillin, 1% streptomycin, and 1% GlutaMax. Cells were transferred onto 35 mm dishes at 50% confluency to be cultured overnight. Transfection was performed on the following day with 1 µg of Cx50 or mutant vector and 2 µL of X-tremeGENE HP DNA transfection reagent (Roche Diagnostics GmbH,

Indianapolis, IN) for 5 hours. Transfection reagent was then replaced with DMEM to culture overnight. On recording day, N2A cells were replated onto 1 cm glass coverslips and incubated for another 1-2 hours prior to electrophysiological recordings; with a few exceptions, a much longer incubation time was needed to obtain a higher experimental yield of stable single channel and macroscopic recordings.

2.3.3 Homology structure modeling

Sequence alignment of mouse Cx50 and human Cx26 demonstrated an overall sequence identity of 49% (Tong et al., 2014; Tong et al., 2015). The crystal structure of Cx26 (2ZW3) was used as a template to construct a structural model for Cx50 (Maeda et al., 2009). Abnormal inter-atomic contact was adjusted manually in COOT and then revised by crystallography and NMR system energy refinement. Manual inspection of the model was done to assess structural validity (Tong et al., 2014). To calculate electrostatic potentials of all atoms in Cx50 and mutations, adaptive Poisson-Boltzmann solver (Baker, Sept, Joseph, Holst, & McCammon, 2001) and PDB2PQR server (http://nbcrc-222.ucsd.edu/pdb2pqr_1.8/) were used set to parameters described previously (Maeda et al., 2009; Tong et al., 2014). PyMOL was used to estimate the GJ pore diameters and construct structural presentations of Cx50 as described earlier (Tong et al., 2014).

2.3.4 Electrophysiological recordings

GJ channel properties of cell pairs expressing either Cx50 or one of its mutants was measured using dual whole-cell patch clamp technique as described previously (Bai, del Corso, Srinivas, & Spray, 2006). A coverslip containing transfected N2A cells was transferred to a recording chamber placed on an upright microscope (BX51WI, Olympus). N2A cells were bathed in an extracellular solution (ECS) at room

temperature containing (in mM): 135 NaCl, 2 CsCl, 2 CaCl₂, 1 MgCl₂, 10 HEPES, 5 KCl, 5 D-glucose, 2 Na pyruvate, and 1 BaCl₂ at pH 7.4, and an osmolarity of 320 mOsm. Isolated cell pairs with green fluorescence (GFP positive), indicating a successful transfection, were selected for dual patch clamp recording. Glass patch micropipettes (resistance 2-4 MΩ) were filled with intracellular fluid solution (ICS) containing (in mM): 130 CsCl, 10 EGTA, 0.5 CaCl₂, and 10 HEPES at pH 7.2, and 295 mOsm. Sensitivity of GJ channels to different [Mg²⁺]_i was tested by adding different amounts of MgCl₂ into the Mg²⁺-free ICS to have 0.1, 1, or 3 mM [MgCl₂]_i.

Whole-cell voltage clamp was performed on each cell in the recorded cell pair. One cell of the pair was clamped at 0 mV while the apposed cell was administered a series of voltage steps ranging from ± 20 mV to ± 100 mV in 20 mV increments for a duration of 7 s per voltage step (Tong et al., 2014; Xin et al., 2010). Recorded gap junction currents were amplified with MultiClamp 700A (Axon Instruments) and digitized using an ADDA converter at a sampling frequency of 10 kHz (Digidata 1322A, Molecular Devices, Sunnyvale, CA).

All unitary channel currents (i_j) and macroscopic junctional currents (I_j) were measured using pClamp9.2 software. All recordings were digitized at 10 kHz and low pass filtered at 200 Hz for analysis.

Selection criteria for single channel analysis were cell pairs expressing one or two operational channels (Tong et al., 2014; Xin et al., 2010). Representative i_j recordings chosen for illustrations underwent digital low-pass filter (200 Hz) with Clampfit (pClamp9, Molecular Devices, Sunnyvale, CA). All-points current amplitude histograms

fitted with two Gaussian functions measured the mean and variance of baseline and open channel current amplitude to determine i_j (Xin et al., 2010). The i_{js} of different cell pairs were averaged under the same transjunctional voltage (V_j), regardless of V_j polarity, to generate an $i_j - V_j$ plot. Linear regression of $i_j - V_j$ plot with 3 to 4 different V_{js} was used to calculate slope unitary conductance (γ_j).

For homotypic Cx50 GJs, V_j induced a macroscopic transjunctional current (I_j). The I_{js} were relatively steady throughout the V_j pulse with $V_j = \pm 20$ mV or lower. Larger I_{js} were recorded with increased V_{js} (± 40 to ± 100 mV), but the I_j declined with time due to V_j -dependent inactivation to a steady state. Steady state I_{js} , found near the end of a V_j -pulse, were normalized to the peak I_{js} , found at the beginning of the pulse to obtain a normalized steady-state conductance ($G_{j,ss}$). $G_{j,ss}$ was plotted at corresponding positive and negative V_{js} to obtain $G_{j,ss}-V_j$ plot, which was fitted with a two-state Boltzmann equation:

$$G_{j,ss} = \frac{G_{\max} - G_{\min}}{1 + e^{A(V_j - V_0)}} + G_{\min}$$

V_0 is the voltage at which conductance is reduced by half $[(G_{\max} - G_{\min})/2]$, G_{\max} is the maximum normalized conductance, G_{\min} is the normalized voltage-insensitive residual conductance, and A defines the slope of the curve, reflecting V_j -gating sensitivity (Harris, Spray, & Bennett, 1981). To avoid voltage clamp errors only cell pairs with a G_j lower than 5 nS were selected for V_j -gating analysis (Bai & Cameron, 2017; Wilders & Jongsma, 1992).

2.3.5 Data analysis

All data are expressed as mean \pm SEM. Student's unpaired t -test and one-way ANOVA followed by a Bonferroni post-hoc test was used to compare slope γ_{js} obtained by linear regression of i_j - V_j plots across several groups of data. Other comparisons and statistical tests used are as indicated.

2.4 Results

2.4.1 Single channel conductance (γ_j) of Cx50 G8EG46EV53E GJ

Representative i_j s of triple mutation G8EG46EV53E (or G8G46V53) and Cx50 GJ in response to V_j pulses of 40, 60, and 80 mV are illustrated in Fig. 2-2A. All-point histograms measured i_j amplitude at the main open state. All-point histograms were constructed for a short segment of i_j s as indicated under each V_j to show i_j amplitudes of G8G46V53 and wildtype Cx50 (Fig. 2-2B). i_j s of different G8G46V53 cell pairs were averaged under the same V_j and were plotted with V_j to obtain $i_j - V_j$ plot (Fig. 2-2C). Linear regression of $i_j - V_j$ plot was used to determine the slope single channel conductance ($\gamma_j = 329 \pm 10$ pS, $n = 5$, $p < 0.001$), which revealed to be significantly larger than the slope γ_j of Cx50 (219 ± 5 pS, $n = 7$, Fig. 2-2C right panel). i_j s of G8G46V53 GJ showed more than one subconductance state (also known as substate or residual state, see Fig. 2-2A). The conductance levels of different subconductance state varied a lot from different cell pairs and from the same pair at different V_j s; therefore, we did not perform detailed conductance analysis of different substates.

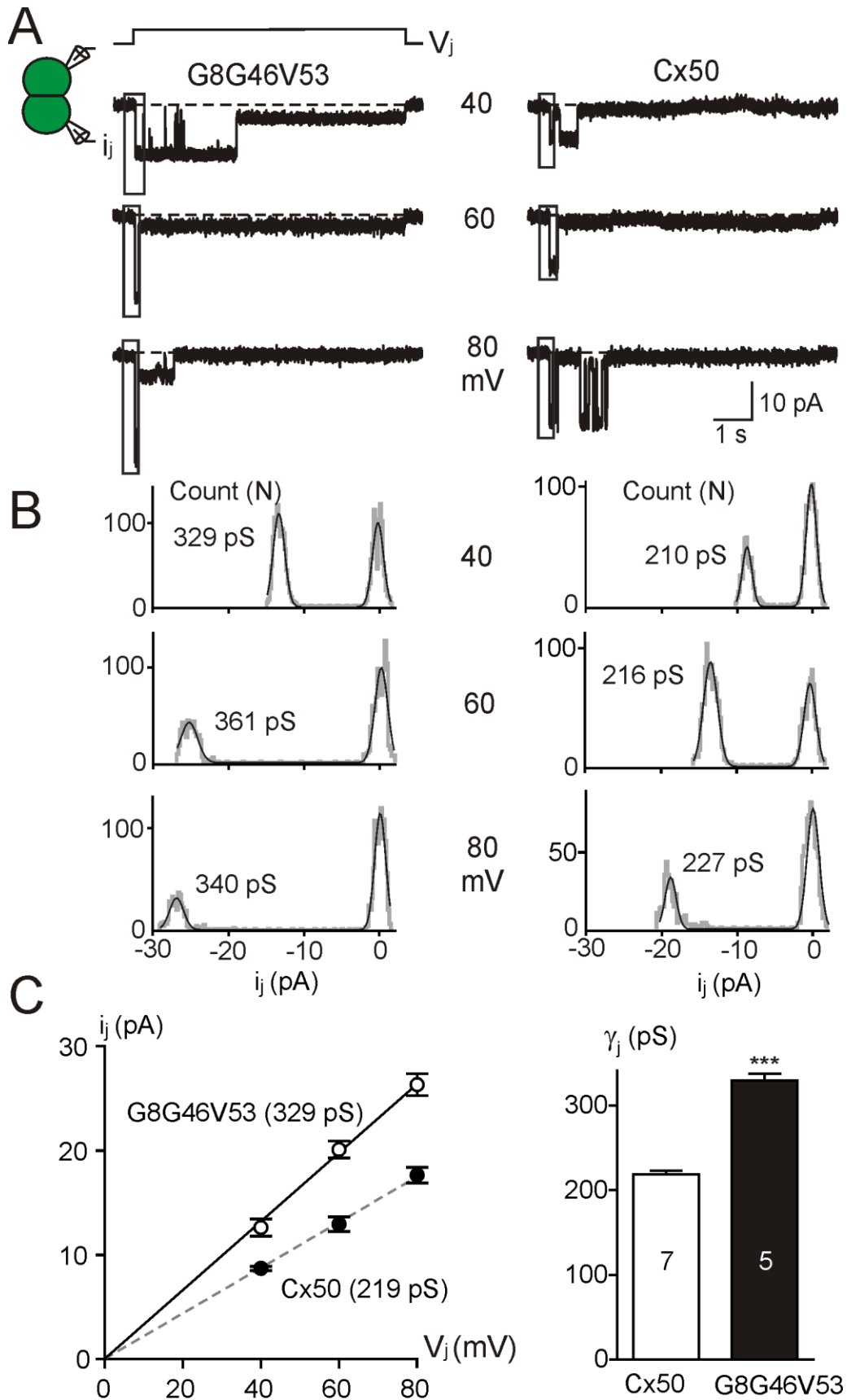


Figure 2-2. The γ_j of Cx50 G8EG46EV53E GJ is drastically higher than that of Cx50.

A. Representative i_j s for Cx50 G8EG46EV53E (G8G46V53) and Cx50 are illustrated in response to indicated V_j . Boxed regions of the currents used for all-point histogram. **B.** All-point histograms of i_j s are shown under different V_j s as indicated. Main open state and baseline were fit with Gaussian functions and the calculated conductances are shown on each of the histograms. **C.** Linear regressions of $i_j - V_j$ plots (shown on the left panel) of Cx50 (grey dashed line, filled circles) and G8G46V53 (black line, open circles) were used to obtain average slope γ_j . Number of cell pairs included in average γ_j analysis is indicated inside the bar graph (right panel). A student's unpaired t-test revealed the γ_j of G8G46V53 GJ is significantly higher than that of Cx50 (***) $p < 0.001$).

2.4.2 γ_j s of G8E, G46E, and V53E GJs

Having learned that the triple mutation increased the γ_j of Cx50 GJ channels, the extent of each residue's contribution to this increase was investigated. Representative i_j s of G8E, G46E, and V53E GJs in response to V_j pulses of 40, 60, and 80 mV are illustrated in Fig. 2-3A. The averaged i_j s were plotted against corresponding V_j s for each single mutation to obtain $i_j - V_j$ plot. Linear regression of $i_j - V_j$ plot was used to obtain each mutant slope γ_j and compared with that of Cx50 (Fig. 2-3B grey dashed line). The slope γ_j s of G8E (254 ± 2 pS, $n = 7$) and G46E (272 ± 9 pS, $n = 7$), but not V53E (230 ± 5 pS, $n = 4$), were significantly higher than that of Cx50 (Fig. 2-3C, $p < 0.001$ for G8E and G46E).

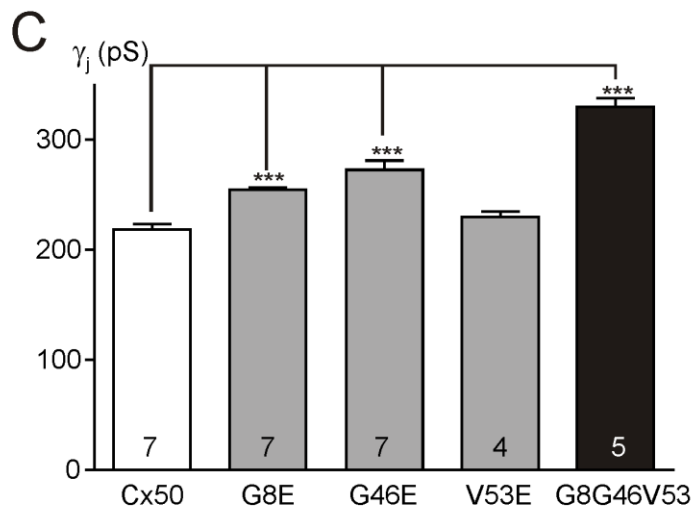
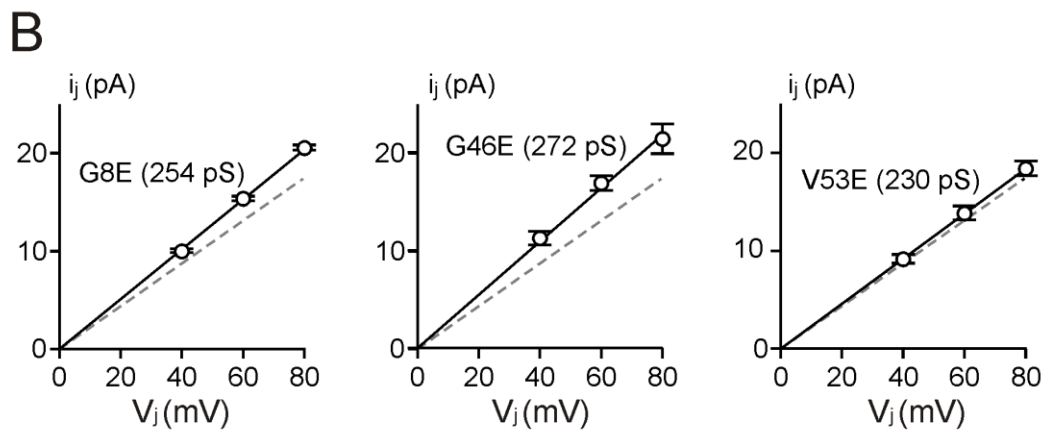
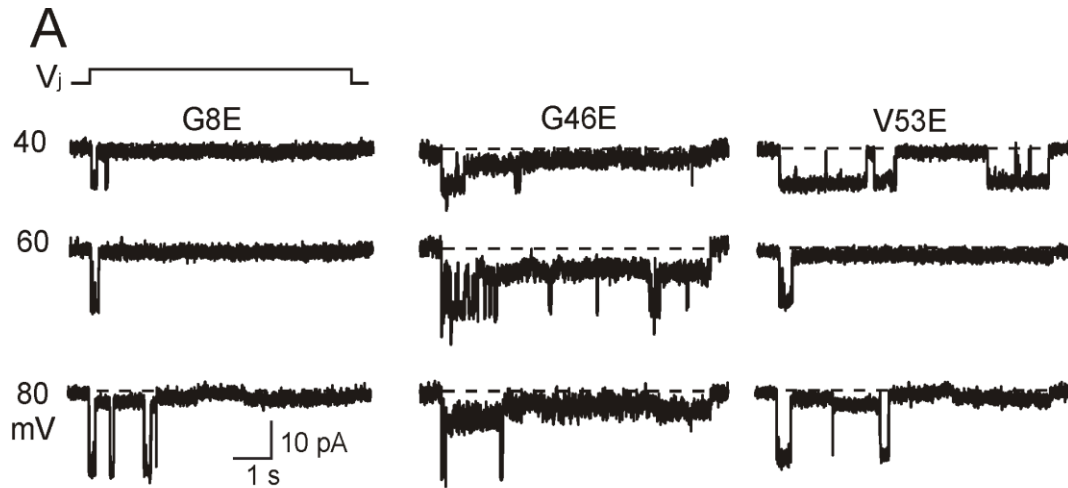


Figure 2-3. γ_j of G8E and G46E, but not V53E, GJ channels were higher than that of Cx50 GJ.

A. Representative i_j for G8E, G46E, and V53E are illustrated in response to indicated V_{js} .

B. Linear regressions of $i_j - V_j$ plots for each single mutation (black line in each panel) were used to obtain slope γ_j . For comparison, Cx50 regression lines (dashed grey lines) obtained from Fig 2-2C were included.

C. The average slope γ_{js} of the GJs of G8G46V53 as well as three individual mutants are plotted as a bar graph. The statistical differences of each mutant in comparison to γ_j Cx50 GJ channel are shown (***) $p < 0.001$).

2.4.3 V_j -gating properties of GJs formed by G8G46V53 and individual mutants

Substantial change in γ_j may alter the V_j distribution along the elongated GJ pore, which could have an effect on the sensor or gate responsible for V_j -gating. To test this, we investigated V_j -gating properties of these mutant GJs. Representative macroscopic transjunctional currents (I_j) from cell pairs expressing Cx50, G8G46V53, G8E, G46E, and V53E GJ channels in response to corresponding V_j s are shown in Fig. 2-4. At higher V_j s (40 – 100 mV), I_j s from all constructs showed a mirror symmetrical V_j -dependent deactivation as those observed from Cx50 GJ (Fig. 2-4). Normalized steady-state junctional conductance ($G_{j,ss}$) was plotted against corresponding V_j s and the obtained plot was fitted with a two-state Boltzmann fitting curve for each polarity of V_j . Each mutant was plotted with wildtype Cx50 GJ for comparison (dashed grey lines in Fig. 2-4). Statistical tests revealed minor alterations when comparing each of the mutant's parameters to those of Cx50 GJs (Table 2-1).

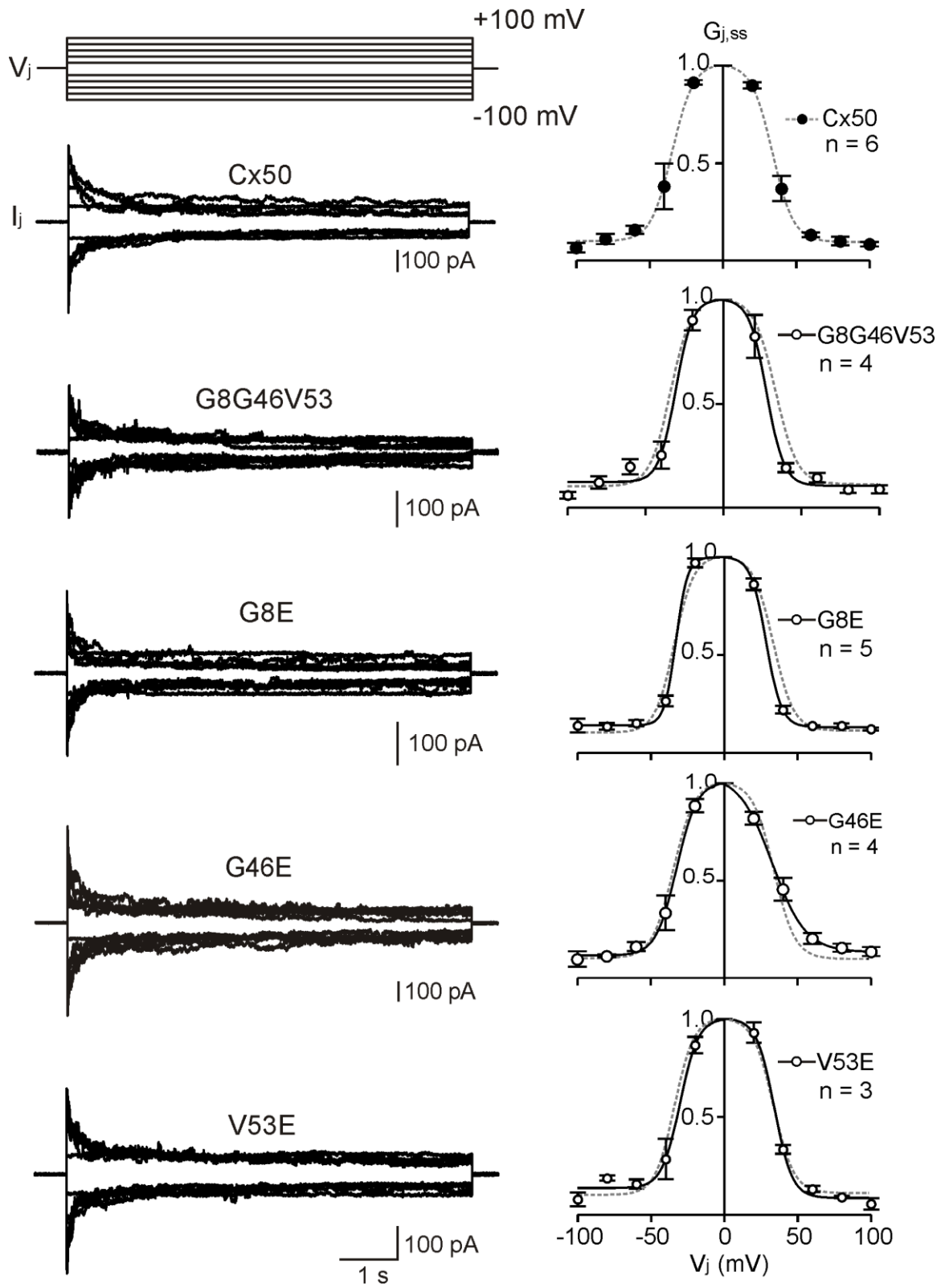


Figure 2-4. The GJs of Cx50 mutants showed little change in V_j -gating.

Representative superimposed I_j for Cx50, G8G46V53, G8E, G46E, and V53E GJ channels in response to the tested V_j s are shown. Normalized steady state to peak junctional conductance ($G_{j,ss}$) are plotted as a function of V_j and fitted with two-state Boltzmann equation on each V_j polarity. Boltzmann fitting curves of each mutant (solid black lines) are plotted with Cx50 (dashed grey lines) for comparison.

Table 2-1. Boltzmann fitting parameters for Cx50 and mutants showed minor differences in V_j -gating parameters.

	V_j polarity	G_{\min}	V_0 (mV)	A
Cx50	+	0.10 ± 0.02	34.0 ± 1.4	0.14 ± 0.02
	-	0.10 ± 0.03	34.4 ± 2.4	0.14 ± 0.04
G8G46V53	+	0.13 ± 0.03	28.0 ± 2.5	0.17 ± 0.04
	-	0.09 ± 0.03	30.3 ± 2.1	0.15 ± 0.03
G8E	+	0.13 ± 0.01	$28.6 \pm 0.8 *$	0.19 ± 0.01
	-	0.14 ± 0.01	33.0 ± 1.6	0.26 ± 0.05
G46E	+	0.14 ± 0.02	32.9 ± 2.2	0.09 ± 0.02
	-	0.12 ± 0.03	32.4 ± 2.1	0.14 ± 0.03
V53E	+	0.09 ± 0.02	34.1 ± 1.3	0.17 ± 0.03
	-	0.14 ± 0.03	30.2 ± 2.5	0.16 ± 0.04

Data are presented as means \pm SEM and V_0 are absolute values. Student's unpaired t -test was used to compare each mutant's parameter to Cx50's parameter of the same V_j polarity. Student's unpaired t -test was used to compare Boltzmann fitting parameters (G_{\min} , V_0 , and A) of each mutant to Cx50 with the same V_j polarity. Statistical differences are shown (* $p < 0.05$).

2.4.4 $[\text{Mg}^{2+}]_i$ modulated the γ_{js} of G8G46V53 and Cx50

To investigate G8G46V53 and Cx50 GJ channel's sensitivity to $[\text{Mg}^{2+}]_i$, three intracellular concentrations of Mg^{2+} (0.1, 1, or 3 mM) were tested in independent cell pairs. No added Mg^{2+} ICS ($[\text{Mg}^{2+}]_i = 0$ mM) used in the previous experiments was used as a baseline control. Representative single channel current recordings of G8G46V53 and Cx50 GJs at different $[\text{Mg}^{2+}]_i$ are illustrated in Fig. 2-5A. The same procedure as described in Fig. 2-2 was used to obtain average slope γ_{js} . The γ_{js} were plotted as bar graphs to compare the dose-dependent modulation by $[\text{Mg}^{2+}]_i$ for G8G46V53 and Cx50 GJs (Fig. 2-5B). With increasing $[\text{Mg}^{2+}]_i$, the γ_{js} decreased significantly for both GJs. The γ_{js} of G8G46V53 GJ showed a larger relative reduction at each dose of $[\text{Mg}^{2+}]_i$ (21%, 31%, and 39% reduction for 0.1, 1, and 3 mM, respectively), while the reduction in the γ_{js} of Cx50 GJ was moderate (5%, 12%, and 20%, respectively, see Fig. 2-5B).

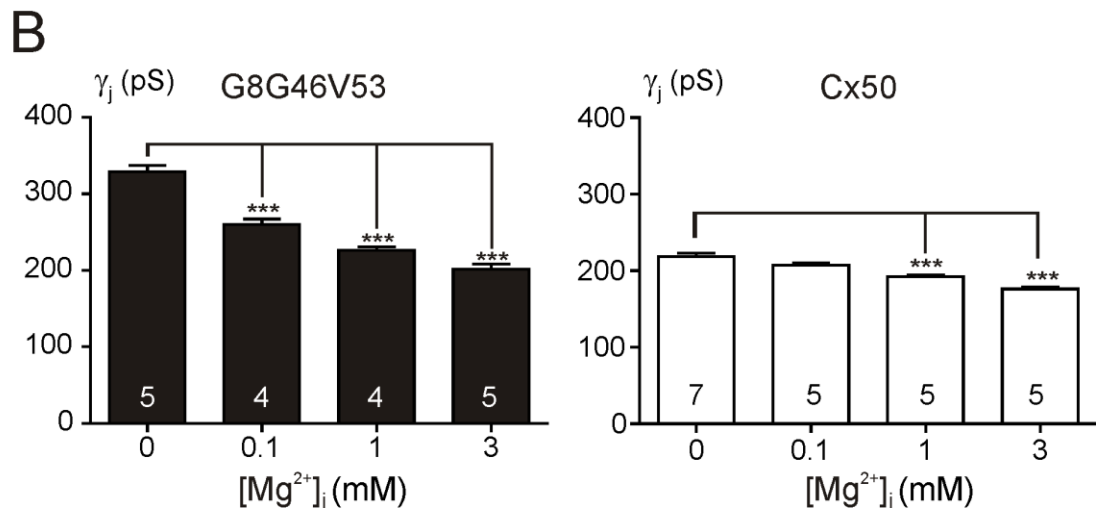
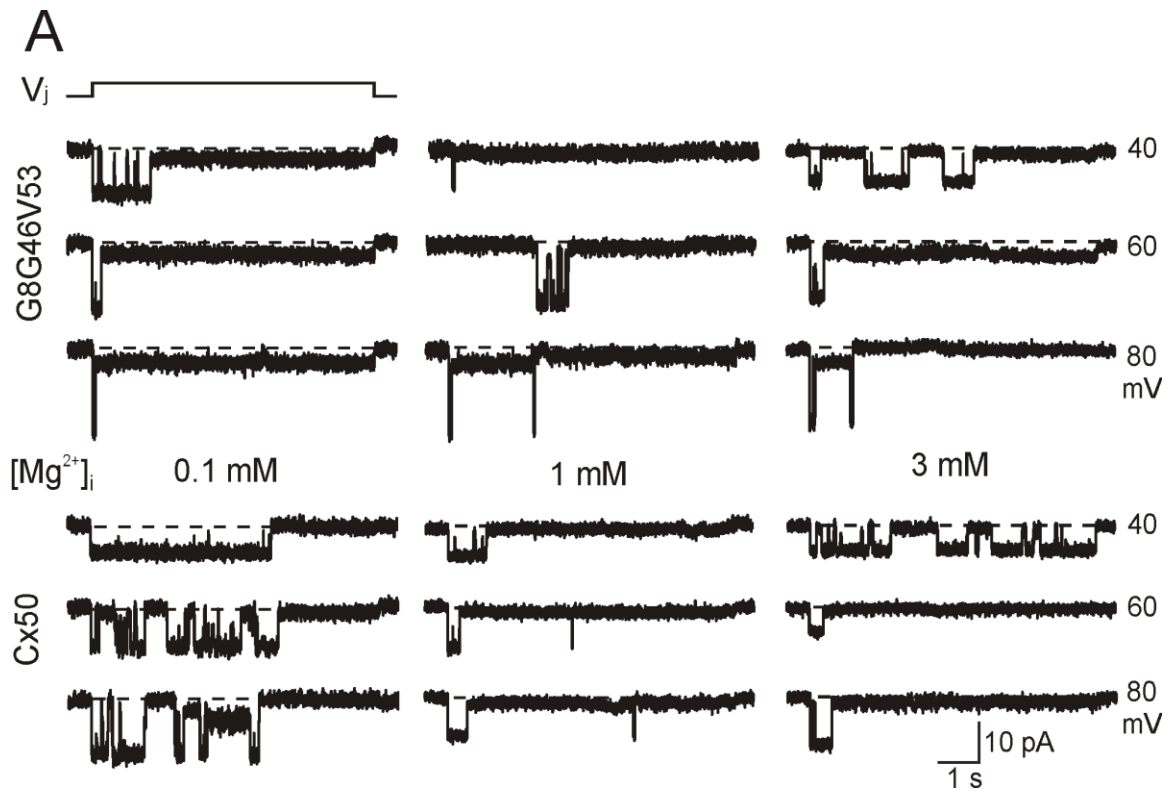


Figure 2-5. G8G46V53 GJ channels shows greater decrease in γ_j with increasing $[\text{Mg}^{2+}]_i$ than Cx50 GJ.

A. Representative i_j for G8G46V53 and Cx50 at 0.1, 1, and 3 mM $[\text{Mg}^{2+}]_i$ are illustrated in response to indicated V_j s. **B.** Average slope γ_j s of G8G46V53 GJ channels (left panel) and Cx50 GJ channels (right panel) at all tested $[\text{Mg}^{2+}]_i$ are shown. The number of cell pairs (numbers on each bar) and statistical differences of the slope γ_j are indicated (***) $p < 0.001$).

2.4.5 $[Mg^{2+}]_i$ modulate γ_{js} of G8E, G46E, and V53E GJs

To examine which residue in the triple mutation was the most sensitive to elevated $[Mg^{2+}]_i$, 3 mM Mg^{2+} - ICS was used to study the GJs of single mutations, G8E, G46E, or V53E. Representative i_{js} in response to corresponding V_{js} are shown in Fig. 2-6A. The averaged i_{js} were plotted against corresponding V_{js} for each single mutation at 3 mM Mg^{2+} - ICS to obtain $i_j - V_j$ plot. Linear regression of $i_j - V_j$ plot was used to obtain each mutant slope γ_j at 3 mM Mg^{2+} - ICS compared with that of their corresponding slopes at 0 mM Mg^{2+} -ICS (Fig. 2-3B). The average γ_{js} of G8E, G46E, and V53E GJs were significantly reduced by 23%, 31%, and 21% respectively (all $p < 0.001$, Fig. 2-6B,C). A summary bar graph of average γ_{js} in 0 mM and 3 mM Mg^{2+} - ICS for each mutant GJs is shown in Fig. 2-6C.

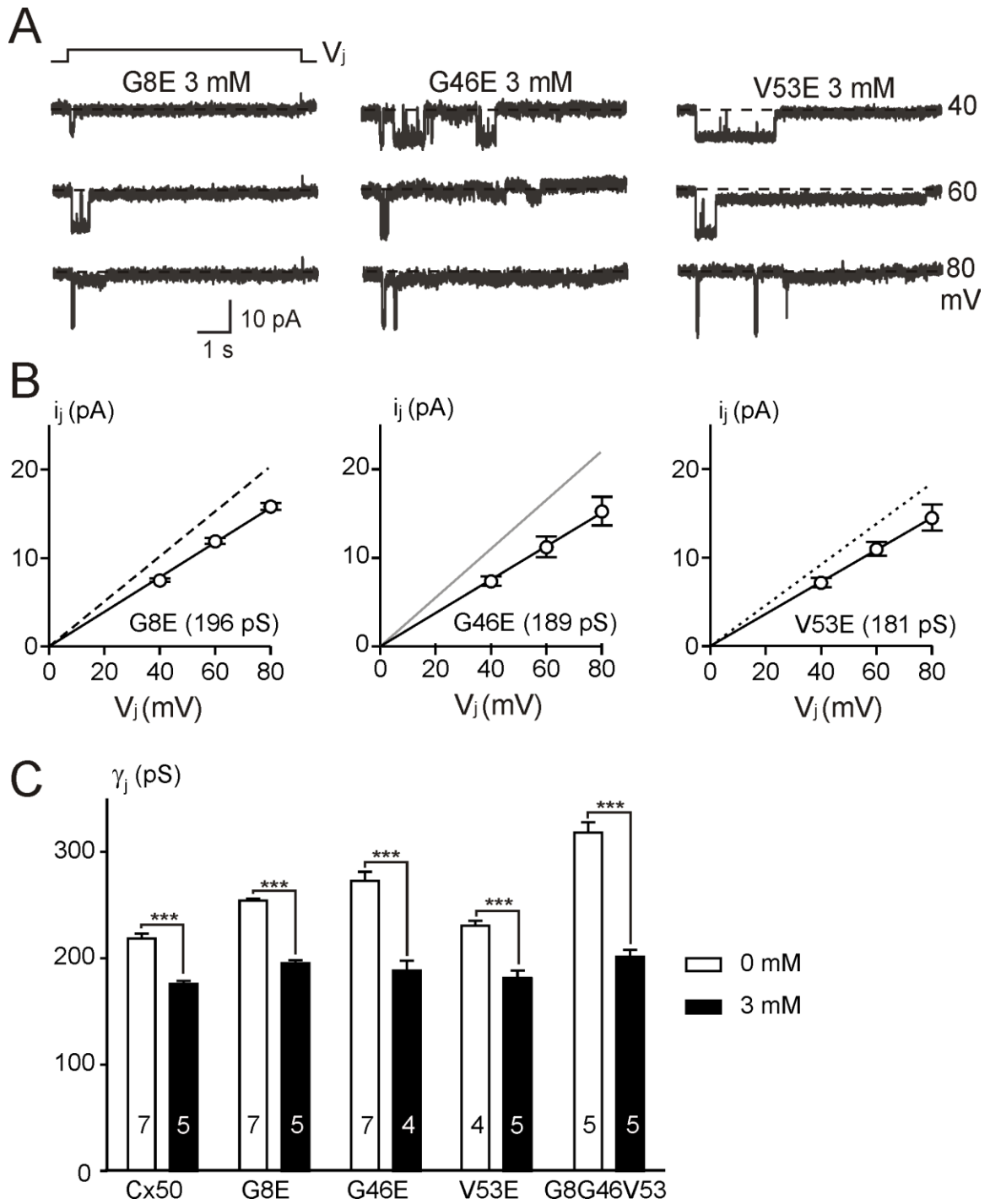


Figure 2-6. The γ_j s of individual mutation GJs reduced in 3 mM $[\text{Mg}^{2+}]_i$.

A. Representative i_j for G8E, G46E, and V53E GJs at 3 mM $[\text{Mg}^{2+}]_i$ are illustrated in response to indicated V_j s. **B.** Linear regressions of $i_j - V_j$ plots of G8E, G46E, and V53E GJs to obtain slope γ_j s in 3 mM $[\text{Mg}^{2+}]_i$. The linear regression lines of the GJs in 0 mM $[\text{Mg}^{2+}]_i$ are also shown for comparison, G8E (dashed black line), G46E (solid grey line), and V53E (dotted black line). **C.** Comparing the average γ_j of Cx50, the triple mutation, and single mutations GJ channels under 0 and 3 mM $[\text{Mg}^{2+}]_i$. Number of cell pairs are indicated in each bar. A two-way ANOVA followed by a Bonferroni post-hoc test was used to compare average slope γ_j of each mutant under 0 and 3 mM $[\text{Mg}^{2+}]_i$. Statistical differences are shown (***) $p < 0.001$).

2.4.6 V_j -gating properties of Cx50 and each mutant GJs under different $[Mg^{2+}]_i$

To determine whether $[Mg^{2+}]_i$ had an effect on V_j -gating properties of Cx50 GJ channels, we studied V_j -gating using pipette solution containing 0.1, 1, and 3 mM $[Mg^{2+}]_i$. Representative I_j s in response to V_j s at different $[Mg^{2+}]_i$ were recorded revealing a mirror symmetrical V_j -dependent deactivation (Fig. 2-7). $G_{j,ss}-V_j$ plots were constructed for Cx50 under 0.1, 1 and 3 mM $[Mg^{2+}]_i$ and the data were well fitted by Boltzmann equations with little difference from that obtained without added Mg^{2+} (Fig. 2-7 right panels). Individual Boltzmann parameters of the V_j -gating under each of these conditions showed minimal change comparing to those obtained from no added Mg^{2+} (Table 2-2).

Since increasing $[Mg^{2+}]_i$ had no dose-dependent effect on Cx50 GJ V_j -gating parameters, only 3 mM Mg^{2+} ICS was used to test the effect of intracellular Mg^{2+} on the Cx50 mutant GJs. Similar to those observed for Cx50 GJs, in the presence of 3 mM Mg^{2+} -ICS, V_j -gating of each of the Cx50 mutant GJs showed no major change compared to those observed without added $[Mg^{2+}]_i$ (Fig. 2-8). Furthermore, $G_{j,ss}-V_j$ plots and Boltzmann fitting curves in the presence of 3 mM $[Mg^{2+}]_i$ for each mutation showed no major differences from those obtained without added intracellular Mg^{2+} . Boltzmann fitting parameters (G_{min} , V_0 , and A) for each mutation at different $[Mg^{2+}]_i$ showed no significant differences (Table 2-3).

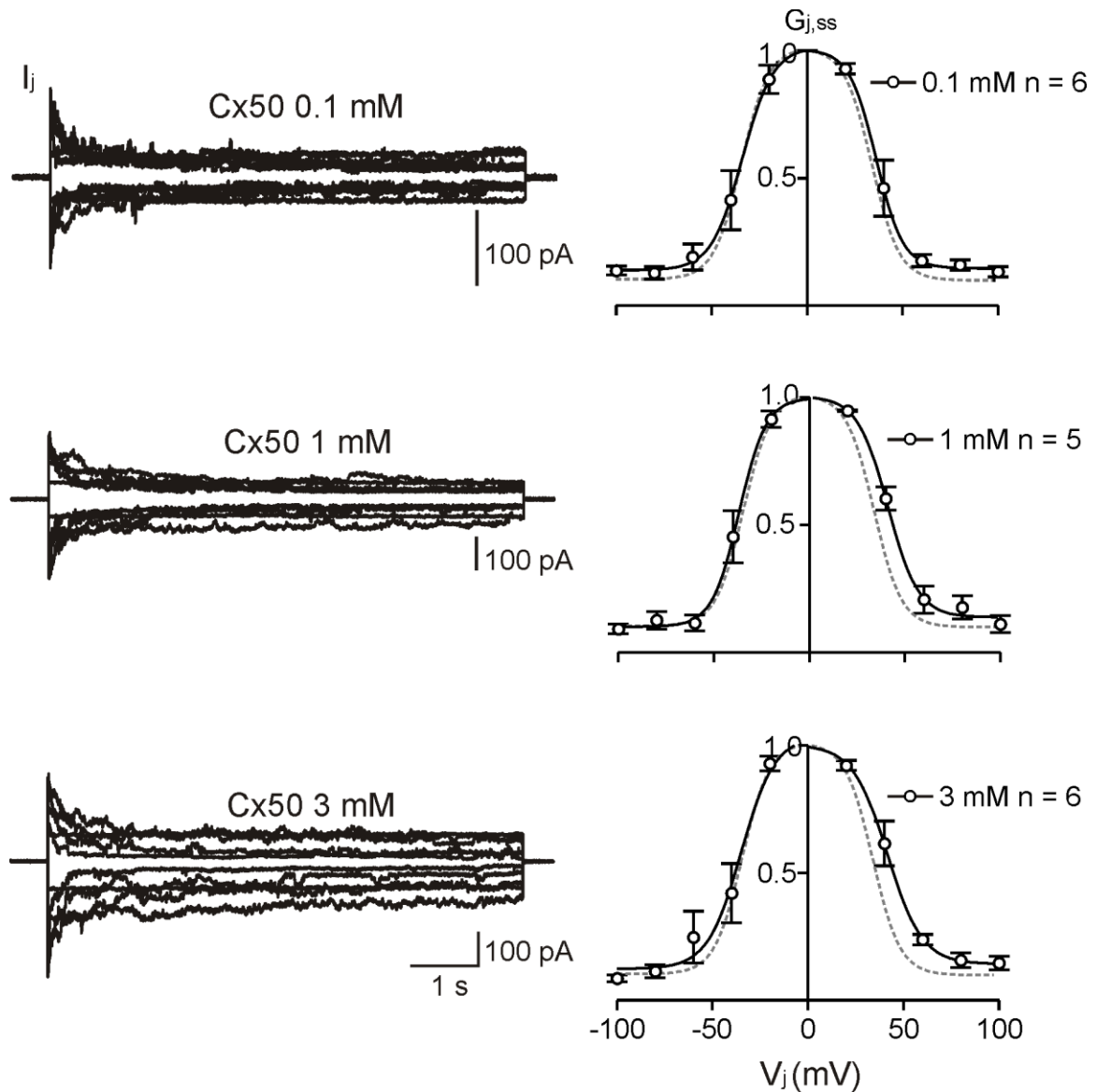


Figure 2-7. $[Mg^{2+}]_i$ showed little influence on the V_j -gating properties of Cx50 GJ.

Representative I_j s for Cx50 GJ channels at 0.1, 1, and 3 mM $[Mg^{2+}]_i$ in response to the same V_j protocol as shown in Fig. 2-4. Normalized steady state to peak junctional conductance ($G_{j,ss}$) are plotted as a function of V_j and fitted with two-state Boltzmann equation. Cx50 GJ at different $[Mg^{2+}]_i$ showed a similar Boltzmann fitting curves (solid black lines) as those obtained without intracellular Mg^{2+} (grey dashed lines).

Table 2-2. Boltzmann fitting parameters for the V_j -gating of Cx50 GJ at different $[Mg^{2+}]_i$.

$[Mg^{2+}]_i$	V_j polarity	G_{min}	V_0 (mV)	A
0 mM	+	0.10 ± 0.02	34.0 ± 1.4	0.14 ± 0.02
	-	0.10 ± 0.03	34.4 ± 2.4	0.14 ± 0.04
0.1 mM	+	0.15 ± 0.03	36.2 ± 2.2	0.14 ± 0.05
	-	0.14 ± 0.04	33.9 ± 3.0	0.12 ± 0.04
1 mM	+	0.14 ± 0.03	$41.2 \pm 1.6^{**}$	0.13 ± 0.03
	-	0.10 ± 0.03	36.8 ± 2.1	0.14 ± 0.04
3 mM	+	0.14 ± 0.3	$41.6 \pm 2.0^*$	0.11 ± 0.03
	-	0.12 ± 0.05	35.0 ± 3.5	0.11 ± 0.04

Data are presented as means \pm SEM and V_0 are absolute values. Student's unpaired t-test was used to compare each Boltzmann fitting parameter of Cx50 GJ at 0.1, 1, and 3 mM $[Mg^{2+}]_i$ to those control parameters obtained without any added Mg^{2+} . Only moderate statistical differences on the V_0 at $+V_j$, but not $-V_j$, of 1 and 3 mM Mg^{2+} -ICS were observed (* $p < 0.05$, ** $p < 0.01$).

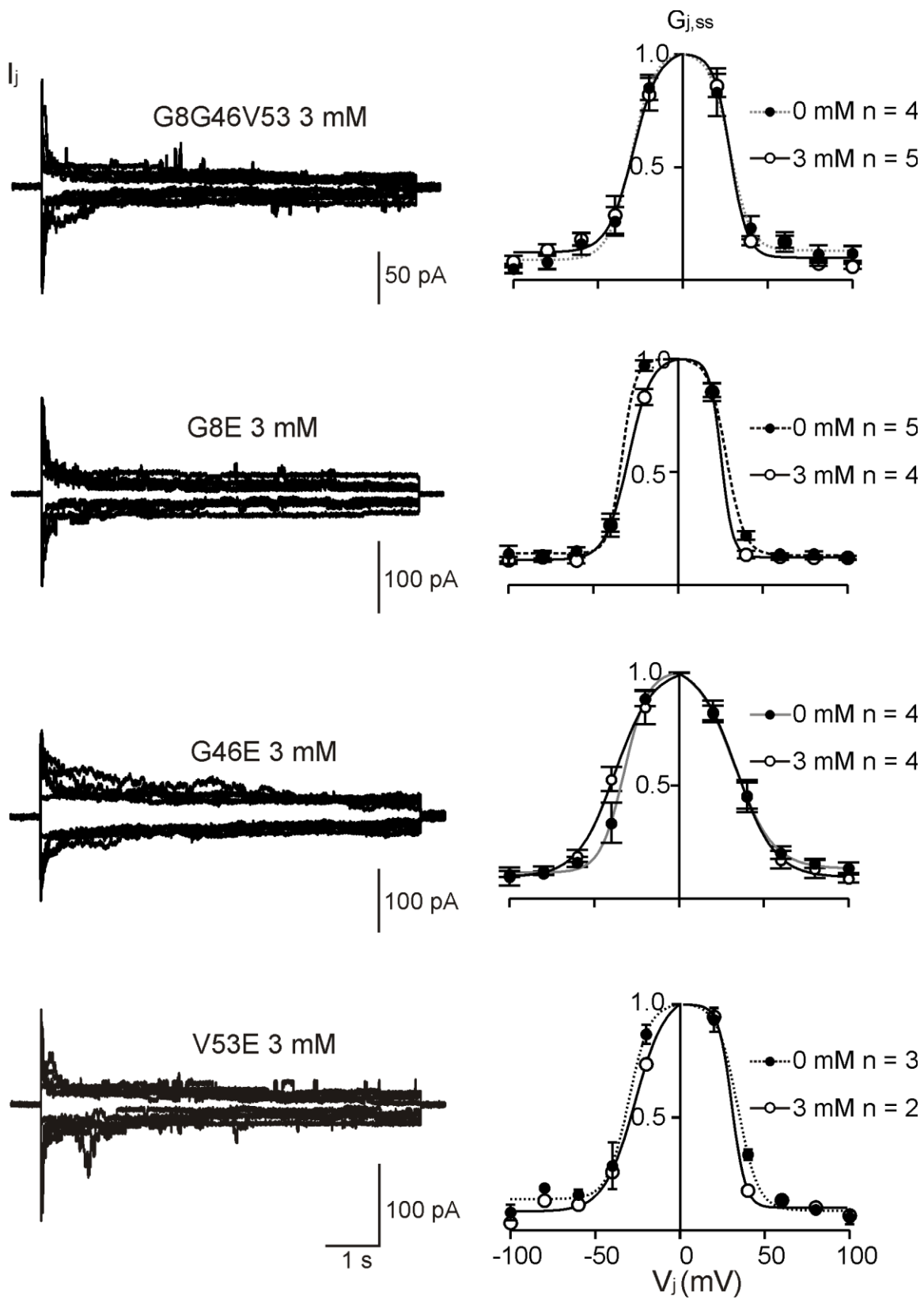


Figure 2-8. $[Mg^{2+}]_i$ showed little influence on the V_j -gating properties of Cx50 mutant GJs.

Representative I_j s for Cx50 mutant GJ channels at 3 mM $[Mg^{2+}]_i$ in response to the same V_j protocol as shown in Fig. 2-4. Normalized steady state to peak junctional conductance ($G_{j,ss}$) are plotted as a function of V_j and fitted with two-state Boltzmann equation for each mutant GJ. These mutant GJ under 3 mM $[Mg^{2+}]_i$ showed a similar Boltzmann fitting curves (solid black lines) as those obtained without intracellular Mg^{2+} (dotted lines).

Table 2-3. Boltzmann fitting parameters for the V_j -gating of Cx50 mutant GJ at different $[Mg^{2+}]_i$.

Cx50 mutant	$[Mg^{2+}]_i$ (mM)	V_j polarity	G_{min}	V_0 (mV)	A
G8G46V53	0	+	0.13 ± 0.03	28.1 ± 2.5	0.17 ± 0.04
	n = 4	-	0.09 ± 0.03	30.3 ± 2.1	0.15 ± 0.03
		3	+	0.09 ± 0.02	28.9 ± 1.6
	n = 4	-	0.12 ± 0.04	29.4 ± 3.1	0.13 ± 0.04
G8E	0	+	0.13 ± 0.01	28.6 ± 0.8	0.19 ± 0.01
	n = 5	-	0.14 ± 0.01	33.0 ± 1.6	0.26 ± 0.05
		3	+	0.12 ± 0.01	25.6 ± 2.0
	n = 3	-	0.12 ± 0.02	28.2 ± 1.4	0.16 ± 0.02
					**
G46E	0	+	0.14 ± 0.02	32.9 ± 2.2	0.09 ± 0.02
	n = 4	-	0.12 ± 0.03	32.4 ± 2.1	0.14 ± 0.03
		3	+	0.10 ± 0.07	34.1 ± 2.8
	n = 4	-	0.10 ± 0.03	37.8 ± 2.5	0.09 ± 0.02

V53E	0	+	0.09 ± 0.02	34.1 ± 1.3	0.17 ± 0.03
	n = 3	-	0.14 ± 0.03	30.2 ± 2.5	0.16 ± 0.04
	3	+	0.10	30.1	0.26
	n = 2	-	0.08	26.6	0.11

Data are presented as means \pm SEM and V_0 are absolute values. Student's unpaired *t*-test was used to compare each Boltzmann fitting parameter of the mutant GJ at 0 and 3 mM $[\text{Mg}^{2+}]_i$. Only moderate statistical differences on the *A* at $+V_j$, but not $-V_j$, of 3 mM $[\text{Mg}^{2+}]_i$ were observed for G8E mutant GJ (** $p < 0.01$).

2.4.7 Homology model and pore surface electrostatic potentials of Cx50, G8E, G46E, V53E, and G8G46V53

High sequence identity between Cx26 and Cx50 enabled the construction of a homology structural model of Cx50 seen in Fig. 2-9A (Maeda et al., 2009; Tong et al., 2014). The homology structural model of Cx50 proposes the glutamate substitutions at positions G8, G46, and V53 in Cx50 reduce pore diameter (Fig. 2-9A). Accordingly, pore surface electrostatic potentials were generated using this structural model. Pore surface electrostatic potentials for Cx50 and each mutant are illustrated in Fig. 2-9B. In comparison to Cx50 GJ, the glutamate substitution of each mutation (G8E, G46E, or V53E) increased local negative surface potentials near the mutation residue location (Fig. 2-9B). The triple mutant showed elevated negative surface potentials in three mutation sites, therefore showed the highest negative surface potential among of these Cx50 mutant GJs (Fig. 2-9B). Since Cx50 GJ is a cation-preferring channel, the increase in negative electrostatic surface potential by these individual and combined mutants may be an important facilitator of ion permeation (Srinivas, Costa, et al., 1999; Tong et al., 2014). In descending ranking order, these mutant GJs according to their slope γ_j , G8G46V53 > G46E > G8E > V53E = Cx50, suggest that negative electrostatic potential near the G46 and G8 positions (the narrowest portion and near the pore entrance, respectively) showed much stronger effect on ion permeation than that of V53 position (middle of the GJ pore).

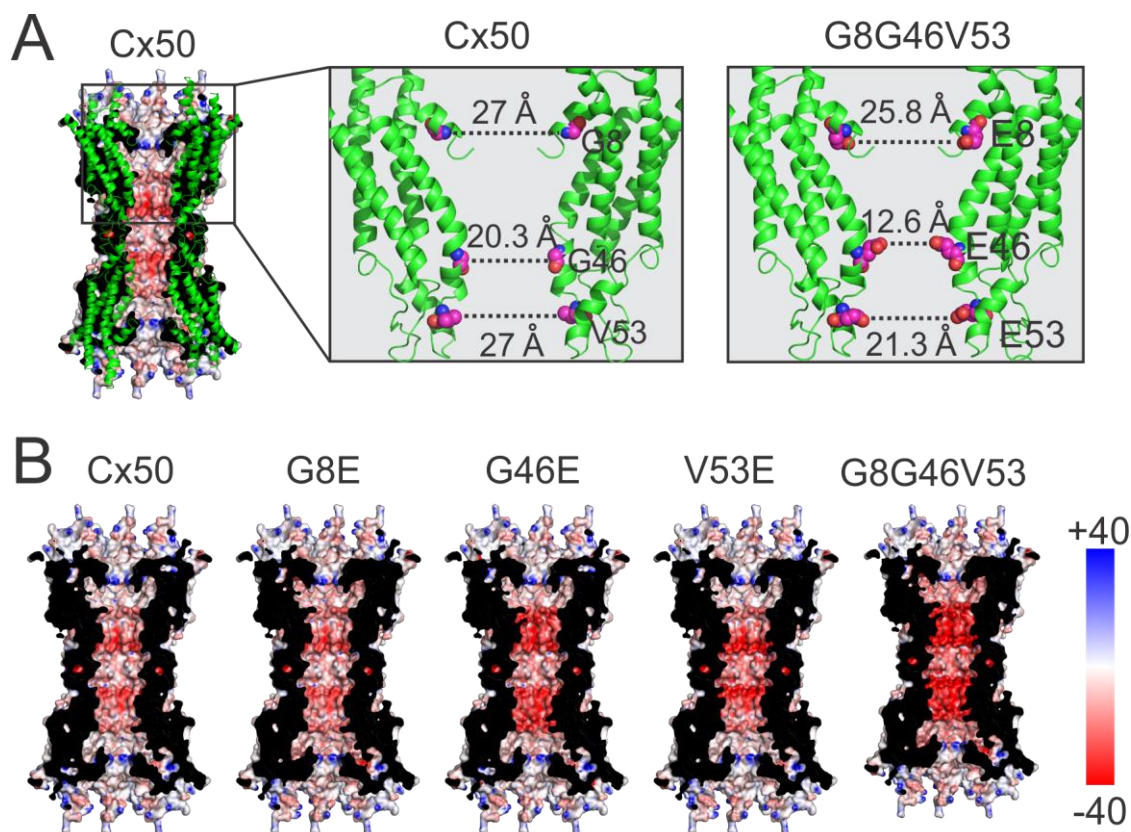


Figure 2-9. Homology models and pore-electrostatic potentials in G8E, G46E, V53E, and G8G46V53 in comparison to Cx50.

A. A side view of Cx50 homology structural model (cartoon view) superimposed with electrostatic surface potential model (left panel). Enlarged portion of pore-lining domains in Cx50 and triple mutation are shown (right panel). Side chains of mutant residues with estimated pore diameters are represented as spheres before (Cx50) and after mutation (G8G46V53) are illustrated. **B.** Side view of cut open Cx50 and mutant GJ channels shows pore surface electrostatic potentials (calculated with an adaptive Poisson-Boltzmann solver) using dielectric constants of 2 (protein) and 80 (solutions) (Baker et al., 2001). Surface electrostatic potentials range from -40 (red) to +40 (blue).

2.5 Discussions

In the present study, we investigated the channel properties of a mutant homotypic GJ channel formed by triple glutamate substitutions in the 8th, 46th, and 53rd positions in Cx50 (G8EG46EV53E). The triple mutant GJ channels drastically increased GJ single channel conductance ($\gamma_j = 329$ pS) approximately 50% higher than that of Cx50. The γ_j of G8EG46EV53E is also larger than the γ_j of Cx37 (~300 pS), the largest known homotypic GJ γ_j (Veenstra et al., 1994). Our homology structural models predict that the triple mutant altered the pore diameters and electrostatic properties at different pore positions. Specifically, replacing small nonpolar hydrophobic residues (glycine or valine) with large hydrophilic negatively charged glutamates is expected to reduce the pore size and increase negative electrostatic potentials of the pore. The fact that γ_j was substantially elevated in the triple mutant GJ channel suggests that increased negativity of electrostatic potentials played a dominant role in facilitating ion permeation of the GJ channel. Investigating individual mutations revealed that G8E and G46E, but not V53E, GJs were also able to increase γ_j , suggesting that these two positions in Cx50 are likely pore-lining and are critical to Cx50 GJ γ_j . Our mutated residues resulted in only minor changes in Cx50 GJ V_j -gating suggesting that a substitution into glutamate at these residues does not likely alter the proposed V_j -sensor or gate in Cx50 GJ. Additionally, we have provided experimental evidence that elevated $[Mg^{2+}]_i$ decreases the γ_j s of Cx50 and the triple mutant GJs. Results from GJs formed by individual mutations suggest that position G46 in Cx50 may play an important role in the γ_j changes in different $[Mg^{2+}]_i$. Our results from mutated residues in NT, M1, and E1 domains of Cx50 GJ are consistent with a

model where these residues either directly line or indirectly affect the pore to alter the rate of ion permeation as well as the modulation by $[Mg^{2+}]_i$.

2.5.1 Structural determinants of γ_j and V_j -gating in Cx50

Previous studies showed that Cx50 GJ channels display prominent deactivation in macroscopic junctional currents (I_j) with increasing V_j s, have higher permeability to cations than anions, and also display the second highest γ_j (200 – 220 pS) of all characterized homotypic GJs (Srinivas, Rozental, et al., 1999; White et al., 1994). Molecular mechanisms underlying these characteristics, particularly V_j -gating and γ_j , are not fully understood. Previous studies exchanging domains of Cx50 with Cx36 and site mutagenesis studies have demonstrated that the NT and M1-E1 border domains in Cx50 influence V_j -gating and γ_j (Tong et al., 2014, 2015; Xin et al., 2010). According to a crystallized structure of Cx26, these domains are assumed to be pore-lining in Cx50, and thus, may be crucial in the involvement in sensing changes along the channel lumen (Maeda et al., 2009). Single point mutations altering electrostatic properties along these proposed pore-lining domains in Cx50 have shown drastic changes in the rate of ion permeation (Tong et al., 2015; Xin et al., 2012). Particularly, substituting a large and negatively charged glutamic acid at position G46 drastically increased GJ γ_j close to that of Cx37 GJs (Tong et al., 2014). This evidence suggests that electrostatic properties of pore-lining residues may be critical in determining Cx50 GJ γ_j .

The effect of mutating any single residue in one connexin is amplified six times in a hemichannel and twelve times in a GJ channel. Therefore, a triple mutation like G8EG46EV53E would create three additional negatively charged glutamate rings in one

hemichannel and six rings in a GJ channel. According to our homology model, these mutations are pore-lining residues which substantially increases the negative pore surface and center electrostatic potentials (Tong et al., 2015, 2014). Our experimental data indicate that the triple mutation GJ increases Cx50 GJ γ_j by nearly 50%, surpassing the highest γ_j attributed to Cx37 GJs (Veenstra et al., 1994). This poses the question of whether there is an upper limit to ion permeation to any GJ channel. Since both Cx50 and Cx37 form cation-preferring GJ channels (Srinivas, Costa, et al., 1999; Veenstra, 1996), increasing negative charges in the pore may facilitate the concentration of local permeating cations, thereby increasing single channel conductance. Our data and the above interpretation parallel studies in high-conducting Ca^{2+} and voltage-activated K^+ (BK) channels as well as nicotinic acetylcholine receptor (AChR) channels as both channels have shown that anionic rings of glutamic acids in pore-lining domains are responsible for a higher rate of ion permeation (Brelidze, Niu, & Magleby, 2003; Carvacho et al., 2008; Imoto et al., 1988; Konno et al., 1991; MacKinnon, Latorre, & Miller, 1989; Wilson, Pascual, Brooijmans, Murray, & Karlin, 2000). We postulate that the difference in γ_j between Cx50 and Cx37 GJs, and potentially other cation-preferring GJs, are likely due to the differences in electrostatic profile in the channel lumen.

Further investigation into the individual mutations revealed that mutational sites showed different ability to increase ion permeation. Homotypic Cx50 GJs expressing mutations G8E and G46E significantly increased Cx50 GJ γ_j by 17% and 24%, respectively, whereas V53E GJs γ_j was approximately equal to wild type. This suggests that residues G8 and G46, but not V53, in Cx50 have a high probability of facing the pore lumen. According to a model proposed by Tong and colleagues (2015), the effect of substituting

glutamic acids in pore-lining regions increases negative charge density in the center of the pore. Our homology model predicts that positions G8 (NT domain) is closest to the pore entrance, G46 (M1–E1 border) is in the narrowest portion of the pore, and V53 (E1 domain) is located in the middle of the GJ pore. We predict that G46E has the strongest electrostatic effect on Cx50 GJ γ_j because the negative charges by six glutamate side chains are concentrated in such a small and narrow region, therefore, substantially increasing the pore's negative charge density. We predict that this would consequently increase the rate of cation permeation traversing through the pore. Similar findings in AChR anionic rings found that mutations in the intermediate glutamine ring, positioned in the narrowest part of the channel, displayed larger effects on ion selectivity than the extracellular and cytoplasmic rings (Konno et al., 1991). The authors suggested that the combination of pore size, pore position, and electrostatic interactions are involved in the effect of the mutation (Konno et al., 1991). This may account for such a drastic increase in γ_j in the triple mutation GJs, as three mutations altered pore size and electrostatic surface potentials at multiple locations. Our results are consistent with a previous study which first demonstrated an increase in Cx50 G46E GJ γ_j (Tong et al., 2014). The previous study had also shown that mutating the 46th position with a glutamic acid had a larger increase in Cx50 GJ γ_j than a mutation with an aspartic acid (D), a negatively charged amino acid with one less methylene group, suggesting that negative electrostatic potential in the center of the pore is a more critical factor for determining Cx50 GJ γ_j (Tong et al., 2014). Our homology model indicates that the G8E mutation is located at the GJ pore entrance and has less impact on the pore diameter (less than 5% reduction) GJs in comparison to E46. As such, negative charge density from the G8E mutation is less

than that of G46E thereby showing less increase in GJ γ_j . In comparison, our homology model indicates that the V53E mutation is located close to the middle of the GJ with E53 side chain orientated into the pore reducing the pore diameter (from 27 to 21.3 Å, a 21% reduction). However, our experimental data indicate that V53E GJs had the least increase in γ_j , suggesting that the V53 position might be less important in affecting Cx50 GJ γ_j .

Our G8E GJs demonstrated a γ_j of 254 pS, which was slightly higher than the previously reported γ_j of 222 pS (Xin et al., 2012). Additionally, our G46E GJs demonstrated a γ_j of 272 pS, which was slightly lower than a previously reported γ_j of 293 pS (Tong et al., 2014). We postulate that these discrepancies are likely due to minor differences in pipette solution, as we excluded both MgATP and Na₂ATP to eliminate their effects on $[Mg^{2+}]_i$ (Xin et al., 2012; Tong et al., 2014). Other possibilities including minor differences in room temperature, extracellular solutions, and/or pH/osmolarity of these solutions could also contribute this minor difference in γ_j .

It was believed that the V_j-sensor involved in initiating GJ V_j-gating consisted of a charged complex formed between NT and M1/E1 domains (Verselis et al., 1994). Furthermore, replacing the NT of Cx50 with the NT of Cx36 was able to alter V_j-gating parameters (Xin et al., 2010). Yet generating a triple mutation, G8EN9RI10L, in the mid-section of Cx50's NT domain did not alter V_j-gating parameters suggesting that not all residues proposed to be in the NT-M1/E1 V_j-sensor complex play a role in this property (Xin et al., 2010). Furthermore, previous work on G46E GJs showed no major alterations in V_j-gating parameters (Tong et al., 2014). Our results are consistent with these findings, as we did not observe any major alterations in V_j-gating in the current study's triple mutation or individual mutations. Nevertheless, changes in Cx50 GJ V_j-gating parameters

have been shown in D3E (NT domain), N9R (substitution to a positively charged amino acid in NT domain), and G46K (substitution to a positively charged amino acid in M1-E1 border), further suggesting that mutation position, size and/or electrostatic potential changes, is critical in determining Cx50 GJ V_j -gating parameters (Tong et al., 2014; Xin et al., 2010, 2012). Systematically mutating non-charged or charged amino acid residues with different side chain charge and size along the proposed pore-lining domains might elucidate the role of size and electrostatic properties in determining Cx50 GJ V_j -gating parameters.

2.5.2 Intracellular magnesium modulation

Increasing $[Mg^{2+}]_i$ has been shown to reduce macroscopic GJ conductance in several different GJs (Noma & Tsuboi, 1987; Oliveira-Castro & Loewenstein, 1971b; Palacios-Prado et al., 2013; Peracchia & Peracchia, 1980). It was proposed that increased $[Mg^{2+}]_i$ reduces open probability and stabilized the closed confirmation of the slow gates (Palacios-Prado et al., 2013). The mechanism by which intracellular Mg^{2+} modulates GJs has not been well studied in connexins on a single channel level. For the first time, we demonstrate increasing $[Mg^{2+}]_i$ reduces rate of ion permeation in Cx50 GJs. By incrementally adding Mg^{2+} into our patch pipette solution, we determined that Mg^{2+} -sensitivity in Cx50 GJs starts approximately around 1 mM and significantly reduces γ_j by ~20% at 3 mM. In comparison, our triple mutation started showing Mg^{2+} -sensitivity at approximately around 0.1 mM and significantly reduced Cx50 GJ γ_j by 39% at 3 mM. Previous studies proposed that negative charges residing in the pore lumen act as Mg^{2+} -sensors (Palacios-Prado et al., 2013). Divalent cations, including Mg^{2+} , aggregate along

the channel lumen and neutralize these negative charges causing the pore to narrow, consequently reducing the amount of current traversing through the channel (Peracchia & Peracchia, 1980). Our results on the triple mutant GJs propose that an increase negative charge along putative pore-lining residues may facilitate Mg^{2+} binding to the pore-lining residues. This enables more Mg^{2+} to aggregate within the channel lumen causing a reduction in the GJ γ_j . The triple mutant GJs are predicted to have more negatively charged residue clusters to serve as binding sites for Mg^{2+} or alternatively, increases affinity to Mg^{2+} at pre-existing sites, thus playing a role in higher sensitivity to low $[Mg^{2+}]_i$ in comparison to Cx50 GJs. This is a simple explanation of our data; of course other additional functional and/or structural evidence is needed to consolidate this model.

GJs of individual single mutations revealed that E46 in Cx50 is a highly Mg^{2+} sensitive residue suggesting the involvement of the M1-E1 border in Mg^{2+} dependent modulation. E8 and E53 in Cx50 also showed Mg^{2+} sensitivity, yet out of the three individual mutations, G46E GJs showed the greatest reduction in γ_j in the presence of 3 mM $[Mg^{2+}]_i$ relative to the reduction in γ_j seen in wild type Cx50. Palacios-Prado and colleagues (2014) demonstrated that putative pore-lining mutations D47G in Cx36 and G46D in Cx43 altered macroscopic GJ conductance with increasing $[Mg^{2+}]_i$; therefore, these positions in their respective connexins are proposed to be Mg^{2+} -sensors in the respective GJs. Our results are consistent with these findings. Referring back to our homology model of Cx50, we predict that G46E is positioned at the narrowest part of the pore, thus, Mg^{2+} -binding at this location would result in larger pore occlusion to reduce ion permeation. In comparison, the homology model predicts G8E and V53E to occupy the pore entrance and center of the GJ, respectively. Since increasing $[Mg^{2+}]_i$ reduces γ_j for

GJs expressing G8E and V53E it is likely that Mg^{2+} is binding at these positions but pore occlusion is less than that of G46E. A fully crystallized structure of Cx50 would aid in elucidating the structural effects of glutamate substitutions in at these residues.

With regards to V_j -gating parameters, Cx50 and all mutant GJs did not show any major changes to increased $[Mg^{2+}]_i$. In comparison to studies done on human Cx37, intracellular Mg^{2+} showed a voltage-dependent modulation of macroscopic currents (Ramanan et al., 1999). Since we generated G8E and V53E mutations in Cx50 based on a sequence alignment with Cx37 it was expected that Cx50 GJ V_j -gating parameters would also be altered in GJs expressing Cx50 mutations with increasing $[Mg^{2+}]_i$. One possible explanation for the lack of changes in V_j -gating parameters in our Cx50 mutated GJs in response to increasing $[Mg^{2+}]_i$ is that these two residues in particular may not be critical to Mg^{2+} modulation on a macroscopic current level. This parallels the results seen in a study investigating the effect of $[Mg^{2+}]_i$ on Cx36 GJ macroscopic currents (Palacios-Prado et al., 2014). Cx36 GJs expressing E1 mutation D47G showed high sensitivity to $[Mg^{2+}]_i$ but not to other E1 residue mutations M52K and V54D demonstrating that not all residues in putative pore-lining domains are responsible for Mg^{2+} modulation on a macroscopic level (Palacios-Prado et al., 2014). As mentioned previously, we suggested that glutamic substitutions at G8, G46, and V53 in Cx50 are not effective at altering Cx50 GJ V_j -gating parameters. As such, these mutations may also not be effective at facilitating Mg^{2+} modulation on a macroscopic current level.

2.5.3 Pathologies associated with mutations in NT, M1, E1 domains

The NT, M1, and E1 domains are mutational hotspots for several disease-linked connexin pathologies such as Cx46 and Cx50 congenital cataracts, Cx32 X-linked Charcot-Marie-Tooth (CMTX) disease, Cx43 oculodentodigital dysplasia (ODDD), and Cx26 Keratitis-ichthyosis-deafness syndrome (KID) (Guleria et al., 2007; Li et al., 2013; Paznekas et al., 2009; Richard et al., 2002; Rubinos et al., 2014; Yoshimura, Satake, Ohnishi, Tsutsumi, & Fujikura, 1998). Disease-linked mutations manifest in modulations at different levels of GJ and hemichannel functioning. Several mice and human Cx50 gene mutations linked to cataract formation are located in the M1-E1 interface, including D47H, V44E, W45S, D47N, and D47A, and often result in impaired trafficking to the plasma membrane and a loss-of-function mutation (Li et al., 2013; Rubinos et al., 2014; Vanita, Singh, Singh, Varon, & Sperling, 2008; Wang, Luo, Wen, Zhang, & Lu, 2011; Xu & Ebihara, 1999). Impairment in hemichannel trafficking is also seen in C53S, a M1-E1 border mutation in Cx32, resulting in CMTX (Yoshimura et al., 1998). In comparison, Cx50 G46V reaches the plasma membrane and enhances hemichannel functioning, compromising cell viability resulting in apoptotic cells (Minogue et al., 2009). Genetic screenings of cataract patients have also identified NT (D3Y) and M1 (R33L) mutations in Cx46 that alters hemichannel voltage sensitivity and cell coupling (Guleria et al., 2007; Schlingmann, Schadzek, Busko, Heisterkamp, & Ngezahayo, 2012). NT mutations G12R and S17F in Cx26 result in a loss-of-function leading to KID (Richard et al., 2002). This suggests that mutations linked to cataracts and other diseases manifest through different mechanisms. Elucidating the functional role of NT, M1, and E1 domains would provide further insight

into the etiology and mechanisms underlying the many disease-linked mutations occurring in these connexin domains.

2.5.4 Resolving the structure-function relationship in NT, M1, E1 domains in Cx50

Human Cx26 is the only connexin to have a near atomic resolution crystalized structure (Maeda et al., 2009). The structural model positioned NT, M1, and E1 domains as pore-lining regions and are critical in ion permeation through the channel lumen (Maeda et al., 2009). Since these domains (in addition to M2, M3, and M4) are highly conserved between connexins, Cx26 has been used as a structural template for other connexins. Substituted cysteine accessibility method (SCAM) and tryptophan scanning in Cx46 and Cx32 propose putative pore-lining residues along the M1-E1 border greatly influence GJ γ_j (Kronengold et al., 2003; Zhou et al., 1997). Domain exchange studies in Cx50 and Cx36 E1 domains further suggest that this domain is responsible for γ_j in Cx50 GJs (Tong et al., 2015). Additionally, changing the amino acid charge at G46 drastically altered Cx50 GJ γ_j (Tong et al., 2014). The results of our present study are consistent with this finding providing further evidence that this residue does play a role in single channel properties.

Previous work in replacing the NT domain of Cx50 with Cx36 in addition to individual NT mutations, N9R and D3E, in Cx50 also suggest that the NT domain is responsible for γ_j (Xin et al., 2010; Xin et al., 2012). Our results suggest that position G8 plays an important role in γ_j and is likely pore-lining. It has also been suggested that the V_j -sensor initiating V_j -gating is composed of a charged complex between NT, M1 and E1 domains

in other connexins (Verselis et al., 1994). Although previous work in these domains demonstrate an effect on Cx50 V_j -gating parameters, none of our generated mutations showed any major alterations (Tong et al., 2015; Xin et al., 2010, 2012). We propose these mutated residues may not be effective at altering Cx50 GJ V_j -gating properties, however, we argue that these positions play a significant role in determining Cx50 GJ γ_j .

2.5.5 Conclusion

Our study demonstrates that collectively increasing negative charges along proposed pore-lining domains through a triple glutamate substitution substantially increases Cx50 GJ γ_j . We propose this increase in negative electrostatic potential in the center of the pore enables Cx50 GJ channels to more efficiently facilitate cation permeation. Furthermore, the increase in negative charges in our triple glutamate substitution may have facilitated Mg^{2+} modulation by providing more available Mg^{2+} -binding sites or increasing the affinity to Mg^{2+} of pre-existing sites. Follow-up studies must be conducted to see if further increasing negative charges along the pore or even higher $[Mg^{2+}]_i$ will influence Cx50 V_j -gating properties or show an upper limit to both effects. It should be noted that these mechanisms are based on a homology model of Cx26. A crystallized structure of Cx50 GJ channel would provide more confirmation and insight into the modulatory effects of pore-lining residues and $[Mg^{2+}]_i$.

2.6 References

- Agarwal, R., Iezhitsa, I., Agarwal, P., & Spasov, A. (2012). Magnesium deficiency: Does it have a role to play in cataractogenesis? *Experimental Eye Research*, *101*, 82–89.
- Agarwal, R., Iezhitsa, I. N., Agarwal, P., & Spasov, A. a. (2013). Mechanisms of cataractogenesis in the presence of magnesium deficiency. *Magnesium Research*, *26*(1), 2–8.
- Agarwal, R., Iezhitsa, L., & Agarwal, P. (2014). Pathogenetic role of magnesium deficiency in ophthalmic diseases. *BioMetals*, *27*(1), 5–18.
- Arora, a, Minogue, P. J., Liu, X., Addison, P. K., Russel-Eggitt, I., Webster, ... Moore, A. T. (2008). A novel connexin50 mutation associated with congenital nuclear pulverulent cataracts. *Journal of Medical Genetics*, *45*(3), 155–60.
- Bai, D., & Cameron, J. A. (2017). Patch clamp analysis of gap junction channel properties. In Bai, D., & Sáez, J.C. (Eds.), *Gap Junction Channels and Hemichannels* (pp. 93-112). Boca Raton, FL: Taylor & Francis Group.
- Bai, D., del Corosso, C., Srinivas, M., & Spray, D. C. (2006). Block of Specific Gap Junction Channel Subtypes by 2-Aminoethoxydiphenyl Borate (2-APB). *Journal of Pharmacology and Experimental Therapeutics*, *319*(3), 1452–1458.
- Bai, D., & Wang, A. H. (2014). Extracellular domains play different roles in gap junction formation and docking compatibility. *The Biochemical Journal*, *458*(1), 1–10.
- Baker, N. A., Sept, D., Joseph, S., Holst, M. J., & McCammon, J. A. (2001). Electrostatics of nanosystems: application to microtubules and the ribosome. *Proceedings of the National Academy of Sciences of the United States of America*, *98*(18), 10037–41.
- Bassnett, S., & Beebe, D. C. (1992). Coincident loss of mitochondria and nuclei during lens fiber cell differentiation. *Developmental Dynamics*, *194*(2), 85–93.

- Bennett, M. V. (1997). Gap junctions as electrical synapses. *Journal of Neurocytology*, 26(6), 349–66.
- Bennett, M. V., & Verselis, V. K. (1992). Biophysics of gap junctions. *Seminars in Cell Biology*, 3(1), 29–47.
- Beyer, E. C., & Berthoud, V. M. (2014). Connexin hemichannels in the lens. *Frontiers in Physiology*, 5, 20.
- Brelidze, T. I., Niu, X., & Magleby, K. L. (2003). A ring of eight conserved negatively charged amino acids doubles the conductance of BK channels and prevents inward rectification. *Proceedings of the National Academy of Sciences of the United States of America*, 100(15), 9017–9022.
- Brennan, M. J., Karcz, J., Vaughn, N. R., Woolwine-Cunningham, Y., DePriest, A. D., Escalona, Y., ... Skerrett, I. M. (2015). Tryptophan Scanning Reveals Dense Packing of Connexin Transmembrane Domains in Gap Junction Channels Composed of Connexin32. *Journal of Biological Chemistry*, 290(28), 17074–17084.
- Bruzzone, R., White, T. W., & Paul, D. L. (1996). Connections with connexins: the molecular basis of direct intercellular signaling. *European Journal of Biochemistry / FEBS*, 238(1), 1–27.
- Bukauskas, F. F., & Peracchia, C. (1997). Two distinct gating mechanisms in gap junction channels: CO₂-sensitive and voltage-sensitive. *Biophysical Journal*, 72(5), 2137–42.
- Bukauskas, F. F., & Verselis, V. K. (2004). Gap junction channel gating. *Biochimica et Biophysica Acta*, 1662(1-2), 42–60.
- Bukauskas, F. F., & Weingart, R. (1994). Voltage-dependent gating of single gap junction channels in an insect cell line. *Biophysical Journal*, 67(2), 613–625.

- Burghardt, R. C., Barhoumi, R., Sewall, T. C., & Bowen, J. a. (1995). Cyclic AMP induces Rapid increases in gap junction permeability and changes in the cellular distribution of connexin43. *New York*, 253, 243–253.
- Burr, G. S., Mitchell, C. K., Keflemariam, Y. J., Heidelberger, R., & O'Brien, J. (2005). Calcium-dependent binding of calmodulin to neuronal gap junction proteins. *Biochemical and Biophysical Research Communications*, 335(4), 1191–1198.
- Carvacho, I., Gonzalez, W., Torres, Y. P., Brauchi, S., Alvarez, O., Gonzalez-Nilo, F. D., & Latorre, R. (2008). Intrinsic electrostatic potential in the BK channel pore: role in determining single channel conductance and block. *The Journal of General Physiology*, 131(2), 147–61.
- Chang, B., Wang, X., Hawes, N. L., Ojakian, R., Davisson, M. T., Lo, W. K., & Gong, X. (2002). A Gja8 (Cx50) point mutation causes an alteration of alpha 3 connexin (Cx46) in semi-dominant cataracts of Lop10 mice. *Hum Mol Genet*, 11(5), 507–513.
- Church, R. L., Wang, J., & Steele, E. (1995). The human lens intrinsic membrane protein MP70 (Cx50) gene: clonal analysis and chromosome mapping. *Current Eye Research*, 14(3), 215–221.
- Decker, R. S. (1976). Hormonal regulation of gap junction differentiation. *The Journal of Cell Biology*, 69(3).
- Dermietzel, R., Traub, O., Hwang, T. K., Beyer, E., Bennett, M. V, Spray, D. C., & Willecke, K. (1989). Differential expression of three gap junction proteins in developing and mature brain tissues. *Proceedings of the National Academy of Sciences*, 86(December), 10148–10152.
- Dilsiz, N., Olcucu, A., & Atas, M. (2000). Determination of calcium, sodium, potassium and magnesium concentrations in human senile cataractous lenses. *Cell Biochemistry and Function*, 18(4), 259–262.

- Dunlap, K., Takeda, K., & Brehm, P. (1987). Activation of a calcium-dependent photoprotein by chemical signalling through gap junctions. *Nature*, 325(6099), 60–62.
- Ebihara, L., Liu, X., & Pal, J. D. (2003). Effect of external magnesium and calcium on human connexin46 hemichannels. *Biophysical Journal*, 84(1), 277–286.
- George, C. H., Kendall, J. M., & Evans, W. H. (1999). Intracellular trafficking pathways in the assembly of connexins into gap junctions. *Journal of Biological Chemistry*, 274(13), 8678–8685.
- Girsch, S. J., & Peracchia, C. (1985). Lens cell-to-cell channel protein: I. Self-assembly into liposomes and permeability regulation by calmodulin. *The Journal of Membrane Biology*, 83(3), 217–25.
- Goldberg, G. S., Lampe, P. D., & Nicholson, B. J. (1999). Selective transfer of endogenous metabolites through gap junctions composed of different connexins. *Nature Cell Biology*, 1(7), 457–459.
- Gómez-Hernández, J. M., de Miguel, M., Larrosa, B., González, D., Barrio, L. C., Gomez-Hernandez, J. M., ... Barrio, L. C. (2003). Molecular basis of calcium regulation in connexin-32 hemichannels. *Proceedings of the National Academy of Sciences of the United States of America*, 100(26), 16030–16035.
- Gong, X., Li, E., Klier, G., Huang, Q., Wu, Y., Lei, H., ... Gilula, N. B. (1997). Disruption of $\alpha 3$ connexin gene leads to proteolysis and cataractogenesis in mice. *Cell*, 91(6), 833–843.
- Gong, X. Q., & Nicholson, B. J. (2001). Size selectivity between gap junction channels composed of different connexins. *Cell Communication & Adhesion*, 8, 187–192.
- González, D., Gómez-Hernández, J. M., & Barrio, L. C. (2007). Molecular basis of voltage dependence of connexin channels: An integrative appraisal. *Progress in Biophysics and Molecular Biology*, 94(1-2), 66–106.

- Goodenough, D. a. (1992). The crystalline lens. A system networked by gap junctional intercellular communication. *Semin Cell Biol*, 3(1), 49–58.
- Gourdie, R., Green, C., Severs, N., & Thompson, R. (1992). Immunolabelling patterns of gap junction connexins in the developing and mature rat heart. *Anatomy and Embryology*, 185(4), 363–378.
- Guleria, K., Sperling, K., Singh, D., Varon, R., Singh, J. R., & Vanita, V. (2007). A novel mutation in the connexin 46 (GJA3) gene associated with autosomal dominant congenital cataract in an Indian family. *Molecular Vision*, 13(April), 1657–65.
- Harris, a L., Spray, D. C., & Bennett, M. V. (1981). Equilibrium Properties of a voltage-dependent junctional conductance. *The Journal of General Physiology*, 77(January), 95–117.
- Harris, A. L., Spray, D. C., & Bennett, M. V. (1981). Kinetic properties of a voltage-dependent junctional conductance. *The Journal of General Physiology*, 77(1).
- Hartzell, H. C., & White, R. E. (1989). Effects of magnesium on inactivation of the voltage-gated calcium current in cardiac myocytes. *The Journal of General Physiology*, 94(4), 745–67.
- Hermans, M. M. P., Kortekaas, P., Jongasma, H. J., & Rook, M. B. (1995). pH sensitivity of the cardiac gap junction proteins, connexin 45 and 43. *Pflügers Archiv European Journal of Physiology*, 431(1), 138–140.
- Hopperstad, M. G., Srinivas, M., & Spray, D. C. (2000). Properties of gap junction channels formed by Cx46 alone and in combination with Cx50. *Biophysical Journal*, 79(4), 1954–66.
- Horie, M., & Irisawa, H. (1987). Rectification of muscarinic K⁺ current by magnesium ion in guinea pig atrial cells. *American Journal of Physiology - Heart and Circulatory Physiology*, 253(1).

- Hu, X., Ma, M., & Dahl, G. (2006). Conductance of Connexin Hemichannels Segregates with the First Transmembrane Segment. *Biophysical Journal*, *90*(1), 140–150.
- Imoto, K., Busch, C., Sakmann, B., Mishina, M., Konno, T., Nakai, J., ... Numa, S. (1988). Rings of negatively charged amino acids determine the acetylcholine receptor channel conductance. *Nature*, *335*(6191), 645–648.
- Johnson, R., Hammer, M., Sheridan, J., & Revel, J. P. (1974). Gap junction formation between reaggregated Novikoff hepatoma cells. *Proc Natl Acad Sci U S A*, *71*(11), 4536–4540.
- Kanter, H. L., Saffitz, J. E., & Beyer, E. C. (1992). Cardiac myocytes express multiple gap junction proteins. *Circulation Research*, *70*(2), 438–444.
- Kennedy, K. G., & Nayler, W. G. (1965). The effect of quinidine on the activity of a sodium-potassium activated, magnesium-dependent ATPase enzyme isolated from toad cardiac muscle. *Biochimica et Biophysica Acta (BBA) - Enzymology and Biological Oxidation*, *110*(1), 174–180.
- Kerscher, S., Church, R. L., Boyd, Y., & Lyon, M. F. (1995). Mapping of four mouse genes encoding eye lens-specific structural, gap junction, and integral membrane proteins: Cryba1 (crystallin beta A3/A1), Crybb2 (crystallin beta B2), Gja8 (MP70), and Lim2 (MP19). *Genomics*, *29*(2), 445–450.
- Kistler, J., Kirkland, B., & Bullivant, S. (1985). Identification of a 70,000-D protein in lens membrane junctional domains. *Journal of Cell Biology*, *101*(1), 28–35.
- Konno, T., Busch, C., von Kitzing, E., Imoto, K., Wang, F., Nakai, J., ... Sakmann, B. (1991). Rings of anionic amino acids as structural determinants of ion selectivity in the acetylcholine receptor channel. *Proc. Biol. Sci.*, *244*(1310), 69–79.
- Kreuzberg, M. M., Söhl, G., Kim, J.-S., Verselis, V. K., Willecke, K., & Bukauskas, F. F. (2005). Functional properties of mouse connexin30.2 expressed in the conduction system of the heart. *Circulation Research*, *96*(11), 1169–77.

- Kronengold, J. (2003). Single-channel SCAM Identifies Pore-lining Residues in the First Extracellular Loop and First Transmembrane Domains of Cx46 Hemichannels. *The Journal of General Physiology*, 122(4), 389–405.
- Kronengold, J., Trexler, E. B., Bukauskas, F. F., Bargiello, T. A., & Verselis, V. K. (2003). Single-channel SCAM Identifies Pore-lining Residues in the First Extracellular Loop and First Transmembrane Domains of Cx46 Hemichannels. *The Journal of General Physiology*, 122(4), 389–405.
- Krutovskikh, V. a, Piccoli, C., & Yamasaki, H. (2002). Gap junction intercellular communication propagates cell death in cancerous cells. *Oncogene*, 21(13), 1989–1999.
- Kumar, N. M., & Gilula, N. B. (1992). Molecular biology and genetics of gap junction channels. *Seminars in Cell Biology*, 3(1), 3–16.
- Kwak, B. R., Hermans, M. M., De Jonge, H. R., Lohmann, S. M., Jongsma, H. J., & Chanson, M. (1995). Differential regulation of distinct types of gap junction channels by similar phosphorylating conditions. *Molecular Biology of the Cell*, 6(12), 1707–1719.
- Laird, D. W. (1996). The life cycle of a connexin: gap junction formation, removal, and degradation. *Journal of Bioenergetics and Biomembranes*, 28(4), 311–318.
- Lawrence, T. S., Beers, W. H., & Gilula, N. B. (1978). Transmission of hormonal stimulation by cell-to-cell communication. *Nature*, 272, 501–506.
- Li, J., Wang, Q., Fu, Q., Zhu, Y., Zhai, Y., Yu, Y., ... Yao, K. (2013). A novel connexin 50 gene (gap junction protein, alpha 8) mutation associated with congenital nuclear and zonular pulverulent cataract. *Molecular Vision*, 19(April), 767–774.
- Loewenstein, W. R., Nakas, M., & Socolar, S. J. (1967). Junctional Membrane Uncoupling: Permeability transformations at a cell membrane junction . *The Journal of General Physiology* , 50 (7) , 1865–1891.

- Loewenstein, W. R., & Rose, B. (1978). Calcium in (Junctional) Intercellular Communication and a Thought on Its Behavior in Intracellular Communication. *Annals of the New York Academy of Sciences*, 307(1), 285–307.
- MacKinnon, R., Latorre, R., & Miller, C. (1989). Role of surface electrostatics in the operation of a high-conductance Ca²⁺-activated K⁺ channel. *Biochemistry*, 28(1985), 8092–8099.
- Maeda, S., Nakagawa, S., Suga, M., Yamashita, E., Oshima, A., Fujiyoshi, Y., & Tsukihara, T. (2009). Structure of the connexin 26 gap junction channel at 3.5 Å resolution. *Nature*, 458(7238), 597–602.
- Maza, J., Mateescu, M., Das Sarma, J., & Koval, M. (2003). Differential oligomerization of endoplasmic reticulum-retained connexin43/connexin32 chimeras. *Cell Communication & Adhesion*, 10, 319–322.
- McGahan, M. C., Chin, B., & Bentley, P. J. (1983). Some Observations on the Magnesium Metabolism of the Rabbit Lens. *Exp. Eye Res*, 36, 67–73.
- Minnich, V., Smith, M. B., Brauner, M. J., & Majerus, P. W. (1971). Glutathione biosynthesis in human erythrocytes. I. Identification of the enzymes of glutathione synthesis in hemolysates. *Journal of Clinical Investigation*, 50(3), 507–513.
- Minogue, P. J., Tong, J. J., Arora, A., Russell-Eggitt, I., Hunt, D. M., Moore, A. T., ... Berthoud, V. M. (2009). A mutant connexin50 with enhanced hemichannel function leads to cell death. *Investigative Ophthalmology and Visual Science*, 50(12), 5837–5845.
- Moreno, a P., Rook, M. B., Fishman, G. I., & Spray, D. C. (1994). Gap junction channels: distinct voltage-sensitive and -insensitive conductance states. *Biophysical Journal*, 67(1), 113–9.
- Noma, a, & Tsuboi, N. (1987). Dependence of junctional conductance on proton, calcium and magnesium ions in cardiac paired cells of guinea-pig. *J. Physiol.*, 382(1), 193–211.

- Oliveira-Castro, G. M., & Loewenstein, W. R. (1971a). Junctional membrane permeability. *The Journal of Membrane Biology*, 5(1), 51–77.
- Oliveira-Castro, G. M., & Loewenstein, W. R. (1971b). Junctional membrane permeability - Effects of divalent cations. *The Journal of Membrane Biology*, 5(1), 51–77.
- Palacios-Prado, N., Chapuis, S., Panjkovich, A., Fregeac, J., Nagy, J. I., & Bukauskas, F. F. (2014). Molecular determinants of magnesium-dependent synaptic plasticity at electrical synapses formed by connexin36. *Nature Communications*, 5, 4667.
- Palacios-Prado, N., Hoge, G., Marandykina, A., Rimkute, L., Chapuis, S., Paulauskas, N., ... Bukauskas, F. F. (2013). Intracellular Magnesium-Dependent Modulation of Gap Junction Channels Formed by Neuronal Connexin36. *J Neurosci.*, 33(11), 4741–4753.
- Paulauskas, N., Pranevicius, M., Pranevicius, H., & Bukauskas, F. F. (2009). A stochastic four-state model of contingent gating of gap junction channels containing two “fast” gates sensitive to transjunctional voltage. *Biophysical Journal*, 96(10), 3936–3948.
- Paznekas, W. a., Karczeski, B., Vermeer, S., Lowry, R. B., Delatycki, M., Laurence, F., ... Jabs, E. W. (2009). GJA1 mutations, variants, and connexin 43 dysfunction as it relates to the oculodentodigital dysplasia phenotype. *Human Mutation*, 30(5), 724–733.
- Peracchia, C., & Peracchia, L. L. (1980). Gap junction dynamics: reversible effects of divalent cations. *The Journal of Cell Biology*, 87(3).
- Pershadsingh, H. a., & McDonald, J. M. (1980). A high affinity calcium-stimulated magnesium-dependent adenosine triphosphatase in rat adipocyte plasma membranes. *Journal of Biological Chemistry*, 255(9), 4087–4093.
- Pfahnl, A., & Dahl, G. (1999). Gating of cx46 gap junction hemichannels by calcium and voltage. *Pflugers Archiv European Journal of Physiology*, 437(3), 345–353.

- Ramanan, S. V., Brink, P. R., Varadaraj, K., Peterson, E., Schirrmacher, K., & Banach, K. (1999). A Three-State Model for Connexin37 Gating Kinetics. *Biophysical Journal*, 76(5), 2520–2529.
- Richard, G., Rouan, F., Willoughby, C. E., Brown, N., Chung, P., Jabs, E. W., ... Russell, L. (2002). Missense Mutations in GJB2 Encoding Connexin-26 Cause the Ectodermal Dysplasia Keratitis-Ichthyosis-Deafness Syndrome, 1341–1348.
- Rong, P., Wang, X., Niesman, I., Wu, Y., Benedetti, L. E., Dunia, I., ... Gong, X. (2002). Disruption of Gja8 (alpha8 connexin) in mice leads to microphthalmia associated with retardation of lens growth and lens fiber maturation. *Development (Cambridge, England)*, 129(1), 167–74.
- Rose, B., Simpson, I., & Loewenstein, W. R. (1977). Calcium ion produces graded changes in permeability of membrane channels in cell junction. *Nature*, 267(5612), 625–627.
- Rubinos, C., Villone, K., Mhaske, P. V, White, T. W., & Srinivas, M. (2014). Functional effects of Cx50 mutations associated with congenital cataracts. *American Journal of Physiology. Cell Physiology*, 306(3), C212–20.
- Sarma, J. Das, Wang, F., & Koval, M. (2002). Targeted gap junction protein constructs reveal connexin-specific differences in oligomerization. *Journal of Biological Chemistry*, 277(23), 20911–20918.
- Schlingmann, B., Schadzek, P., Busko, S., Heisterkamp, A., & Ngezahayo, A. (2012). Cataract-associated D3Y mutation of human connexin46 (hCx46) increases the dye coupling of gap junction channels and suppresses the voltage sensitivity of hemichannels. *Journal of Bioenergetics and Biomembranes*, 44(5), 607–614.
- Schütte, M., Chen, S., Buku, A., & Wolosin, J. M. (1998). Connexin50, a Gap Junction Protein of Macrogliia in the Mammalian Retina and Visual Pathway. *Experimental Eye Research*, 66(5), 605–613.

- Segretain, D., & Falk, M. M. (2004). Regulation of connexin biosynthesis, assembly, gap junction formation, and removal. *Biochimica et Biophysica Acta - Biomembranes*, 1662(1-2), 3–21.
- Shiels, a, Mackay, D., Ionides, a, Berry, V., Moore, a, & Bhattacharya, S. (1998). A missense mutation in the human connexin50 gene (GJA8) underlies autosomal dominant “zonular pulverulent” cataract, on chromosome 1q. *American Journal of Human Genetics*, 62(3), 526–32.
- Simpson, I., Rose, B., & Loewenstein, W. R. (1977). Size limit of molecules permeating the junctional membrane channels. *Science (New York, N.Y.)*, 195(4275), 294–6.
- Sohl, G. (2004). Gap junctions and the connexin protein family. *Cardiovascular Research*, 62(2), 228–232.
- Söhl, G., & Willecke, K. (2004). Gap junctions and the connexin protein family. *Cardiovascular Research*, 62(2), 228–232.
- Srinivas, M., Costa, M., Gao, Y., Fort, a, Fishman, G. I., & Spray, D. C. (1999). Voltage dependence of macroscopic and unitary currents of gap junction channels formed by mouse connexin50 expressed in rat neuroblastoma cells. *The Journal of Physiology*, 517 (Pt 3, 673–89.
- Srinivas, M., Rozental, R., Kojima, T., Dermietzel, R., Mehler, M., Condorelli, D. F., ... Spray, D. C. (1999). Functional properties of channels formed by the neuronal gap junction protein connexin36. *The Journal of Neuroscience : The Official Journal of the Society for Neuroscience*, 19(22), 9848–9855.
- Swanson, A. a., & Truesdale, A. W. (1971). Elemental analysis in normal and cataractous human lens tissue. *Biochemical and Biophysical Research Communications*, 45(6), 1488–1496.
- Takaya, J., Higashino, H., & Kobayashi, Y. (2000). Can magnesium act as a second messenger? Current data on translocation induced by various biologically active

substances. *Magnesium Research : Official Organ of the International Society for the Development of Research on Magnesium*, 13(2), 139–146.

- Tong, J.-J., Minogue, P. J., Guo, W., Chen, T.-L., Beyer, E. C., Berthoud, V. M., & Ebihara, L. (2011). Different consequences of cataract-associated mutations at adjacent positions in the first extracellular boundary of connexin50. *American Journal of Physiology. Cell Physiology*, 300(5), C1055–64.
- Tong, X., Aoyama, H., Sudhakar, S., Chen, H., Shilton, B. H., & Bai, D. (2015). The first extracellular domain plays an important role in unitary channel conductance of Cx50 gap junction channels. *PLoS ONE*, 10(12), 1–20.
- Tong, X., Aoyama, H., Tsukihara, T., & Bai, D. (2014). Charge at the 46th residue of connexin 50 is crucial for the gap-junctional unitary conductance and transjunctional voltage-dependent gating. *The Journal of Physiology*, 592(23), 5187–5202.
- Török, K., Stauffer, K., & Evans, W. H. (1997). Connexin 32 of gap junctions contains two cytoplasmic calmodulin-binding domains. *The Biochemical Journal*, 326 (Pt 2, 479–83.
- Umeda, I. O., Kashiwa, Y., Nakata, H., & Nishigori, H. (2003). Predominant phosphatase in the ocular lens regulated by physiological concentrations of magnesium and calcium. *Life Sciences*, 73(9), 1161–1173.
- Vandenberg, C. a. (1987). Inward rectification of a potassium channel in cardiac ventricular cells depends on internal magnesium ions. *Proceedings of the National Academy of Sciences*, 84(8), 2560–2564.
- Vanita, V., Singh, J. R., Singh, D., Varon, R., & Sperling, K. (2008). A novel mutation in GJA8 associated with jellyfish-like cataract in a family of Indian origin. *Molecular Vision*, 14(August 2007), 323–326.
- Veenstra, R. D. (1996). Size and selectivity of gap junction channels formed from different connexins. *Journal of Bioenergetics and Biomembranes*, 28(4), 327–37.

- Veenstra, R. D., Wang, H. Z., Beyer, E. C., Ramanan, S. V., & Brink, P. R. (1994). Connexin37 forms high conductance gap junction channels with subconductance state activity and selective dye and ionic permeabilities. *Biophysical Journal*, 66(June), 1915–1928.
- Verselis, V. K., Ginter, C. S., & Bargiello, T. a. (1994). Opposite voltage gating polarities of two closely related connexins. *Nature*, 368, 348–351.
- Wang, L., Luo, Y., Wen, W., Zhang, S., & Lu, Y. (2011). Another evidence for a D47N mutation in GJA8 associated with autosomal dominant congenital cataract. *Molecular Vision*, 17(May), 2380–2385.
- Weber, P. a, Chang, H. C., Spaeth, K. E., Nitsche, J. M., & Nicholson, B. J. (2004). The permeability of gap junction channels to probes of different size is dependent on connexin composition and permeant-pore affinities. *Biophys J*, 87(2), 958–973.
- White, T. W., Bruzzone, R., Goodenough, D. a, & Paul, D. L. (1992). Mouse Cx50, a functional member of the connexin family of gap junction proteins, is the lens fiber protein MP70. *Molecular Biology of the Cell*, 3(7), 711–20.
- White, T. W., Bruzzone, R., Wolfram, S., Paul, D. L., & Goodenough, D. a. (1994). Selective interactions among the multiple connexin proteins expressed in the vertebrate lens: The second extracellular domain is a determinant of compatibility between connexins. *Journal of Cell Biology*, 125(4), 879–892.
- White, T. W., Goodenough, D. a., & Paul, D. L. (1998). Targeted ablation of connexin50 in mice results in microphthalmia and zonular pulverulent cataracts. *Journal of Cell Biology*, 143(3), 815–825.
- Wilders, R., & Jongsma, H. J. (1992). Limitations of the dual voltage clamp method in assaying conductance and kinetics of gap junction channels. *Biophysical Journal*, 63(4), 942–53.

- Wilson, G. G., Pascual, J. M., Brooijmans, N., Murray, D., & Karlin, a. (2000). The intrinsic electrostatic potential and the intermediate ring of charge in the acetylcholine receptor channel. *J Gen Physiol*, *115*(2), 93–106.
- Wolosin, J. M., Schütte, M., & Chen, S. (1997). Connexin distribution in the rabbit and rat ciliary body: A case for heterotypic epithelial gap junctions. *Investigative Ophthalmology and Visual Science*, *38*(2), 341–348.
- Xin, L., Gong, X. Q., & Bai, D. (2010). The role of amino terminus of mouse Cx50 in determining transjunctional voltage-dependent gating and unitary conductance. *Biophysical Journal*, *99*(7), 2077–2086.
- Xin, L., Nakagawa, S., Tsukihara, T., & Bai, D. (2012). Aspartic Acid Residue D3 Critically Determines Cx50 Gap Junction Channel Transjunctional Voltage-Dependent Gating and Unitary Conductance. *Biophysj*, *102*(5), 1022–1031.
- Yeager, M., Unger, V. M., & Falk, M. M. (1998). Synthesis, assembly and structure of gap junction intercellular channels. *Current Opinion in Structural Biology*, *8*(4), 517–524.
- Yoshimura, T., Satake, M., Ohnishi, a, Tsutsumi, Y., & Fujikura, Y. (1998). Mutations of connexin32 in Charcot-Marie-Tooth disease type X interfere with cell-to-cell communication but not cell proliferation and myelin-specific gene expression. *Journal of Neuroscience Research*, *51*(2), 154–61.
- Zhou, X. W., Pfahnl, a, Werner, R., Hudder, a, Llanes, a, Luebke, a, & Dahl, G. (1997). Identification of a pore lining segment in gap junction hemichannels. *Biophysical Journal*, *72*(5), 1946–53.

Chapter 3 – Discussions

3.1 Overall Study

The present study aimed to further understand the molecular mechanisms underlying Cx50 GJ properties including γ_j and V_j -gating. Experimental evidence increasingly emphasizes the importance of the influence of pore surface electrostatics on GJ γ_j (Tong, Aoyama, Tsukihara, & Bai, 2014; Xin, Nakagawa, Tsukihara, & Bai, 2012). Here we examined the effect of introducing negative charges at putative pore-lining domains on Cx50 GJ γ_j and V_j -gating. Our data from the triple mutation (G8G46V53) demonstrate that increasing the amount of negatively charged glutamate residues at the NT, M1-E1 border, and E1 domain of Cx50 dramatically increases γ_j . Furthermore, single mutations G8E and G46E, but not V53E, increase γ_j suggesting that these two positions in Cx50 are critical residues in determining γ_j . Although previous studies propose the NT and E1 domains to be responsible for V_j -gating properties, none of the Cx50 mutations tested in the present study elicited any major alterations (Maeda et al., 2009; Tong et al., 2014; Xin, Gong, & Bai, 2010). This suggests that glutamate substitutions at these positions are more pertinent to γ_j but not V_j -gating properties. Furthermore, increasing $[Mg^{2+}]_i$ was shown to reduce γ_j Cx50 and triple mutant GJ channels. Negatively charged putative pore-lining residues may mediate Mg^{2+} -dependent modulation by providing additional Mg^{2+} -binding sites or increase the affinity of pre-existing binding sites. Overall, putative pore-lining residues and $[Mg^{2+}]_i$ are key factors in determining Cx50 GJ γ_j .

3.2 The role of pore-lining residues in γ_j and V_j -gating

Structural determinants underlying the broad range of GJ γ_j and V_j -gating parameters observed in different connexins are not fully understood. Many studies have suggested that pore-lining properties of connexin GJ structure, such as pore diameter and electrostatic surface potential, are responsible for these functional differences, in particular γ_j . Pore size was initially hypothesized to create a physical restriction to channel conductance, yet experimental evidence has shown little correlation between pore diameter and rate of ion permeation (Gong & Nicholson, 2001; Tong et al., 2015; Veenstra et al., 1994; Weber et al., 2004). This weak correlation has been seen in Cx50 when comparing varying predicted pore diameters of several Cx50 mutant channels to single GJ channel γ_j (Tong et al., 2015). Instead, evidence suggests surface electrostatic potential in the pore is a main contributor to determining Cx50 GJ γ_j (Tong et al., 2015; Tong et al., 2014). Single point mutations altering electrostatic surface potential in Cx50's M1-E1 border have shown drastic changes in ion permeation (Tong et al., 2014). Particularly, a substitution of negatively charged glutamic acid at position G46 drastically increased Cx50 GJ γ_j close to that of Cx37 GJs (Tong et al., 2014). Accumulation of negative charges in our triple mutation substantially increased Cx50 GJ γ_j surpassing the highest γ_j attributed to Cx37 (Veenstra et al., 1994). Several connexins, including Cx50 and Cx37, form GJs that are modestly selective for cations (Srinivas, Costa, et al., 1999; Veenstra, 1996). Introducing negatively charged residues at putative pore-lining positions may facilitate an increase in concentration of local permeating cations thereby increasing single channel conductance. A comparative study between BK channels and lower-conducting K^+ channels revealed that differences in single channel conductance was due

to the ring of negative charges in BK channels facilitating the rate of K^+ permeation (Brelidze et al., 2003). Our results suggest that the difference in γ_j between Cx50 and Cx37 GJs, and potentially other cation preferring connexins, are likely due to differences in electrostatic profile in the channel lumen.

The structural homology model generated speculates that the substitution to glutamic acid at positions G8, G46, and V53 in Cx50 increased negative electrostatic potential in the center of the pore and reduced pore diameter. Analyzing individual mutations revealed that each position showed different extents of increase in γ_j . Although these positions were assumed to be pore-lining, this suggests that determinants of Cx50 GJ γ_j is residue specific such that G8 and G46 play a more critical role in determining single channel properties than V53. Individual mutation G46E has previously been shown to drastically increase Cx50 GJ γ_j (Tong et al., 2014). Out of the three single mutations, G46E GJs demonstrated the highest increase in γ_j but was also predicted to have the smallest estimated pore diameter, providing further evidence that this position is critical to determining Cx50 γ_j . While studies in most connexins show a weak correlation between channel conductance and pore size, the diameter may help facilitate the electrostatic field influence on γ_j (Konno et al., 1991; Tong et al., 2015). AChR channels also show differential effects on single channel conductance based on pore position (Imoto et al., 1988; Konno et al., 1991; Wilson et al., 2000). AChR channels have anionic rings near the extracellular region, cytoplasmic region, and an intermediate region found between the extracellular and cytoplasmic rings (Imoto et al., 1988). Through mutagenesis, the intermediate ring, which resides in the narrowest part of the channel, was identified as the major determinant in channel conductance (Konno et al., 1991; Wilson et al., 2000). It

was suggested that a combination of pore size, pore position, and electrostatic interactions are involved in the effect of the mutation (Konno et al., 1991). Our results show that the additive effect of individual mutation GJ γ_j s is not equivalent to the high γ_j expressed by the triple mutation GJ. While individual mutation V53E did not significantly increase Cx50 GJ γ_j , its electrostatic interactions with the other mutations in the triple mutation may have facilitated such a high γ_j .

Previous studies on Cx26 and Cx32 suggest the V_j -sensor consists of a charged complex between NT and M1/E1 domains (Verselis et al., 1994). Surprisingly, none of the mutations tested in the present study significantly altered Cx50 GJ V_j -gating parameters. However, consistent with our findings, previous work on G46E GJs also showed no major alterations in V_j -gating parameters (Tong et al., 2014). Instead, a substitution to a positively charged lysine at this position (G46K) was able to alter V_j -gating parameters. Similarly, a substitution to a positively charged arginine at position N9 in the NT domain of Cx50 resulted in distinct V_j -gating parameters from wild type Cx50 GJs (Xin et al., 2010). It was suggested that the positively charged residues introduced in this area created an electrical barrier in this cation-preferring GJ channel, decreasing sensitivity of the V_j -sensor and abolishing V_j -gating (Tong et al., 2014). Based on these observations, we cannot discredit electrostatic surface potential as a potential molecular determinant to Cx50 GJ V_j -gating parameters.

3.3 Intracellular magnesium modulation in Cx50 mutant GJ channels

Mg^{2+} is a major cation involved in several biological processes and has been shown to regulate ionic channels including AChR channels, a variety of K^+ channels, and Ca^{2+} channels (Hartzell & White, 1989; Horie & Irisawa, 1987; Imoto et al., 1988; Takaya, Higashino, & Kobayashi, 2000; Vandenberg, 1987). The mechanisms underlying its modulatory effects on intercellular communication via GJ channel regulation are not fully understood. Increasing $[Mg^{2+}]_i$ has been shown to dose-dependently reduce junctional conductance resulting in cellular uncoupling in GJs expressed in cardiac cells, salivary gland cells, and calf lens fiber GJs (Noma & Tsuboi, 1987; Oliveira-Castro & Loewenstein, 1971b; Peracchia & Peracchia, 1980). Moreover, homotypic GJs expressing Cx36, Cx26, Cx32, Cx45, and Cx47 have also shown a reduction in junctional conductance in response to increasing $[Mg^{2+}]_i$ (Palacios-Prado et al., 2013). It has been proposed that the sensorial domain within the channel lumen contains Mg^{2+} binding sites (Palacios-Prado et al., 2013). A previous study identified a negatively charged aspartic acid at position 47 (D47) in Cx36's E1 domain to be a critical Mg^{2+} -sensor as a substitution to glycine abolished Mg^{2+} -sensitivity and altered V_j -gating properties (Palacios-Prado et al., 2014). Proposed E1 Mg^{2+} -binding sites have also been identified in hCx46 hemichannels (Ebihara, Liu, & Pal, 2003). $[Mg^{2+}]_i$ modulatory effects on single channel conductance has yet to be fully investigated in connexins. Here we demonstrate that Cx50 GJ does indeed show a significant reduction in γ_j with increasing $[Mg^{2+}]_i$. Introducing negative charges at three putative pore-lining residues, our triple mutation

GJs demonstrated a reduction in γ_j at higher $[\text{Mg}^{2+}]_i$ and a greater reduction in γ_j overall in comparison to GJs expressing Cx50. Studies on AChR channels also demonstrated intracellular anionic rings interacting with intracellular Mg^{2+} (Imoto et al., 1988). Evidence from our triple mutation provides further support for the probable involvement of the pore's electrostatic profile in intracellular Mg^{2+} -modulation. Triple mutation GJs may also be more sensitive to smaller amounts of $[\text{Mg}^{2+}]_i$ in comparison to Cx50 GJs due to the higher probability of Mg^{2+} binding within the pore. Furthermore, GJs expressing single mutations revealed G8, G46, and V53 in Cx50 to be Mg^{2+} sensitive residues. Out of the three mutations, G46E showed the greatest sensitivity to increased $[\text{Mg}^{2+}]_i$ suggesting that this residue in the M1-E1 border may be a Mg^{2+} sensor.

Comparatively, Ca^{2+} modulatory effects have been extensively studied. Numerous studies have demonstrated that a rise in $[\text{Ca}^{2+}]_i$ results in a reduction in junctional conduction and reversible GJ uncoupling (Ebihara et al., 2003; Gómez-Hernández et al., 2003; Loewenstein & Rose, 1978; Pfahnl & Dahl, 1999; Rose, Simpson, & Loewenstein, 1977). Physiologically, uncoupling was thought to be a protective mechanism for healthy cells to seal themselves from unhealthy cells (Loewenstein & Rose, 1978). It has been proposed that Ca^{2+} binds to several spots throughout the GJ channel directly or through calmodulin (CaM) activity (Burr, Mitchell, Keflemariam, Heidelberger, & O'Brien, 2005; Girsch & Peracchia, 1985; Török, Stauffer, & Evans, 1997). Similar to the mechanism of Mg^{2+} modulation proposed in our present study, Ca^{2+} was shown to bind directly to a ring of negatively charged aspartic acids in Cx32 hemichannels, thereby occluding the pore resulting in a reduction in junctional permeability (Gómez-Hernández et al., 2003). Furthermore, Ca^{2+} -dependent CaM binds at a higher affinity to NT than CT

in Cx32, while CaM has more binding sites in the CT of neuronal connexins such as Cx36 (Burr et al., 2005; Török et al., 1997). Differences in binding sites suggest that molecular determinants underlying Ca^{2+} modulation may be connexin-specific. Based on this observation, molecular determinants of Mg^{2+} modulation may also be connexin-specific.

3.4 Physiological and pathological role of intracellular magnesium in the lens

Mg^{2+} is one of the most abundant intracellular regulatory cations and is involved in many cellular activities. Among the many enzymes it regulates, $\text{Na}^+\text{-K}^+\text{-ATPase}$ and $\text{Ca}^{2+}\text{-ATPase}$ activity are highly dependent on Mg^{2+} for the maintenance of the intracellular ionic environment (Kennedy & Nayler, 1965; Pershadsingh & McDonald, 1980). This activity is critical for maintaining a precise intracellular ionic composition of low levels of Ca^{2+} and Na^+ and high levels of K^+ and Mg^{2+} in the lens (Dilsiz et al., 2000). Ionic homeostasis is crucial for maintaining structural and functional integrity in the lens tissues (Agarwal et al., 2014). Moreover, Mg^{2+} has been shown to regulate a lens specific Mg^{2+} -dependent phosphatase which accounts for most phosphatase activity in the lens (Umeda et al., 2003). Additionally, Mg^{2+} is involved in the synthesis of ATP and glutathione peroxidase, an antioxidant required to protect the lens from oxidative stress (Agarwal et al., 2013; Minnich et al., 1971). It is apparent that Mg^{2+} plays a crucial role in maintaining ionic and metabolic homeostasis in the lens.

Disturbances in intracellular Mg^{2+} levels can lead to many pathological conditions, such as ophthalmic diseases like cataracts, glaucoma, and diabetic retinopathy (Agarwal et al.,

2014). These pathologies are prevalent in older populations, as $[Mg^{2+}]_i$ typically show a gradual decrease with age (Swanson & Truesdale, 1971). Pathologically low $[Mg^{2+}]_i$ interferes with proper Na^+ - K^+ - and Ca^{2+} -ATPase activity, reversing proper intracellular ionic composition (Agarwal et al., 2013). Studies done in human lens epithelial cells have demonstrated that Mg^{2+} -deficient medium induces activation of nitric oxide (NO) synthase which enhances cytotoxic NO production. This decreases ATP levels, in turn abolishes ATP ion channel functionality and accelerates the progression of lens opacification (Nagai, Fukuhata, & Ito, 2007). The administration of Mg^{2+} -containing diet supplements and deep-sea drinking water containing Mg^{2+} in Shumiya cataract rats shows promising attenuation in the progression of cataract development (Nagai, Ito, Tai, Hataguchi, & Nakagawa, 2006; Nagai, Ito, Inomata, et al., 2006). Understanding the mechanisms underlying $[Mg^{2+}]_i$ modulation of Cx50 GJs would provide further insight into GJs involvement in the etiology of ophthalmic pathologies and how exogenous Mg^{2+} treatment through supplementation might affect GJ functionality.

3.5 Limitations and future directions

Observations presented in this study establish a critical role of pore-lining residues and $[Mg^{2+}]_i$ as determinants in Cx50 GJ γ_j . Furthermore, our study provides evidence supporting the importance of electrostatics in facilitating ion permeation. However, it should be noted that there are limitations to consider when interpreting our results. Currently, Cx26 is the only connexin that has a high-resolution near atomic GJ structure (Maeda et al., 2009). The homology structure generated for Cx50 is therefore only a homology model based on the structural template provided by Cx26. Due to the high degree of sequence identity within the connexin family, Cx26 has been commonly used

as an acceptable structural template for many structure-function studies. GJ properties, including γ_j and V_j -gating, are thus conserved within similar domains. Nevertheless, variability within connexin structure does exist and is likely the reason for the range in GJ properties. Without a high resolution of Cx50's crystal structure we cannot fully confirm whether the residues mutated in this study face the pore lumen in an active GJ channel; therefore we are unable to make definite conclusions on the molecular mechanisms proposed. Based on previous studies, alterations in GJ properties, particularly changes in γ_j , caused by site mutagenesis, provide support for pore-lining residues. Since G8E and G46E altered Cx50 GJ γ_j in both Mg^{2+} -free and Mg^{2+} -containing ICS, it is highly probable that these positions line the pore. Without a fully crystalized structure, creating systematic mutagenic changes to amino acid residues along the pore lining regions could provide a more extensive molecular analysis and further elucidate the role of putative pore-lining residues in Cx50 GJ channels.

Like previous studies, we predict that negative electrostatic profile of the pore increases γ_j in cation-preferring GJs. These observations were generated through the substitution to negatively charged glutamates at three potential pore-lining positions in Cx50. To follow up on this observation, future studies should simultaneously mutate several putative pore-lining residues to determine the potential upper limit negative pore electrostatic potential has on Cx50 GJ properties. It may be interesting to investigate whether increasing negatively charged amino acids in pore-lining regions amplifies γ_j of connexins that exhibit low GJ γ_j , such as mCx30.2 (9 pS) (Kreuzberg et al., 2005). Increasing negative electrostatic profile of the pore would further determine if increasing intracellular Mg^{2+} modulates Cx50 GJ γ_j by binding non-selectively to multiple negative charges along the

pore or if there are in fact critical Mg^{2+} sensing residues. To further our understanding of electrostatics in determining channel properties, future studies should consider either neutralizing charged amino acid residues or substituting to positively charged residues along the pore.

As previously mentioned, $[Mg^{2+}]_i$ is not uniform throughout the lens (McGahan et al., 1983). Investigating the effect of higher $[Mg^{2+}]_i$ would address any potential upper limit of Mg^{2+} modulation that might be seen in outer layers of the lens tissue. It would also be worth investigating the effects of $[Mg^{2+}]_i$ in other lens connexins, Cx43 and Cx46, to provide further insight into how intracellular Mg^{2+} modulates GJ properties. However, it should be noted that this is an *in vitro* study and that assumptions are limited to how $[Mg^{2+}]_i$ modulates GJs in N2A cells. We cannot confirm any physiological mechanisms, specifically in the lens, without the aid of *in vivo* studies.

3.6 Summary

Here we have provided experimental evidence to highlight the importance of pore-lining residues and $[Mg^{2+}]_i$ in Cx50 GJ γ_j . A significant increase in γ_j in GJs expressing G8E, G46E, and G8G46V53 suggest that these positions are likely pore-lining and greatly influence γ_j in Cx50 GJ channels. Since Cx50 forms cation-preferring GJ channels, increasing negatively charged residues along pore-lining domains may facilitate the concentration of local permeating cations, thereby increasing single channel conductance. We predict that differences in electrostatic pore profiles between connexins may account for the large range seen in GJ γ_j . Future studies investigating the effect of increasing negative electrostatic pore potentials in connexins with GJs displaying lower γ_j would provide further insight into the importance of electrostatics in determining γ_j .

Furthermore, our results demonstrate a decrease in γ_j in GJs expressing Cx50, G8E, G46E, V53E, and G8G46V53 with increasing $[\text{Mg}^{2+}]_i$. The decrease in γ_j in these individual GJs suggests that these positions likely contribute to Mg^{2+} -binding. The drastic reduction in γ_j in GJs expressing G8G46V53 suggests that increasing negative charges in the pore may increase the availability of Mg^{2+} binding sites or increase affinity of pre-existing sites. Follow up studies should investigate whether there is an upper limit when higher $[\text{Mg}^{2+}]_i$ is introduced. A high-resolution crystallized atomic structure of Cx50 would provide more confirmation on whether these positions are pore-lining and would further confirm Mg^{2+} modulatory effects.

3.7 References

- Agarwal, R., Iezhitsa, I., Agarwal, P., & Spasov, A. (2012). Magnesium deficiency: Does it have a role to play in cataractogenesis? *Experimental Eye Research*, *101*, 82–89.
- Agarwal, R., Iezhitsa, I. N., Agarwal, P., & Spasov, A. a. (2013). Mechanisms of cataractogenesis in the presence of magnesium deficiency. *Magnesium Research*, *26*(1), 2–8.
- Agarwal, R., Iezhitsa, L., & Agarwal, P. (2014). Pathogenetic role of magnesium deficiency in ophthalmic diseases. *BioMetals*, *27*(1), 5–18.
- Arora, a, Minogue, P. J., Liu, X., Addison, P. K., Russel-Eggitt, I., Webster, ... Moore, A. T. (2008). A novel connexin50 mutation associated with congenital nuclear pulverulent cataracts. *Journal of Medical Genetics*, *45*(3), 155–60.
- Bai, D., & Cameron, J. A. (2017). Patch clamp analysis of gap junction channel properties. In Bai, D., & Sáez, J.C. (Eds.), *Gap Junction Channels and Hemichannels* (pp. 93-112). Boca Raton, FL: Taylor & Francis Group.
- Bai, D., del Corso, C., Srinivas, M., & Spray, D. C. (2006). Block of Specific Gap Junction Channel Subtypes by 2-Aminoethoxydiphenyl Borate (2-APB). *Journal of Pharmacology and Experimental Therapeutics*, *319*(3), 1452–1458.
- Bai, D., & Wang, A. H. (2014). Extracellular domains play different roles in gap junction formation and docking compatibility. *The Biochemical Journal*, *458*(1), 1–10.
- Baker, N. A., Sept, D., Joseph, S., Holst, M. J., & McCammon, J. A. (2001). Electrostatics of nanosystems: application to microtubules and the ribosome. *Proceedings of the National Academy of Sciences of the United States of America*, *98*(18), 10037–41.
- Bassnett, S., & Beebe, D. C. (1992). Coincident loss of mitochondria and nuclei during lens fiber cell differentiation. *Developmental Dynamics*, *194*(2), 85–93.

- Bennett, M. V. (1997). Gap junctions as electrical synapses. *Journal of Neurocytology*, 26(6), 349–66.
- Bennett, M. V., & Verselis, V. K. (1992). Biophysics of gap junctions. *Seminars in Cell Biology*, 3(1), 29–47.
- Beyer, E. C., & Berthoud, V. M. (2014). Connexin hemichannels in the lens. *Frontiers in Physiology*, 5, 20.
- Brelidze, T. I., Niu, X., & Magleby, K. L. (2003). A ring of eight conserved negatively charged amino acids doubles the conductance of BK channels and prevents inward rectification. *Proceedings of the National Academy of Sciences of the United States of America*, 100(15), 9017–9022.
- Brennan, M. J., Karcz, J., Vaughn, N. R., Woolwine-Cunningham, Y., DePriest, A. D., Escalona, Y., ... Skerrett, I. M. (2015). Tryptophan Scanning Reveals Dense Packing of Connexin Transmembrane Domains in Gap Junction Channels Composed of Connexin32. *Journal of Biological Chemistry*, 290(28), 17074–17084.
- Bruzzone, R., White, T. W., & Paul, D. L. (1996). Connections with connexins: the molecular basis of direct intercellular signaling. *European Journal of Biochemistry / FEBS*, 238(1), 1–27.
- Bukauskas, F. F., & Peracchia, C. (1997). Two distinct gating mechanisms in gap junction channels: CO₂-sensitive and voltage-sensitive. *Biophysical Journal*, 72(5), 2137–42.
- Bukauskas, F. F., & Verselis, V. K. (2004). Gap junction channel gating. *Biochimica et Biophysica Acta*, 1662(1-2), 42–60.
- Bukauskas, F. F., & Weingart, R. (1994). Voltage-dependent gating of single gap junction channels in an insect cell line. *Biophysical Journal*, 67(2), 613–625.

- Burghardt, R. C., Barhoumi, R., Sewall, T. C., & Bowen, J. a. (1995). Cyclic AMP induces Rapid increases in gap junction permeability and changes in the cellular distribution of connexin43. *New York*, 253, 243–253.
- Burr, G. S., Mitchell, C. K., Keflemariam, Y. J., Heidelberger, R., & O'Brien, J. (2005). Calcium-dependent binding of calmodulin to neuronal gap junction proteins. *Biochemical and Biophysical Research Communications*, 335(4), 1191–1198.
- Carvacho, I., Gonzalez, W., Torres, Y. P., Brauchi, S., Alvarez, O., Gonzalez-Nilo, F. D., & Latorre, R. (2008). Intrinsic electrostatic potential in the BK channel pore: role in determining single channel conductance and block. *The Journal of General Physiology*, 131(2), 147–61.
- Chang, B., Wang, X., Hawes, N. L., Ojakian, R., Davisson, M. T., Lo, W. K., & Gong, X. (2002). A Gja8 (Cx50) point mutation causes an alteration of alpha 3 connexin (Cx46) in semi-dominant cataracts of Lop10 mice. *Hum Mol Genet*, 11(5), 507–513.
- Church, R. L., Wang, J., & Steele, E. (1995). The human lens intrinsic membrane protein MP70 (Cx50) gene: clonal analysis and chromosome mapping. *Current Eye Research*, 14(3), 215–221.
- Decker, R. S. (1976). Hormonal regulation of gap junction differentiation. *The Journal of Cell Biology*, 69(3).
- Dermietzel, R., Traub, O., Hwang, T. K., Beyer, E., Bennett, M. V, Spray, D. C., & Willecke, K. (1989). Differential expression of three gap junction proteins in developing and mature brain tissues. *Proceedings of the National Academy of Sciences*, 86(December), 10148–10152.
- Dilsiz, N., Olcucu, A., & Atas, M. (2000). Determination of calcium, sodium, potassium and magnesium concentrations in human senile cataractous lenses. *Cell Biochemistry and Function*, 18(4), 259–262.

- Dunlap, K., Takeda, K., & Brehm, P. (1987). Activation of a calcium-dependent photoprotein by chemical signalling through gap junctions. *Nature*, 325(6099), 60–62.
- Ebihara, L., Liu, X., & Pal, J. D. (2003). Effect of external magnesium and calcium on human connexin46 hemichannels. *Biophysical Journal*, 84(1), 277–286.
- George, C. H., Kendall, J. M., & Evans, W. H. (1999). Intracellular trafficking pathways in the assembly of connexins into gap junctions. *Journal of Biological Chemistry*, 274(13), 8678–8685.
- Girsch, S. J., & Peracchia, C. (1985). Lens cell-to-cell channel protein: I. Self-assembly into liposomes and permeability regulation by calmodulin. *The Journal of Membrane Biology*, 83(3), 217–25.
- Goldberg, G. S., Lampe, P. D., & Nicholson, B. J. (1999). Selective transfer of endogenous metabolites through gap junctions composed of different connexins. *Nature Cell Biology*, 1(7), 457–459.
- Gómez-Hernández, J. M., de Miguel, M., Larrosa, B., González, D., Barrio, L. C., Gomez-Hernandez, J. M., ... Barrio, L. C. (2003). Molecular basis of calcium regulation in connexin-32 hemichannels. *Proceedings of the National Academy of Sciences of the United States of America*, 100(26), 16030–16035.
- Gong, X., Li, E., Klier, G., Huang, Q., Wu, Y., Lei, H., ... Gilula, N. B. (1997). Disruption of $\alpha 3$ connexin gene leads to proteolysis and cataractogenesis in mice. *Cell*, 91(6), 833–843.
- Gong, X. Q., & Nicholson, B. J. (2001). Size selectivity between gap junction channels composed of different connexins. *Cell Communication & Adhesion*, 8, 187–192.
- González, D., Gómez-Hernández, J. M., & Barrio, L. C. (2007). Molecular basis of voltage dependence of connexin channels: An integrative appraisal. *Progress in Biophysics and Molecular Biology*, 94(1-2), 66–106.

- Goodenough, D. a. (1992). The crystalline lens. A system networked by gap junctional intercellular communication. *Semin Cell Biol*, 3(1), 49–58.
- Gourdie, R., Green, C., Severs, N., & Thompson, R. (1992). Immunolabelling patterns of gap junction connexins in the developing and mature rat heart. *Anatomy and Embryology*, 185(4), 363–378.
- Guleria, K., Sperling, K., Singh, D., Varon, R., Singh, J. R., & Vanita, V. (2007). A novel mutation in the connexin 46 (GJA3) gene associated with autosomal dominant congenital cataract in an Indian family. *Molecular Vision*, 13(April), 1657–65.
- Harris, a L., Spray, D. C., & Bennett, M. V. (1981). Equilibrium Properties of a voltage-dependent junctional conductance. *The Journal of General Physiology*, 77(January), 95–117.
- Harris, A. L., Spray, D. C., & Bennett, M. V. (1981). Kinetic properties of a voltage-dependent junctional conductance. *The Journal of General Physiology*, 77(1).
- Hartzell, H. C., & White, R. E. (1989). Effects of magnesium on inactivation of the voltage-gated calcium current in cardiac myocytes. *The Journal of General Physiology*, 94(4), 745–67.
- Hermans, M. M. P., Kortekaas, P., Jongasma, H. J., & Rook, M. B. (1995). pH sensitivity of the cardiac gap junction proteins, connexin 45 and 43. *Pflügers Archiv European Journal of Physiology*, 431(1), 138–140.
- Hopperstad, M. G., Srinivas, M., & Spray, D. C. (2000). Properties of gap junction channels formed by Cx46 alone and in combination with Cx50. *Biophysical Journal*, 79(4), 1954–66.
- Horie, M., & Irisawa, H. (1987). Rectification of muscarinic K⁺ current by magnesium ion in guinea pig atrial cells. *American Journal of Physiology - Heart and Circulatory Physiology*, 253(1).

- Hu, X., Ma, M., & Dahl, G. (2006). Conductance of Connexin Hemichannels Segregates with the First Transmembrane Segment. *Biophysical Journal*, *90*(1), 140–150.
- Imoto, K., Busch, C., Sakmann, B., Mishina, M., Konno, T., Nakai, J., ... Numa, S. (1988). Rings of negatively charged amino acids determine the acetylcholine receptor channel conductance. *Nature*, *335*(6191), 645–648.
- Johnson, R., Hammer, M., Sheridan, J., & Revel, J. P. (1974). Gap junction formation between reaggregated Novikoff hepatoma cells. *Proc Natl Acad Sci U S A*, *71*(11), 4536–4540.
- Kanter, H. L., Saffitz, J. E., & Beyer, E. C. (1992). Cardiac myocytes express multiple gap junction proteins. *Circulation Research*, *70*(2), 438–444.
- Kennedy, K. G., & Nayler, W. G. (1965). The effect of quinidine on the activity of a sodium-potassium activated, magnesium-dependent ATPase enzyme isolated from toad cardiac muscle. *Biochimica et Biophysica Acta (BBA) - Enzymology and Biological Oxidation*, *110*(1), 174–180.
- Kerscher, S., Church, R. L., Boyd, Y., & Lyon, M. F. (1995). Mapping of four mouse genes encoding eye lens-specific structural, gap junction, and integral membrane proteins: Cryba1 (crystallin beta A3/A1), Crybb2 (crystallin beta B2), Gja8 (MP70), and Lim2 (MP19). *Genomics*, *29*(2), 445–450.
- Kistler, J., Kirkland, B., & Bullivant, S. (1985). Identification of a 70,000-D protein in lens membrane junctional domains. *Journal of Cell Biology*, *101*(1), 28–35.
- Konno, T., Busch, C., von Kitzing, E., Imoto, K., Wang, F., Nakai, J., ... Sakmann, B. (1991). Rings of anionic amino acids as structural determinants of ion selectivity in the acetylcholine receptor channel. *Proc. Biol. Sci.*, *244*(1310), 69–79.
- Kreuzberg, M. M., Söhl, G., Kim, J.-S., Verselis, V. K., Willecke, K., & Bukauskas, F. F. (2005). Functional properties of mouse connexin30.2 expressed in the conduction system of the heart. *Circulation Research*, *96*(11), 1169–77.

- Kronengold, J. (2003). Single-channel SCAM Identifies Pore-lining Residues in the First Extracellular Loop and First Transmembrane Domains of Cx46 Hemichannels. *The Journal of General Physiology*, 122(4), 389–405.
- Kronengold, J., Trexler, E. B., Bukauskas, F. F., Bargiello, T. A., & Verselis, V. K. (2003). Single-channel SCAM Identifies Pore-lining Residues in the First Extracellular Loop and First Transmembrane Domains of Cx46 Hemichannels. *The Journal of General Physiology*, 122(4), 389–405.
- Krutovskikh, V. a, Piccoli, C., & Yamasaki, H. (2002). Gap junction intercellular communication propagates cell death in cancerous cells. *Oncogene*, 21(13), 1989–1999.
- Kumar, N. M., & Gilula, N. B. (1992). Molecular biology and genetics of gap junction channels. *Seminars in Cell Biology*, 3(1), 3–16.
- Kwak, B. R., Hermans, M. M., De Jonge, H. R., Lohmann, S. M., Jongsma, H. J., & Chanson, M. (1995). Differential regulation of distinct types of gap junction channels by similar phosphorylating conditions. *Molecular Biology of the Cell*, 6(12), 1707–1719.
- Laird, D. W. (1996). The life cycle of a connexin: gap junction formation, removal, and degradation. *Journal of Bioenergetics and Biomembranes*, 28(4), 311–318.
- Lawrence, T. S., Beers, W. H., & Gilula, N. B. (1978). Transmission of hormonal stimulation by cell-to-cell communication. *Nature*, 272, 501–506.
- Li, J., Wang, Q., Fu, Q., Zhu, Y., Zhai, Y., Yu, Y., ... Yao, K. (2013). A novel connexin 50 gene (gap junction protein, alpha 8) mutation associated with congenital nuclear and zonular pulverulent cataract. *Molecular Vision*, 19(April), 767–774.
- Loewenstein, W. R., Nakas, M., & Socolar, S. J. (1967). Junctional Membrane Uncoupling: Permeability transformations at a cell membrane junction . *The Journal of General Physiology* , 50 (7) , 1865–1891.

- Loewenstein, W. R., & Rose, B. (1978). Calcium in (Junctional) Intercellular Communication and a Thought on Its Behavior in Intracellular Communication. *Annals of the New York Academy of Sciences*, 307(1), 285–307.
- MacKinnon, R., Latorre, R., & Miller, C. (1989). Role of surface electrostatics in the operation of a high-conductance Ca²⁺-activated K⁺ channel. *Biochemistry*, 28(1985), 8092–8099.
- Maeda, S., Nakagawa, S., Suga, M., Yamashita, E., Oshima, A., Fujiyoshi, Y., & Tsukihara, T. (2009). Structure of the connexin 26 gap junction channel at 3.5 Å resolution. *Nature*, 458(7238), 597–602.
- Maza, J., Mateescu, M., Das Sarma, J., & Koval, M. (2003). Differential oligomerization of endoplasmic reticulum-retained connexin43/connexin32 chimeras. *Cell Communication & Adhesion*, 10, 319–322.
- McGahan, M. C., Chin, B., & Bentley, P. J. (1983). Some Observations on the Magnesium Metabolism of the Rabbit Lens. *Exp. Eye Res*, 36, 67–73.
- Minnich, V., Smith, M. B., Brauner, M. J., & Majerus, P. W. (1971). Glutathione biosynthesis in human erythrocytes. I. Identification of the enzymes of glutathione synthesis in hemolysates. *Journal of Clinical Investigation*, 50(3), 507–513.
- Minogue, P. J., Tong, J. J., Arora, A., Russell-Eggitt, I., Hunt, D. M., Moore, A. T., ... Berthoud, V. M. (2009). A mutant connexin50 with enhanced hemichannel function leads to cell death. *Investigative Ophthalmology and Visual Science*, 50(12), 5837–5845.
- Moreno, a P., Rook, M. B., Fishman, G. I., & Spray, D. C. (1994). Gap junction channels: distinct voltage-sensitive and -insensitive conductance states. *Biophysical Journal*, 67(1), 113–9.
- Noma, a, & Tsuboi, N. (1987). Dependence of junctional conductance on proton, calcium and magnesium ions in cardiac paired cells of guinea-pig. *J. Physiol.*, 382(1), 193–211.

- Oliveira-Castro, G. M., & Loewenstein, W. R. (1971a). Junctional membrane permeability. *The Journal of Membrane Biology*, 5(1), 51–77.
- Oliveira-Castro, G. M., & Loewenstein, W. R. (1971b). Junctional membrane permeability - Effects of divalent cations. *The Journal of Membrane Biology*, 5(1), 51–77.
- Palacios-Prado, N., Chapuis, S., Panjkovich, A., Fregeac, J., Nagy, J. I., & Bukauskas, F. F. (2014). Molecular determinants of magnesium-dependent synaptic plasticity at electrical synapses formed by connexin36. *Nature Communications*, 5, 4667.
- Palacios-Prado, N., Hoge, G., Marandykina, A., Rimkute, L., Chapuis, S., Paulauskas, N., ... Bukauskas, F. F. (2013). Intracellular Magnesium-Dependent Modulation of Gap Junction Channels Formed by Neuronal Connexin36. *J Neurosci.*, 33(11), 4741–4753.
- Paulauskas, N., Pranevicius, M., Pranevicius, H., & Bukauskas, F. F. (2009). A stochastic four-state model of contingent gating of gap junction channels containing two “fast” gates sensitive to transjunctional voltage. *Biophysical Journal*, 96(10), 3936–3948.
- Paznekas, W. a., Karczeski, B., Vermeer, S., Lowry, R. B., Delatycki, M., Laurence, F., ... Jabs, E. W. (2009). GJA1 mutations, variants, and connexin 43 dysfunction as it relates to the oculodentodigital dysplasia phenotype. *Human Mutation*, 30(5), 724–733.
- Peracchia, C., & Peracchia, L. L. (1980). Gap junction dynamics: reversible effects of divalent cations. *The Journal of Cell Biology*, 87(3).
- Pershadsingh, H. a., & McDonald, J. M. (1980). A high affinity calcium-stimulated magnesium-dependent adenosine triphosphatase in rat adipocyte plasma membranes. *Journal of Biological Chemistry*, 255(9), 4087–4093.
- Pfahnl, A., & Dahl, G. (1999). Gating of cx46 gap junction hemichannels by calcium and voltage. *Pflugers Archiv European Journal of Physiology*, 437(3), 345–353.

- Ramanan, S. V., Brink, P. R., Varadaraj, K., Peterson, E., Schirrmacher, K., & Banach, K. (1999). A Three-State Model for Connexin37 Gating Kinetics. *Biophysical Journal*, 76(5), 2520–2529.
- Richard, G., Rouan, F., Willoughby, C. E., Brown, N., Chung, P., Jabs, E. W., ... Russell, L. (2002). Missense Mutations in GJB2 Encoding Connexin-26 Cause the Ectodermal Dysplasia Keratitis-Ichthyosis-Deafness Syndrome, 1341–1348.
- Rong, P., Wang, X., Niesman, I., Wu, Y., Benedetti, L. E., Dunia, I., ... Gong, X. (2002). Disruption of Gja8 (alpha8 connexin) in mice leads to microphthalmia associated with retardation of lens growth and lens fiber maturation. *Development (Cambridge, England)*, 129(1), 167–74.
- Rose, B., Simpson, I., & Loewenstein, W. R. (1977). Calcium ion produces graded changes in permeability of membrane channels in cell junction. *Nature*, 267(5612), 625–627.
- Rubinos, C., Villone, K., Mhaske, P. V., White, T. W., & Srinivas, M. (2014). Functional effects of Cx50 mutations associated with congenital cataracts. *American Journal of Physiology. Cell Physiology*, 306(3), C212–20.
- Sarma, J. Das, Wang, F., & Koval, M. (2002). Targeted gap junction protein constructs reveal connexin-specific differences in oligomerization. *Journal of Biological Chemistry*, 277(23), 20911–20918.
- Schlingmann, B., Schadzek, P., Busko, S., Heisterkamp, A., & Ngezahayo, A. (2012). Cataract-associated D3Y mutation of human connexin46 (hCx46) increases the dye coupling of gap junction channels and suppresses the voltage sensitivity of hemichannels. *Journal of Bioenergetics and Biomembranes*, 44(5), 607–614.
- Schütte, M., Chen, S., Buku, A., & Wolosin, J. M. (1998). Connexin50, a Gap Junction Protein of Macrogliia in the Mammalian Retina and Visual Pathway. *Experimental Eye Research*, 66(5), 605–613.

- Segretain, D., & Falk, M. M. (2004). Regulation of connexin biosynthesis, assembly, gap junction formation, and removal. *Biochimica et Biophysica Acta - Biomembranes*, 1662(1-2), 3–21.
- Shiels, a, Mackay, D., Ionides, a, Berry, V., Moore, a, & Bhattacharya, S. (1998). A missense mutation in the human connexin50 gene (GJA8) underlies autosomal dominant “zonular pulverulent” cataract, on chromosome 1q. *American Journal of Human Genetics*, 62(3), 526–32.
- Simpson, I., Rose, B., & Loewenstein, W. R. (1977). Size limit of molecules permeating the junctional membrane channels. *Science (New York, N.Y.)*, 195(4275), 294–6.
- Sohl, G. (2004). Gap junctions and the connexin protein family. *Cardiovascular Research*, 62(2), 228–232.
- Söhl, G., & Willecke, K. (2004). Gap junctions and the connexin protein family. *Cardiovascular Research*, 62(2), 228–232.
- Srinivas, M., Costa, M., Gao, Y., Fort, a, Fishman, G. I., & Spray, D. C. (1999). Voltage dependence of macroscopic and unitary currents of gap junction channels formed by mouse connexin50 expressed in rat neuroblastoma cells. *The Journal of Physiology*, 517 (Pt 3, 673–89.
- Srinivas, M., Rozental, R., Kojima, T., Dermietzel, R., Mehler, M., Condorelli, D. F., ... Spray, D. C. (1999). Functional properties of channels formed by the neuronal gap junction protein connexin36. *The Journal of Neuroscience : The Official Journal of the Society for Neuroscience*, 19(22), 9848–9855.
- Swanson, A. a., & Truesdale, A. W. (1971). Elemental analysis in normal and cataractous human lens tissue. *Biochemical and Biophysical Research Communications*, 45(6), 1488–1496.
- Takaya, J., Higashino, H., & Kobayashi, Y. (2000). Can magnesium act as a second messenger? Current data on translocation induced by various biologically active

substances. *Magnesium Research : Official Organ of the International Society for the Development of Research on Magnesium*, 13(2), 139–146.

- Tong, J.-J., Minogue, P. J., Guo, W., Chen, T.-L., Beyers, E. C., Berthoud, V. M., & Ebihara, L. (2011). Different consequences of cataract-associated mutations at adjacent positions in the first extracellular boundary of connexin50. *American Journal of Physiology. Cell Physiology*, 300(5), C1055–64.
- Tong, X., Aoyama, H., Sudhakar, S., Chen, H., Shilton, B. H., & Bai, D. (2015). The first extracellular domain plays an important role in unitary channel conductance of Cx50 gap junction channels. *PLoS ONE*, 10(12), 1–20.
- Tong, X., Aoyama, H., Tsukihara, T., & Bai, D. (2014). Charge at the 46th residue of connexin 50 is crucial for the gap-junctional unitary conductance and transjunctional voltage-dependent gating. *The Journal of Physiology*, 592(23), 5187–5202.
- Török, K., Stauffer, K., & Evans, W. H. (1997). Connexin 32 of gap junctions contains two cytoplasmic calmodulin-binding domains. *The Biochemical Journal*, 326 (Pt 2, 479–83.
- Umeda, I. O., Kashiwa, Y., Nakata, H., & Nishigori, H. (2003). Predominant phosphatase in the ocular lens regulated by physiological concentrations of magnesium and calcium. *Life Sciences*, 73(9), 1161–1173.
- Vandenberg, C. a. (1987). Inward rectification of a potassium channel in cardiac ventricular cells depends on internal magnesium ions. *Proceedings of the National Academy of Sciences*, 84(8), 2560–2564.
- Vanita, V., Singh, J. R., Singh, D., Varon, R., & Sperling, K. (2008). A novel mutation in GJA8 associated with jellyfish-like cataract in a family of Indian origin. *Molecular Vision*, 14(August 2007), 323–326.
- Veenstra, R. D. (1996). Size and selectivity of gap junction channels formed from different connexins. *Journal of Bioenergetics and Biomembranes*, 28(4), 327–37.

- Veenstra, R. D., Wang, H. Z., Beyer, E. C., Ramanan, S. V., & Brink, P. R. (1994). Connexin37 forms high conductance gap junction channels with subconductance state activity and selective dye and ionic permeabilities. *Biophysical Journal*, 66(June), 1915–1928.
- Verselis, V. K., Ginter, C. S., & Bargiello, T. a. (1994). Opposite voltage gating polarities of two closely related connexins. *Nature*, 368, 348–351.
- Wang, L., Luo, Y., Wen, W., Zhang, S., & Lu, Y. (2011). Another evidence for a D47N mutation in GJA8 associated with autosomal dominant congenital cataract. *Molecular Vision*, 17(May), 2380–2385.
- Weber, P. a, Chang, H. C., Spaeth, K. E., Nitsche, J. M., & Nicholson, B. J. (2004). The permeability of gap junction channels to probes of different size is dependent on connexin composition and permeant-pore affinities. *Biophys J*, 87(2), 958–973.
- White, T. W., Bruzzone, R., Goodenough, D. a, & Paul, D. L. (1992). Mouse Cx50, a functional member of the connexin family of gap junction proteins, is the lens fiber protein MP70. *Molecular Biology of the Cell*, 3(7), 711–20.
- White, T. W., Bruzzone, R., Wolfram, S., Paul, D. L., & Goodenough, D. a. (1994). Selective interactions among the multiple connexin proteins expressed in the vertebrate lens: The second extracellular domain is a determinant of compatibility between connexins. *Journal of Cell Biology*, 125(4), 879–892.
- White, T. W., Goodenough, D. a., & Paul, D. L. (1998). Targeted ablation of connexin50 in mice results in microphthalmia and zonular pulverulent cataracts. *Journal of Cell Biology*, 143(3), 815–825.
- Wilders, R., & Jongsma, H. J. (1992). Limitations of the dual voltage clamp method in assaying conductance and kinetics of gap junction channels. *Biophysical Journal*, 63(4), 942–53.

- Wilson, G. G., Pascual, J. M., Brooijmans, N., Murray, D., & Karlin, a. (2000). The intrinsic electrostatic potential and the intermediate ring of charge in the acetylcholine receptor channel. *J Gen Physiol*, *115*(2), 93–106.
- Wolosin, J. M., Schütte, M., & Chen, S. (1997). Connexin distribution in the rabbit and rat ciliary body: A case for heterotypic epithelial gap junctions. *Investigative Ophthalmology and Visual Science*, *38*(2), 341–348.
- Xin, L., Gong, X. Q., & Bai, D. (2010). The role of amino terminus of mouse Cx50 in determining transjunctional voltage-dependent gating and unitary conductance. *Biophysical Journal*, *99*(7), 2077–2086.
- Xin, L., Nakagawa, S., Tsukihara, T., & Bai, D. (2012). Aspartic Acid Residue D3 Critically Determines Cx50 Gap Junction Channel Transjunctional Voltage-Dependent Gating and Unitary Conductance. *Biophysj*, *102*(5), 1022–1031.
- Yeager, M., Unger, V. M., & Falk, M. M. (1998). Synthesis, assembly and structure of gap junction intercellular channels. *Current Opinion in Structural Biology*, *8*(4), 517–524.
- Yoshimura, T., Satake, M., Ohnishi, a, Tsutsumi, Y., & Fujikura, Y. (1998). Mutations of connexin32 in Charcot-Marie-Tooth disease type X interfere with cell-to-cell communication but not cell proliferation and myelin-specific gene expression. *Journal of Neuroscience Research*, *51*(2), 154–61.
- Zhou, X. W., Pfahnl, a, Werner, R., Hudder, a, Llanes, a, Luebke, a, & Dahl, G. (1997). Identification of a pore lining segment in gap junction hemichannels. *Biophysical Journal*, *72*(5), 1946–53.

Curriculum Vitae

Name: Mary Grace Mangurali Tejada

Post-secondary Education and Degrees: The University of Western Ontario
London, Ontario, Canada
2015-2017 M.Sc. (*Expected Fall 2017*)

McMaster University
Hamilton, Ontario, Canada
2010-2014 H.B.Sc

Honours and Awards: Dean's Honors List
McMaster University
2012-2013, 2013-2014

Distinction
McMaster University
2010-2014

Related Work Experience Teaching Assistant
The University of Western Ontario
2015-2017

Research Assistant
McMaster University
2014-2015

Publications:

Heisz, J. J., Tejada, M. G. M., Paolucci, E. M., & Muir, C. (2016). Enjoyment for high-intensity interval exercise increases during the first six weeks of training: Implications for promoting exercise adherence in sedentary adults. *PLoS ONE*, *11*(12), 1–10.

Presentations:

Invited Speaker, Nexxin Forum, London, ON, 2017

Poster Presentation, London Health Research Day, London, ON, 2017

McMaster PNB Undergraduate Poster Day, Hamilton, ON 2014